Fakultät für Medizin

Klinik und Poliklinik für Innere Medizin III, Hämatologie und Onkologie, Klinikum rechts der Isar der Technischen Universität München

Dissection of immune responses against naturally presented HLA ligands on native human melanoma identified by mass spectrometry

Eva Mechthild Bräunlein

Vollständiger Abdruck der von der Fakultät für Medizin der Technischen Universität München zur Erlangung des akademischen Grades eines

Doctor of Philosophy (Ph.D.)

genehmigten Dissertation.

Vorsitzender:	Prof. Dr. Dr. Stefan Engelhardt
Betreuerin:	Prof. Dr. Angela Krackhardt

Prüfer der Dissertation:

1. Prof. Dr. Dirk H. Busch

2. Prof. Dr. Ulrike Protzer

3. Prof. Dr. Kirsten Lauber

Die Dissertation wurde am 14.06.2017 bei der Fakultät für Medizin der Technischen Universität München eingereicht und durch die Fakultät für Medizin am 28.02.2018 angenommen.

Table of Content

Parts of this thesis have already been published:

M. Bassani-Sternberg*, E. Bräunlein*, R. Klar, T. Engleitner, P. Sinitcyn, S. Audehm, M. Straub, J. Weber, J. Slotta-Huspenina, K. Specht, M. E. Martignoni, A. Werner, R. Hein, D. H. Busch, C. Peschel, R. Rad, J. Cox, M. Mann, A. M. Krackhardt. Direct identification of clinically relevant neoepitopes presented on native human melanoma tissue by mass spectrometry. Nat. Commun. 7, 13404 doi: 10.1038/ncomms13404 (2016). (*equal contribution)

Summary

The interdependence of cancer and the immune system has been intensively investigated for several decades resulting in the development of promising novel strategies to treat malignant diseases summarized as cancer immunotherapy. Emerging broader clinical applications especially with regard to immune checkpoint blockade, but also adoptive T-cell transfer, show promising results and demand a detailed understanding of determinants involved in immune-mediated tumor eradication. This includes the identification of target structures exposed on the surface of tumor cells, but also the assessment and characterization of potent T-cell responses. Within the proposed study, we sought to investigate the immunogenic potential of human leukocyte antigen (HLA)-bound ligands extracted from primary human melanoma tissue. Peptide ligands were identified by discovery-based mass spectrometry analyses. In a first approach, a selection of the detected peptides derived from tumor-associated antigens was used for in-vitro stimulations of healthy donor-derived naïve T cells in an HLA-mismatched setting. T cells responding to two different epitopes were expanded and further characterized aiming at the isolation of specific T-cell receptors (TCR). However, a more detailed investigation of observed reactivities revealed undesired recognition of target cells lacking respective antigen expression. These results emphasize the importance of a thorough characterization of potential target and TCR candidates as a basis for rational proceedings towards clinical translation.

In a second approach, exome sequencing of melanoma tumors from five patients was performed and used as library containing tumor-related mutations. Search across analyzed mass spectra resulted in the identification of eleven naturally presented mutated peptide ligands. Eight of these peptides were found in the tumor of one single patient, Mel15, and subjected to detailed analysis of immune responses of the patient's own T cells against these target structures. Two of these mutations elicited a T-cell response at several time points of blood withdrawals within a time frame of six months. Moreover, reactivity against one of these neoepitopes, SYTL4^{S363F}, was observed in tumor-infiltrating lymphocytes expanded from a second metastatic lesion from patient Mel15. Isolation of neoantigen-directed T-cell clones revealed an oligoclonal immune response providing insights into the complexity of tumor-directed cytotoxic reactivity. Two other peptide ligands, that were detected by mass spectrometry but not found to elicit an immune response in the autologous host, were immunogenic when tested in HLA-matched in-vitro stimulations with peripheral blood mononuclear cells (PBMC) from healthy donors. Further functional characterization of immune reactivity against one of these ligands, AKAP6^{M1482I}, revealed recognition of the non-mutated peptide as well, although with a lower functional avidity and multifunctional capacity. Thus, four of eleven identified mutated ligands elicited immune responses.

Taken together, conducted analyses provide profound insights into immunogenic features of naturally presented human leukocyte antigen (HLA) ligands and may contribute to a better understanding of immune-related recognition of tumors. Moreover, the high percentage of truly immunogenic mutated peptides amongst identified ligands render the combination of exome sequencing and mass spectrometry immunopeptidomics as an attractive approach for the efficient detection of clinically relevant neoepitopes.

Zusammenfassung

Die Wechselbeziehung zwischen Krebs und dem Immunsystem wird seit Jahrzehnten intensiv erforscht mit dem Ergebnis der Entwicklung vielversprechender neuartiger Strategien der Krebstherapie, zusammengefasst unter dem Begriff der Krebsimmuntherapie. Daraus hervorgehende breitere klinische Anwendungen, insbesondere Immun-Checkpoint-Blockade, aber auch adoptiver T-Zell-Transfer, zeigen vielversprechende Ergebnisse und fordern ein detailliertes Verständnis jener Bestimmungsgrößen, die an der immunvermittelten Tumorvernichtung beteiligt sind. In der vorgestellten Studie untersuchten wir das immunogene Potential humaner Leukozytenantigen (HLA)-gebundener Liganden, welche von primärem humanem Melanomgewebe extrahiert wurden. Die Peptidliganden wurden durch massenspektrometrische Analysen identifiziert. In einem ersten Ansatz wurde eine Selektion der detektierten Peptide abstammend von Tumor-assoziierten Antigenen für in-vitro Stimulationen von naiven T-Zellen gesunder Spender in einer HLA-diskrepanten Umgebung hergenommen. T-Zellen, welche zwei verschiedene Epitope erkannten, wurden expandiert und weitergehend charakterisiert mit dem Ziel der Isolation tumorspezifischer T-Zell-Rezeptoren (TZR). Allerdings ergab eine detaillierte Untersuchung der beobachteten Reaktivitäten eine unerwünschte Erkennung von Zielzellen, die das jeweilige Antigen nicht exprimieren. Diese Ergebnisse unterstreichen die Wichtigkeit einer sorgfältigen Charakterisierung potentieller Ziel- und TCR-Kandidaten als eine Grundlage rationaler Fortschritte in Richtung klinischer Translation.

In einem zweiten Ansatz wurden Exom-Sequenzierungen von Melanomtumoren fünf ausgewählter Patienten durchgeführt und als Bibliothek für die enthaltenen tumorspezifischen Mutationen verwendet. Die Suche innerhalb der analysierten Massenspektren ergab die Identifikation von elf natürlich präsentierten mutierten Peptidliganden. Acht dieser Peptide wurden im Tumor eines einzelnen Patienten, Mel15, detektiert und einer detaillierten Analyse patienteneigener T-Zell-Antworten gegen diese Zielstrukturen unterzogen. Zwei dieser Mutationen riefen Immunantworten von T-Zellen aus Blutproben von unterschiedlichen Zeitpunkten innerhalb einer Spanne von sechs Monaten hervor. Darüber hinaus wurden Reaktivitäten gegen eines dieser Neoepitope, SYTL4^{S363F}, auch in Tumor-infiltrierenden Lymphozyten beobachtet, welche aus einer zweiten Metastase des Patienten Mel15 expandiert wurden. Die Isolation Neoantigen-gerichteter T-Zell-Klone zeigte eine oligoklonale Immunantwort und bot damit Einblicke in die Komplexität der Tumor-gerichteten zytotoxischen Reaktivität. Zwei weitere Peptidliganden, welche massenspektrometrisch detektiert wurden, für die aber kein Auslösen einer Immunantwort im autologen Wirt gezeigt werden konnte, zeigten sich jedoch als immunogen bei in-vitro Stimulationen mit PBMC von gesunden HLA-identischen Spendern. Eine weiterführende funktionelle Charakterisierung von Immunantworten

gegen einen dieser Liganden, AKAP6^{M1482I}, zeigte eine zusätzliche Erkennung des nicht-mutierten Peptids, wenn auch mit einer niedrigeren funktionellen Avidität und multifunktionalen Kapazität. Demnach konnten bei vier der elf identifizierten mutierten Liganden Immunantworten detektiert werden.

Zusammenfassend zeigten die durchgeführten Analysen tiefgreifende Einblicke in die immunogenen Eigenschaften natürlich präsentierter HLA Liganden und können einen Beitrag zum besseren Verständnis immunvermittelter Tumorerkennung leisten. Zudem unterstützt der hohe prozentuale Anteil tatsächlich immunogener mutierter Peptide innerhalb der identifizierten Liganden die Kombination aus Exom-Sequenzierung und Massenspektrometrie-basierten Immunopeptidomics als einen attraktiven Ansatz für die effiziente Detektion klinisch relevanter Neoepitope.

1 Introduction

1.1 Cancer Immunotherapy

The Science Journal denoted Cancer Immunotherapy as the "breakthrough of the year 2013" delighted by the fact of unprecedented proceedings in tumor therapy (Couzin-Frankel, 2013). This was reasoned by the introduction of immune checkpoint inhibitors, so called immune modulators unleashing the immune system to recognize and subsequently eliminate cancer. Evidence for the coherence of cancer and the immune system traces far back into the 20th century, as the immunogenicity of tumors has been assessed using different mouse models (J. C. Rosenberg, Assimacoupoulos, Lober, Rosenberg, & Zimmermann, 1961; Shu & Rosenberg, 1985) or by ex vivo analysis of tumor material. Thereby, tumor composition was investigated including immune infiltrates (Belldegrun, Kasid, Uppenkamp, Topalian, & Rosenberg, 1989) and immune responses were analyzed by isolation of tumor-infiltrating lymphocytes (TIL) (Svennevig, Lovik, & Svaar, 1979), cultivation of tumor cells and co-culture experiments with lymphocytes (Strausser, Mazumder, Grimm, Lotze, & Rosenberg, 1981; Topalian, Solomon, & Rosenberg, 1989) only to name a few. Several tumors have been found to be immunogenic, i.e. in principle recognizable by the immune system, such as melanoma or sarcoma (Morton et al., 1970). Many of these findings have contributed to the development and clinical application of various immunotherapeutic strategies against cancer as shortly outlined in the following.

1.1.1 Antibody-based therapies

1.1.1.1 Checkpoint modulators

Immune checkpoint inhibitors, such as Programmed cell death (PD)-1 and Cytotoxic T-lymphocyte associated protein (CTLA) 4, lead to a systemic modulation of T-cell responses against target cells expressing respective ligands. Antibodies directed against different molecules of the immune checkpoint synapse are able to disrupt this signaling pathway by ligand binding leading to an enhanced activation of T cells after TCR activation inhibited throughout this mode of action. Since the clinical application of PD-1, PD-L1 and CTLA4 inhibitory antibodies, therapy options for several malignancies, preceded by malignant melanoma have changed dramatically. Ipilimumab in comparison to conventional chemotherapy has led to significant improvement of response rates, progression-free survival and overall survival (Hodi et al., 2010), even outperformed by anti-PD-1 antibodies (Hamid et al., 2013; Topalian et al., 2012). The combination of both therapy strategies showed an improved outcome compared to single agents, however with increased rates of immune-related side effects (Larkin et al., 2015; Postow et al., 2015). Immunomodulatory agents also in an

adjuvant treatment, as Ipilimumab therapy of patients undergone complete resection of metastatic lesions resulted in improved survival compared to placebo-treated patients (Eggermont et al., 2016). As a complementary approach to checkpoint inhibition, the direct co-activation of T cells by agonistic antibodies targeting members of the tumor necrosis factor (TNF) receptor superfamily, such as TNF receptor superfamily member 4 (TNFRSF4 = OX40) or member 9 (TNFRSF9 = 4-1BB), have shown promising results in mouse models (Kohrt et al., 2014; Melero et al., 1997) and first clinical application (Curti et al., 2013). In preclinical studies, synergistic effects were observed in combination approaches (Yu et al., 2016) providing rational for further investigation.

1.1.1.2 Antibodies targeting tumor antigens

In the course of target identification of immunogenic structures expressed on the tumor cells, several antibodies have been developed for the treatment of different malignant diseases. Depending on the selected antigen, tumors are targeted throughout different mechanisms, including but not limited to antibody-dependent cell-mediated cytotoxicity (ADCC), complement-dependent cytotoxicity (CDC) or alterations of cellular signaling pathways (Vacchelli et al., 2015). One prime example represents the group of antibodies directed against human epidermal growth factor receptor 2 (HER2) which are successfully used for therapy against breast cancer (Piccart-Gebhart et al., 2005; Slamon et al., 2001) and gastric cancer (Bang et al., 2010). As a second member of the HER protein family, epidermal growth factor receptor (EGFR), has been identified as a promising target for antibody-mediated therapy in several cancers including colorectal cancer (Jonker et al., 2007) and EGFR-positive non-small-cell lung cancer (NSCLC) (Pirker et al., 2009). Another class of antibodies targets differentiation antigens, which are expressed in in a very small defined subset of healthy cells, but also in tumors derived from this cell type. As a successful example, Rituximab has been developed, which is directed against the marker CD20 preferentially expressed by B cells. The antibody targets various B-cell malignancies including non-Hodgkin's lymphoma (Maloney et al., 1997), mantle-cell lymphoma (Foran et al., 2000), diffuse large-B-cell lymphoma (Coiffier et al., 2002) and B-lineage acute lymphoblastic leukemia (Maury et al., 2016). A further promising strategy lies within targeting antigens associated with the malignant phenotype of a tumor. As an example, the application of a monoclonal antibody targeting vascular endothelial growth factor (VEGF), Bevacizumab, resulted in improvement of therapy outcome in cervical cancer (Tewari et al., 2014), ovarian cancer (Perren et al., 2011) and triple-negative breast cancer (von Minckwitz et al., 2012).

1.1.2 Peptide and DC-based vaccinations

Vaccinations may be used as a prevention or active therapy of malignant diseases. The idea to recruit patient's own immune cells for specific tumor targeting has been pursued using different vaccination strategies, such as the application of defined peptides (Lawson et al., 2015; S. A. Rosenberg et al.,

1998; Scheibenbogen et al., 2000), peptide-loaded and antigen-expressing dendritic cells (DC) (Engell-Noerregaard, Hansen, Andersen, Thor Straten, & Svane, 2009) or tumor lysates (Nestle et al., 1998; Palmer et al., 2009). However, these studies presumably observed only limited therapy efficacy. Vaccination approaches represent a promising strategy especially against virally induced cancers, as these tumors express viral epitopes on their surface and can thereby be recognized by virus-specific T cells (Gudgeon, Taylor, Long, Haigh, & Rickinson, 2005; Ressing et al., 1995).

1.1.3 Adoptive T-cell transfer

1.1.3.1 Tumor-infiltrating lymphocytes

First approaches of cellular therapy in melanoma go back to the 1970s, when tumor-infiltrating lymphocytes (TIL) could be extracted and analyzed for reactivity against tumor cells. Re-infusion of ex vivo expanded TIL conferring durable tumor regression provided early evidence for the feasibility of lymphocyte-based immunotherapies (S. A. Rosenberg et al., 1988; S. A. Rosenberg, Spiess, & Lafreniere, 1986). In a larger study reporting on patients receiving ex-vivo expanded TIL, therapy efficacy was even observed in patient with progression on several previous treatments (Besser et al., 2013; S. A. Rosenberg et al., 2011). However, the composition of infused cell products is heterogeneous and largely unknown and several studies aim at the identification of determinants and cell subsets influencing therapy response (Chandran et al., 2015; Dudley et al., 2001; Radvanyi et al., 2012). One attempt to enrich for cell subsets responsible for tumor activity was pursued by the comparison of conventional TIL products with CD8-enriched TIL to focus on cytotoxic T cells, but no superior performance of selected TIL could be observed (Dudley et al., 2013).

1.1.3.2 CAR-engineered T cells

As a possibility to precisely define the specificity of infused cell products, receptors with known and well-characterized specificity can be used for genetic transfer and redirection of T cells. Chimeric antigen receptors (CAR) are synthetic constructs composed of a target-specific extracellular domain, mostly derived from the variable region of an antibody with desired specificity, and an intracellular signaling domain resembling the structure of TCR constant regions and consisting of different components for activation and co-stimulation (Barrett, Singh, Porter, Grupp, & June, 2014). If effector cells are genetically engineered with such constructs, target domains are recognized accordingly leading to a specific activation of engineered T cells and a cytotoxic cellular immune response. The most intensively investigated CAR construct targets CD19, a molecule expressed on the surface of B cells and various B-cell malignances, with clinical application of CD19-CAR transgenic T cells conferring impressive results (Grupp et al., 2013; Maude et al., 2014; Porter, Levine, Kalos, Bagg, & June, 2011). Within the last decades, CARs targeting various surface antigens have been

developed (Carpenito et al., 2009; Hudecek et al., 2013; Stancovski et al., 1993). As mainly surface molecules are targeted, the application of CAR-based therapies focuses on those proteins that are stably expressed on the tumor surface.

1.1.3.3 TCR-transgenic T cells

The genetic transfer of a T-cell receptor (TCR) with predefined specificity has been developed as a smart strategy for the redirection of T cells (Cole et al., 1995; Dembic et al., 1986). Since the first clinical application of T cells transgenic for a MART-1-specific TCR reported on encouraging anti-tumor efficacy (Morgan et al., 2006), different TCR with specificity for previously described tumor-associated antigens found the way towards translational therapy (Johnson et al., 2009; Parkhurst et al., 2011; Robbins et al., 2011; van den Berg et al., 2015). Due to the partially severe side effects observed in several studies, obtained results emphasize the high need of thorough characterization of potential TCR candidates, but also close monitoring in the course of such highly powerful therapy strategies.

1.1.4 Other approaches

With respect to the complexity of the interaction between tumor and the immune system, attempts to foster immune-mediated tumor recognition reach far beyond the engagement of cytotoxic T-cell reactivity. As one of many examples, regulatory T cells (Treg) have been identified as an important player in suppression of tumor-directed immune responses. Inhibition of Treg activity may be achieved by application of low-dose Cyclophosphamide (Hirschhorn-Cymerman et al., 2009) or immune modulatory antibodies (Sugiyama et al., 2013; Turk et al., 2004). As a further reasonable strategy, the investigations on oncolytic viruses have conferred promising preclinical results throughout the direct lysis of tumor cells and the induction of immunogenic cell death (Donnelly et al., 2013; Koks et al., 2015).

1.2 Strategies of epitope identification and TCR selection

Antigens presented on tumor cells and recognized by the immune system were firstly identified using tumor-derived deoxyribonucleic acid (DNA) libraries or autologous antibody screenings resulting in the identification of several tumor-associated antigens (Chen et al., 1997; van der Bruggen et al., 1991; Wolfel et al., 1987). However, these strategies were largely time-consuming and required sufficient patient material for analysis (Viatte, Alves, & Romero, 2006).

1.2.1 Reverse immunology

Other approaches, later summarized as reverse immunology, started with the prediction of potential candidates derived from genes with preferential tumor expression. Immunogenic peptides were then

identified experimentally in large screening approaches (Viatte et al., 2006). It has been shown that several malignancies, such as malignant melanoma, inherit a relatively high mutational load (Alexandrov et al., 2013) and that this mutational load correlates with response to immunotherapy in diverse diseases (Hugo et al., 2016; Rizvi, Hellmann, et al., 2015; Snyder et al., 2014; Van Allen et al., 2015). Especially melanoma has been investigated since a long time with regard to immunogenic mutations providing the hypothesis that even the majority of tumor-reactive T cells might be mutation-specific (Lennerz et al., 2005). In order to systematically investigate structures responsible for neoantigen-driven immune response, recent studies with the focus on mutation-bearing epitopes implemented a tumor-specific, whole genomic analysis into the reverse immunology approach (Matsushita et al., 2012). Target structures were identified by the combination of exome and transcriptome sequencing of patient samples with subsequent in-silico neoepitope prediction. As shown in Table 1, several studies led to the successful identification of immunogenic mutated peptide ligands, however only with a rather low yield of mutations actually eliciting an immune response in relation to all tested mutations (Cohen et al., 2015; Gros et al., 2016; Gubin et al., 2014; Kreiter et al., 2015; Linnemann et al., 2015; Lu et al., 2014; McGranahan et al., 2016; Robbins et al., 2013; Tran et al., 2015).

Table 1: Published investigations with implementation of reverse immunology for neoepitope identification.

Ref.	Workflow of mutation identification	Tumor origin	Classification of tumor-specific T cells	Evaluation of specificity	Immunogenic mutations / tested mutations
(Robbins et al., 2013)	Sequencing, MHC binding prediction	Cell lines 2098mel, 2369mel and 3309mel (from melanoma patients)	TILs	IFNγ release upon stimulation of TILs with minigene-transduced cell lines or peptide-pulsed cell lines	2098mel: 4/55 (7.27%) 2369mel: 3/53 (5.66%) 3309mel: 4/75 (5.33%)
(Lu et al., 2014)	Whole exome sequencing, construction of tandem minigene library	Melanoma patients 2359 and 2591	Expanded TILs from each patient without further specification	IFNγ release upon stimulation of TILs with autologous tumor, minigene-transduced cell lines or peptide-pulsed cell lines	Patient 2359: 1 / 71 (1.41%) Patient 2591: 1 / 217 (0.46%)
(Gubin et al., 2014)	DNA capture sequencing, MHC-I binding prediction + filtering for high processing probability by immune proteasome + higher binding prediction of mutated ligand compared to wt ligand	Murine tumor d42m1-T3	CD8+ TIL	Multimer; IFNγ and TNFα release upon coculture of T cells with peptide-pulsed splenocytes; improved OS after vaccination of tumor-bearing mice with mutated ligands; combination with checkpoint blockade (altered functional phenotype)	2 / 66 (3.03%)

(Linnemann et al., 2015)	Whole-exome-sequencing and RNA-sequencing	Melanoma patients NKIRTIL018, NKIRTIL034 and NKIRTIL045	CD4+ TILs (94% CD4+ after conventional REP)	IFNγ release upon stimulation of TILs with peptide-pulsed B cells, IFNγ secretion of clones upon coculture with autologous tumor	NKIRTIL018: 3/ 188 (1.60%) NKIRTIL034: 1 / 173 (0.58%) NKIRTIL045: 0 / 99 (0%) NKIRTIL027: 1 / 582 (0.17%)
(Kreiter et al., 2015)	Exome sequencing, bioinformatic prioritization + MHC-I binding prediction	Murine tumors B16F10, CT26, 4T1	Predominantly (~80%) CD4+ mediated responses	B16F10: in-vivo tumor control mediated by a single mutated MHC-II restricted epitope; CT26: vaccination with RNA coding for 5 mutated epitopes leads to tumor rejection in vivo	~ 30%, taking high MHC I binding into account
(Cohen et al., 2015)	Whole-exome and RNA sequencing (RNA-seq)	melanoma patients: 3713, 3879, 3466, 3919, 3703, 3903, 3702, 3926	Fresh tumor digest, PBL, TIL	Multimer staining, peptide-pulsed T2, fresh tumor digests or melanoma lines from 4 patients (not further specified)	3713: 3 / 48 (6.25%) 3879: 1 / 78 (1.28%) 3466: 3 / 32 (9.38%) 3919: 1 / 16 (6.25%) 3703: 1 / 75 (1.33%) 3903 0 /38 3702 0 / 28 3926: 0 / 53
(Tran et al., 2015)	Whole exome or whole genome sequencing	Human GI cancer; construction of 264 putative tandem minigene constructs for first patient (4007)	Specific reacitivities of CD8^{+} TIL (assessed by FACS)	CD137 expression and IFNγ release upon stimulation with tandem-minigene transduced autologous DC; no primary tumor material tested	21 / 1452 (1.45%)
(Gros et al., 2016)	Tumor exome and transcriptome analysis	melanoma patients NCI-3998, NCI-3784, NCI-3903, NCI-3713, NCI-3926	PBMC	CD137 expression and IFNg release upon stimulation with tandem-minigene transduced autologous DC and cell lines (COS7) or peptide pulsed targets; reactivity against autologous tumor (digested + cultured, mutations confirmed)	NCI-3998: 3 / 115 (2.60%), NCI-3784: 3 /140 (2.14%), NCI-3903: 1 / 308 (0.32%), NCI-3926 0 /128 NCI-3713 6 / 7 minimal epitopes (reactivity for those epitopes already shown before acc. to personal communications)
(McGranahan et al., 2016)	Whole exome sequencing, MHC-I binding prediction (<500 nM)	NSCLC; patients with analysis of immune repsonse: L011, L012	TIL	pMHC (mutated vs. WT epitope), further flow cytometric characterization based on pMHC staining combined with CTLA4, PD-1, Granzyme B, LAG3 and other	Whole exome sequencing, MHC-I binding prediction (<500 nM)

1.2.2 Mass-spectrometry based immunopeptidomics

An alternative to the reverse immunology approach provides the direct determination of human leukocyte antigen (HLA)-bound peptides by mass spectrometry (MS). Ligands presented on the cell surface are for example obtained by immune precipitation of peptide-HLA complexes within cell lysates using an anti-HLA antibody, followed by elution of peptides and analysis of peptide composition in a high-resolution MS instrument (Caron et al., 2015). Since its first application (Hunt et al., 1992), the method of MS-based immmunopeptidomics has been used in several approaches for the investigation of naturally presented HLA ligands on murine and human tumor cells (Bassani-Sternberg, Pletscher-Frankild, Jensen, & Mann, 2015; Berlin et al., 2015; Walz et al., 2015). In addition, screening of selected ligands for T-cell recognition led to the successful isolation of specific T cells with high potential for clinical application (Hombrink et al., 2013; Klar et al., 2014).

1.2.3 Different TCR repertoires as sources for cancer-specific T cells

Some of the TCR described in section 1.1.3.3 have been isolated from patient material. In addition, healthy donor-derived T cells may serve as an alternative pool for the isolation of TCR directed against tumor antigens (Visseren et al., 1995), especially for those patients lacking endogenous immune responses against immunogenic tumor antigens (Overwijk, 2005). Given the nature of thymus selection, most of tumor-associated antigens are presented to the maturating T cells leading to the eradication of potential auto-reactive T cells, thereby eventually eliminating the vast majority of effector cells capable of tumor recognition (D'Orsogna, Roelen, Doxiadis, & Claas, 2012). Thus, the HLA- or major histocompatibility complex (MHC)-mismatched repertoire provides a meaningful source for peptide-specific T cells with high functional avidity (Bellantuono et al., 2002; Obst, Munz, Stevanovic, & Rammensee, 1998; Sadovnikova, Jopling, Soo, & Stauss, 1998; Schuster et al., 2007). In order to facilitate stimulation in a setting with only one single HLA mismatch, in-vitro transcribed ribonucleic acid (RNA) encoding respective HLA molecule may be electroporated into autologous target cells, thereby reducing the risk of unspecific allogeneic stimulation by other unmatched HLA alleles (Klar et al., 2014; Kumari et al., 2014; Wilde et al., 2012; Wilde et al., 2009). In addition, T cells with undesired HLA-alloreactivity can be removed by activation-induced depletion (Wehler et al., 2007). However, optimal stimulation conditions and properties for universal selection of individual cancer-specific T cells has not been determined yet, demanding a broad exploitation of tumor-directed immune responses across different TCR repertoires.

Aim of this study

Malignant Melanoma is known as an aggressive, but highly immunogenic malignancy. Current therapy options, especially regarding immune checkpoint inhibitors, show encouraging efficacy, but not all patients respond to checkpoint blockade. Besides, determinants of response are still not completely understood. We sought to investigate the cancer-related immunopeptidome for the identification of naturally presented peptide candidates and investigation of their immunogenic potential.

In cooperation with the Max-Planck Institute of Biochemistry, the immunopeptidomes of tumors derived from 25 melanoma patients were analyzed resulting in the detection of more than 95 000 naturally presented HLA ligands. In a first approach taking five of these immunopeptidomes into consideration, a workflow should be established for the rational selection of peptides with preferential tumor restriction within the peptide-pool of unaltered ligands as a model to identify suitable target antigens. Promising peptide candidates should be used for in-vitro stimulations in the HLA-mismatched setting. In case of the detection of peptide-specific responses, T cells and respective T-cell receptor (TCR) should be isolated and characterized with regard to its potential for future clinical applications within an adoptive T-cell transfer.

In a second approach, analyzed immunopeptidomes from five different patients were mined for the presence of mutation-bearing peptides as a proof of principle. In case of detection of such neoepitopes, immunogenicity of these ligands should be assessed within the autologous host as well as in HLA-matched healthy donor-derived T cells. In case of observation of specific immune responses, deeper functional analysis should follow, such as assessment of cross-reactivity against the non-mutated ligand, functional avidity and recognition of endogenously processed epitopes. Composition of immune responses, such as clonality and occurrence of T-cell clones within different compartments, should be investigated for a better understanding of neoantigen-driven immunoreactivity and identification of novel individualized biomarkers.

Altogether, these studies should give deeper knowledge of tumor-specific immunoreactivity with regard to a potential transfer into a clinical setting, such as individualized vaccination approaches or adoptive cell therapy.

2 Material and Methods

2.1 Material

2.1.1 Technical Equipment

Device	Company
Analytical balance SI-64	Denver Instrument / Sartorius AG, Göttingen, Germany
APOLLO Liquid nitrogen vacuum container	Cryotherm, Kirchen/Sieg, Germany
Autoclave Systec V95	Systec GmbH, Linden, Germany
BD™ LSR II	BD Biosciences, Franklin Lakes, USA
BioDocAnalyze Gel documentation system	Biometra GmbH, Göttingen, Germany
Biometra Mitsubishi P95 Printer	Biometra GmbH, Göttingen, Germany
BIOSAFE MD sample container	Cryotherm, Kirchen/Sieg, Germany
Centrifuge 5417R	Eppendorf AG, Hamburg, Germany
Centrifuge 5417R	Eppendorf AG, Hamburg, Germany
Centrifuge 5810R	Eppendorf AG, Hamburg, Germany
Centrifuge with vortex 7-0040	neoLab Migge GmbH, Heidelberg, Germany
Centrifuge with vortex 7-0040	neoLab Migge GmbH, Heidelberg, Germany
Compact M Horizontal Gel Electrophoresis Apparatus	Biometra GmbH, Göttingen, Germany
Digital microtiter shaker MTS 2/4	IKA®-Werke GmbH & CO. KG, Staufen, Germay
Dynal MPC™-L Magnetic Particle Concentrator	Invitrogen Dynal AS, Oslo, Norway
DynaMag™-2 Magnet	Invitrogen Dynal AS, Oslo, Norway
EcoVac Vacuum Pump	schuett-biotec GmbH, Göttingen, Germany
Elelctrophoresis Apparatus i-Mupid	Cosmo Bio Co., LTD, Tokyo, Japan
FACSAria III	BD Biosciences, Franklin Lakes, USA
Fume cupboard 2-453-DXNN	Köttermann GmbH & Co KG, Uetze/Hänigsen, Germany
Gene Pulser Xcell™ Electroporation System	Bio-Rad Laboratories GmbH, München, Germany
Growth chamber WTC	BINDER GmbH, Tuttlingen, Germany
HERAfreeze™ BASIC -86°C Freezer	Thermo Fisher scientific, Waltham, USA
ImmunoSpot S6 Ultra-V Analyzer	CTL - Europe GmbH, Bonn, Germany
Incubator BBD 6220	Heraeus Holding GmbH, Hanau, Germany
Incubator CB 150	BINDER GmbH, Tuttlingen, Germany
Innova 4000 Incubator Shaker	New Brunswick Scientific, Edison, USA
Irradiation chamber Cs137 Type Ob 29/902-1	Buchler GmbH, Braunschweig, Germany
Laminar flow HERAsafe KS 15	Heraeus Holding GmbH, Hanau, Germany
LS6000 sample container	tec-lab GmbH, Taunusstein, Germany

MACS MultiStand	Miltenyi Biotec GmbH, Bergisch Gladbach, Germany
MACSmix Tube Rotator	Miltenyi Biotec GmbH, Bergisch Gladbach, Germany
Magnetic stirrer RH basic 2	IKA®-Werke GmbH & CO. KG, Staufen, Germay
Microscope Axiovert 40 C	Carl Zeiss AG, Feldbach, Schweiz
MidiMACS Separator	Miltenyi Biotec GmbH, Bergisch Gladbach, Germany
Minishaker MS2	IKA®-Werke GmbH & CO. KG, Staufen, Germay
Multichannel pipets	Eppendorf AG, Hamburg, Germany
Multifuge 3 S-R	Heraeus Holding GmbH, Hanau, Germany
Multifuge 3s	Heraeus Holding GmbH, Hanau, Germany
NALGENE Cryo 1°C Freezing Container	Thermo Fisher scientific, Waltham, USA
NanoDrop Spectrophotometer ND1000	PeqLab / VWR International GmbH, Darmstadt, Germany
Neubauer improved counting chamber	Karl Hecht GmbH & Co KG, Sondheim/Röhn, Deutschland
OctoMACS Separator	Miltenyi Biotec GmbH, Bergisch Gladbach, Germany
Pipets	Eppendorf AG, Hamburg, Germany
Pipette controller	INTEGRA Biosciences GmbH, Biebertal, Germany
Precision balance 440	KERN & SOHN GmbH, Balingen, Germany
Premium -20°C Freezer	Liebherr-International Deutschland GmbH, Biberach an der Riß, Germany
Refrigerator Profi line	Liebherr-International Deutschland GmbH, Biberach an der Riß, Germany
Rotina 420R	Andreas Hettich GmbH & Co.KG, Tuttlingen, Germany
StepOnePlus™ Real-Time PCR System	Fisher Scientific GmbH, Schwerte, Germany
SunriseTM absorbance reader	Tecan Group Ltd., Männedorf, Switzerland
TGradient	Biometra GmbH, Göttingen, Germany
Thermomixer Compact	Eppendorf AG, Hamburg, Germany
Titramax 1000 shaker	Heidolph Instruments GmbH & Co.KG, Schwabach, Germany
TProfessional Thermocycler	Biometra GmbH, Göttingen, Germany
UV Transilluminator	Biometra GmbH, Göttingen, Germany
Vortex Mixer 7-2020	neoLab Migge GmbH, Heidelberg, Germany
Vortexer Reax top	Heidolph Instruments GmbH & Co.KG, Schwabach, Germany
Vortex-Genie 2	Scientific Industries, Inc., New York, USA
VWR Power Source 300V	VWR International GmbH, Darmstadt, Germany
Waterbath	Memmert GmbH + Co. KG, Schwabach, Germany
Ziegra Ice machine	ZIEGRA Eismaschinen GmbH, Isernhagen, Germany

2.1.2 Consumables

Consumable	Company
neoScrew Micro tubes 1.5ml brown	neoLab Migge GmbH, Heidelberg, Germany
Cell culture flask (T25, T75, T175)	Greiner Bio-One GmbH, Frickenhausen, Germany
Cell scraper	TPP Techno Plastic Products AG, Trasadingen, Schweiz

CyroPure tubes	Sarstedt AG & Co., Nümbrecht, Germany
EIA/RIA plates	Corning, New York, USA
Falcons (15ml, 50 ml)	BD Biosciences, Franklin Lakes, USA
Filcon 30 µm filter	Syntec International, Dublin, Ireland
Gene Pulser® Electroporation Cuvettes 0.4 cm gap	Bio-Rad Laboratories GmbH, München, Germany
Gloves Dermatril P	KCL GmbH, Eichenzell, Germany
LD/LS columns	Miltenyi Biotec GmbH, Bergisch Gladbach, Germany
MAHAS4510 MultiScreen-HA 0.45 µm ELIspot plate	Merck KGaA, Darmstadt, Germany
Microtubes (1.2 ml)	Alpha Laboratories, Hampshire, UK
Nitrile gloves	Abena A/Sm Aabenraa, Denmark
Non-tissue culture treated plates (6-/24-well)	BD Biosciences, Franklin Lakes, USA
Nunc™ Cell culture flask (80cm2)	Thermo Fisher scientific, Waltham, USA
Parafilm M® laboratory film	Pechiney Plastic Packaging, Chicago, USA
PCR reaction tubes (0.5 ml)	VWR International GmbH, Darmstadt, Germany
Pipet tips (10/20/300/1250 µl)	Sarstedt AG & Co., Nümbrecht, Germany
QIAshredder Homogenizer	QIAGEN GmbH, Hilden, Germany
MicroAmp Fast Optical 96well Reaction Plate with Barcode	Thermo Fisher scientific, Waltham, USA
qPCR seal	4titude Ltd., Surrey, UK
Reaction tubes (1.5, 2 ml)	Sarstedt AG & Co., Nümbrecht, Germany
Screw Cap Micro Tubes	Sarstedt AG & Co., Nümbrecht, Germany
Sealing foil (ELISA)	Alpha Laboratories, Hampshire, UK
Serological Pipets (5 ml, 10 ml, 25 ml, 50 ml)	Sarstedt AG & Co., Nümbrecht, Germany
Stericup/Steritop 0.22 µm filters	Merck KGaA, Darmstadt, Germany
Syringe filters (0.2, 0.45 µm)	TPP Techno Plastic Products AG, Trasadingen, Schweiz
Tissue culture-treated plates (48-well)	BD Biosciences, Franklin Lakes, USA
Tissue culture-treated plates (6-/12-/24-well, round/flat bottom 96-well)	TPP Techno Plastic Products AG, Trasadingen, Schweiz

2.1.3 Primary human material

Written informed consent of healthy volunteers and all involved patients was obtained according to the local review board of the Faculty of Medicine, TU München, and principles of the Helsinki declaration. Information of analyzed patients is listed in 6.1. For those patients with additional exome sequencing, further relevant aspects and clinical courses are depicted in 6.2 and 6.3, respectively. HLA types of healthy donors are listed in Table 2.

Table 2: HLA alleles of healthy donors

Healthy donor	HLA-A*	HLA-B*
HD1	02; 03	07; 50
HD2	01; 31	16; 41
HD3	24; 68	14; 15
HD4	02:05; 24	51; 58
HD5	03; 24	07; -
HD6	02; 03	35; 51
HD7	11; 32	35; 44
HD8	02; 03	07; 14:01
HD9	02; 03	*unknown*
HD10	03:01; 29:02	27:05; 44:03
HD11	01; 31	08; 51
HD12	02; 03	15; 40
HD13	02:01; 26:01	44:02; 56:01
HD14	02:01	07:02; 15:01

2.1.4 Cell lines

Table 3: Cell lines

Cell lines	Characteristics	Source/Origin
293T	Human embryonic kidney cell line; used as packaging cell line for production of retroviral particles	ATCC, Manassas, USA
888mel	Human melanoma cell line	NIH, Bethesda, USA
888mel-A1	888mel, transduced with HLA-A*01:01-P2A-eGFP	[1]
888mel-B7	888mel, transduced with HLA-B*07:02-P2A-eGFP	[1]
C1R	Human plasma leukemia cell line	Stefan Stevanovic, Tübingen
C1R-A1	C1R, transduced with HLA-A*01:01-P2A-eGFP	[1]
C1R-B7	C1R, transduced with HLA-B*07:02-P2A-eGFP	[1]
K562	Human lymphoblast cell line (CML)	ATCC, Manassas, USA
K562-A1	K562, transduced with HLA-A*01:01-P2A-eGFP	[1]
K562-B7	K562, transduced with HLA-B*07:02-P2A-eGFP	[1]
ML2	Human acute myelomonocytic leukemia	The Cabri consortium
ML2-B7	ML2, transduced with HLA-B*07:02-P2A-eGFP	[1]
MOLT4	Human T-lymphoblastic leukemia	CLS, Eppelheim, Germany
MOLT4-A1	K562, transduced with HLA-A*01:01-P2A-eGFP	[1]
MOLT4-B7	K562, transduced with HLA-B*07:02-P2A-eGFP	[1]
RD114	HEK 293-based packaging cell line	BioVec Pharma Inc., Québec, Canada
T2	T-cell leukemia/B-cell hybridoma; TAP-deficient	ATCC, Manassas, USA

[1] These cell lines were retrovirally transduced and cloned jointly by members of Prof. Krackhardt's group.

T2-A1	T2, transduced with HLA-A*01:01-P2A-eGFP	[1]
T2-A3	T2, transduced with HLA-A*03:01-P2A-eGFP	[1]
T2-B7	T2, transduced with HLA-B*07:02-P2A-eGFP	[1]
T2-B27	T2, transduced with HLA-B*27:05-P2A-dsRed	[1]

Table 4: Lymphoblastoid cell lines

LCL	HLA-A*	HLA-B*	IHW[2] number
LCL1	03:01:01	27:05:02	IHW09005
LCL2	02:01:01; 03:01:01	35:02:01 ; B*38:01:01	IHW09216
LCL HD2	01; 31	16; 41	-
LCL HD14	02:01	07:02; 15:01	-

2.1.5 Reagents and chemicals

Reagent/Chemical	Company
1-Bromo-3-chloropropane	Sigma-Aldrich Chemie GmbH, Taufkirchen, Germany
6x loading buffer	Thermo Fisher scientific, Waltham, USA
3-Amino-9-ethylcarbazole (AEC) tablets	Sigma-Aldrich Chemie GmbH, Taufkirchen, Germany
7-Aminoactinomycin D (7-AAD)	Sigma-Aldrich Chemie GmbH, Taufkirchen, Germany
AccuCheck COUNTING BEADS	Thermo Fisher scientific, Waltham, USA
Acetic acid ($C_2H_4O_2$)	Merck KGaA, Darmstadt, Germany
Ampicillin	Sigma-Aldrich Chemie GmbH, Taufkirchen, Germany
Agarose NEEO Ultra-Qualität	Carl Roth GmbH + Co. KG, Karlsruhe, Germany
AIM V™	Thermo Fisher scientific, Waltham, USA
Anti-APC microbeads	Miltenyi Biotec GmbH, Bergisch Gladbach, Germany
Bovine Serum Albumine (BSA)	Sigma-Aldrich Chemie GmbH, Taufkirchen, Germany
CD45RO microbeads	Miltenyi Biotec GmbH, Bergisch Gladbach, Germany
CD57 microbeads	Miltenyi Biotec GmbH, Bergisch Gladbach, Germany
Cyclosporin A	Klinikum rechts der Isar der Technischen Universität, München, Germany
DEPC H_2O	Thermo Fisher scientific, Waltham, USA
Dulbecco's Modified Eagle Medium (DMEM)	Thermo Fisher scientific, Waltham, USA
Dimethylformamide (DMF)	Sigma-Aldrich Chemie GmbH, Taufkirchen, Germany
Dimethyl sulfoxide (DMSO)	Sigma-Aldrich Chemie GmbH, Taufkirchen, Germany
DNA ladder (100 bp, 1 kbp)	PeqLab / VWR International GmbH, Darmstadt, Germany
dNTP (2 /10 mM each)	Thermo Fisher scientific, Waltham, USA
Ethanol	Merck KGaA, Darmstadt, Germany
Ethidium bromide solution	Sigma-Aldrich Chemie GmbH, Taufkirchen, Germany
Fetal calf serum (FCS)	Thermo Fisher scientific, Waltham, USA
Ficoll	Biochrom GmbH, Berlin, Germany

[2] International HLA Workshop

Gentamycin	Biochrom GmbH, Berlin, Germany
Hydrogen Peroxide Solution	Sigma-Aldrich Chemie GmbH, Taufkirchen, Germany
HEPES	Thermo Fisher scientific, Waltham, USA
Human serum (HS)	Technische Universität München, Germany
Ionomycin	Merck KGaA, Darmstadt, Germany
Isopropanol	Merck KGaA, Darmstadt, Germany
L-Glutamine	Thermo Fisher scientific, Waltham, USA
Milk powder	Sigma-Aldrich Chemie GmbH, Taufkirchen, Germany
Non-essential amio acids (NEAA)	Thermo Fisher scientific, Waltham, USA
Opti-MEM® I	Thermo Fisher scientific, Waltham, USA
Paraformaldehyde (PFA)	Sigma-Aldrich Chemie GmbH, Taufkirchen, Germany
PBS (Gibco)	Thermo Fisher scientific, Waltham, USA
PBS powder without Ca^{2+}, Mg^{2+}	Merck KGaA, Darmstadt, Germany
Penicilline/Streptomycin	Thermo Fisher scientific, Waltham, USA
Phorbol 12-myristate 13-acetate (PMA)	Sigma-Aldrich Chemie GmbH, Taufkirchen, Germany
Propidium Iodide (PI)	Sigma-Aldrich Chemie GmbH, Taufkirchen, Germany
Prostaglandine E_2 (PGE_2)	Sigma-Aldrich Chemie GmbH, Taufkirchen, Germany
Protamine Sulfate	MP Biomedicals GmbH, Illkirch, France
RetroNectin	Takara Bio Inc., Japan
RPMI-1640	Thermo Fisher scientific, Waltham, USA
S.O.C. medium	New England Biolabs Inc., Ipswich, USA
Sodium acetate ($C_2H_3NaO_2$)	Merck KGaA, Darmstadt, Germany
Sodium azide (NaN_3)	Merck KGaA, Darmstadt, Germany
Sodium carbonate (Na_2CO_3)	Merck KGaA, Darmstadt, Germany
Sodium hydrogen carbonate ($NaHCO_3$)	Merck KGaA, Darmstadt, Germany
Sodium Pyruvate	Thermo Fisher scientific, Waltham, USA
Streptavidin-HRP	Mabtech AB, Nacka Strand, Sweden
Sulfuric acid	Carl Roth GmbH + Co. KG, Karlsruhe, Germany
T4 ligase	Thermo Fisher scientific, Waltham, USA
TransIT transfection reagent	Mirus Bio LLC, Madison, USA
TRIzol reagent	Thermo Fisher scientific, Waltham, USA
Trypane blue	Sigma-Aldrich Chemie GmbH, Taufkirchen, Germany
Trypsine/EDTA	Thermo Fisher scientific, Waltham, USA
Tween 20	Sigma-Aldrich Chemie GmbH, Taufkirchen, Germany
VLE-RPMI 1640	Biochrom GmbH, Berlin, Germany
Yeast tRNA	Thermo Fisher scientific, Waltham, USA

2.1.6   Kits

Table 5: Kits

Kit	Purpose	Company
AffinityScript Multiple Temperature cDNA Synthesis Kit	Reverse transcription of mRNA into cDNA	Agilent Technologies, Santa Clara, USA

Ambion™ Poly(A) Tailing Kit	Polyadenylation of in vitro transcribed RNA	Thermo Fisher scientific, Waltham, USA
BD OptEIA™ Human IL-2 ELISA Set	Cytokine measurement in cell culture supernatants	BD Biosciences, Franklin Lakes, USA
BD OptEIA™ Human IFN-γ ELISA Set	Cytokine measurement in cell culture supernatants	BD Biosciences, Franklin Lakes, USA
BD OptEIA™ TMB Substrate Reagent Set	Cytokine measurement in cell culture supernatants	BD Biosciences, Franklin Lakes, USA
DNA blood and tissue kit	gDNA isolation from tumor Mel15	QIAGEN GmbH, Hilden, Germany
Dynabeads® Untouched™ Human CD8 T Cells Kit	CD8+ T-cell isolation from PBMC	Thermo Fisher scientific, Waltham, USA
eBioscience™ Intracellular Fixation & Permeabilization Buffer Set	Intracellular cytokine staining	Thermo Fisher scientific, Waltham, USA
HotStarTaq Plus Master Mix Kit	TCR repertoire PCR	QIAGEN GmbH, Hilden, Germany
Human total RNA Master Panel II	RNA expression of TAA in healthy tissues	Clontech Laboratories, Inc., Mountain View, USA
JETSTAR™ 2.0 Plasmid Purification Kit	Large-scale purification of DNA plasmids coding for HLA and minigene constructs; Miniprep	Genomed, Löhne, Germany
KAPA PROBE FAST qPCR Kit	Real-time PCR with dual-labeled hybridization probes	PeqLab / VWR International GmbH, Darmstadt, Germany
KAPA SYBR® Fast qPCR Master Mix (2X) Universal	Real-time PCR (antigen expression)	PeqLab / VWR International GmbH, Darmstadt, Germany
KOD Hot Start Polymerase Kit	PCR	Merck KGaA, Darmstadt, Germany
mMESSAGE mMACHINE® T7 Transcription Kit	In vitro transcription of HLA constructs	Thermo fisher scientific, Waltham, USA
NEB® 5-alpha Competent E. coli	Transformation of vector products	New England BioLabs Inc., Frankfurt am Main, Germany
NucleoBond® Xtra Maxi EF	Endotoxin-free plasmid purification of TCR constructs	MACHEREY-NAGEL GmbH & Co. KG, Düren, Germany
Nucleospin Gel and PCR Cleanup kit	Purification of DNA from Gel and PCR mixtures	MACHEREY-NAGEL GmbH & Co. KG, Düren, Germany
RNeasy Mini Kit	RNA extraction (tumor Mel15)	QIAGEN GmbH, Hilden, Germany
Venor GeM mycoplasma detection kit	Testing of cell lines for absence of mycoplasma infection	Minerva Biolabs GmbH, Berlin, Germany

2.1.7 Media and buffers

Table 6: Composition of buffers and solutions

Buffer/solution	Application	Ingredients
Permeabilization buffer (1x Perm Buffer)	Intracellular cytokine staining	H_2O + 10% Permeabilization Buffer (10x, contained in eBioscience™ Intracellular Fixation & Permeabilization Buffer Set)
TAE buffer (1x)	Gel electrophoresis	H_2O + 10% Invitrogen TAE buffer (10x stock solution, Thermo Fisher scientific)
Acetate buffer	ELIspot	46.9 ml H_2O + 4.6 ml $C_2H_4O_2$ (0.2M) + 11 ml $C_2H_3NaO_2$ (0.2M)
AEC buffer	ELIspot	500 µl AEC solution + 9.5 ml Acetate buffer, filtered (0.45 µm)
AEC solution	ELIspot	AEC tablet dissolved in 2.5 ml DMF
Blocking solution	ELISA	PBS + 1% (w/v) milk powder
ΔFCS	Multiple applications	FCS, inactivated for 20 min at 58°C
ΔHS	Multiple applications	HS, inactivated for 20 min at 58°C
ELISA coating buffer	ELISA	H_2O + 0.1 mol/l $NaHCO_3$, 0.03 mol/l Na_2CO_3, pH = 9.5
FACS buffer	Stainings for flow cytometry	PBS + 1% ΔFCS
FACS-azide buffer	Intracellular cytokine staining	PBS + 1% ΔFCS + 2 mM EDTA + 0.09% NaN_3
HRP-complex solution	ELIspot	10ml PBS + 50 µl von Strp. / HRP + 50 µl ΔFCS
Isolation buffer	T-cell isolation	PBS + 2% ΔHS, 2 mM EDTA
Multimer staining buffer	Tetramer and Pentamer staining	PBS + 50% ΔFCS, 2 mM EDTA
Washing buffer	ELIspot, ELISA	PBS + 0.05% v/v Tween 20

Table 7: Composition of media.

Medium	Ingredients
AIM-V	AIM-V (Thermo Fisher scientific), no supplements
cDMEM	DMEM supplemented with 10% ΔFCS, 10 mM non-essential amino acids, 1 mM sodium pyruvate, 2 mM L-Glutamine, 100 U/ml Penicillin and 100 µg/ml Streptomycin
cRPMI	RPMI supplemented with 10% ΔFCS, 10 mM non-essential amino acids, 1 mM sodium pyruvate, 2 mM L-Glutamine, 100 U/ml Penicillin and 100 µg/ml Streptomycin
DC Medium	VLE RPMI supplemented with 1,5% ΔHS
Freezing medium	90% ΔFCS + 10% DMSO
LB medium	10 g Bacto-Tryptone, 5 g Bacto-Yeast extract and 10 g NaCl dissolved in 1l H_2O → autoclaved after preparation
OptiMEM	OptiMEM (Thermo Fisher scientific), no supplements
T-cell medium (TCM)	RPMI 1640 supplemented with 5% v/v ΔFCS, 5% ΔHS, 10 mM non-

	essential amino acids, 1 mM sodium pyruvate, 2 mM L-Glutamine, 100 U/ml Penicillin, 100 µg/ml Streptomycin, 10 mM HEPES buffer and 16.6 µg/ml Gentamycin
Tumor digestion medium	RPMI supplemented with 0.1 mg/ml DNase type I, 100 µg/ml Hyaluronidase, 1 mg/ml Collagenase type IV, 100 U/ml Penicillin, 100 µg/ml Streptomycin and 10 µg/ml Gentamycin

2.1.8 Recombinant cytokines and TLR ligands

Table 8: Cytokines and TLR ligands

Substance	Company
CL075	InvivoGen, San Diego, USA
OKT-3	Kindly provided by Elisabeth Kremmer, Helmholtz Zentrum München
Poly-I:C	InvivoGen, San Diego, USA
rh GM-CSF	PeproTech, London, UK
rh IFN-g	PeproTech, London, UK
rh IL-15	PeproTech, London, UK
rh IL-1b	PeproTech, London, UK
rh IL-21	PeproTech, London, UK
rh IL-4	PeproTech, London, UK
rh IL-7	PeproTech, London, UK
rh TNF-a	PeproTech, London, UK

2.1.9 Peptides

Table 9: Peptides used for analysis of responses against tumor-associated antigens

Peptide	Sequence	Company
$ATAD2_1$	KPPISKKKAVL	Max-Planck-Institute for Biochemistry, Martinsried, Germany
$ATAD2_2$	SVYENGLSQK	Max-Planck-Institute for Biochemistry, Martinsried, Germany
$CASC5_1$	HVSKERIQQSL	Max-Planck-Institute for Biochemistry, Martinsried, Germany
$CCDC110_1$	QTDPDVHRNGKY	Max-Planck-Institute for Biochemistry, Martinsried, Germany
$CDK4_1$	KARDPHSGHFVAL	Max-Planck-Institute for Biochemistry, Martinsried, Germany
$CTAG1A_1$	TPMEAELARRSL	Max-Planck-Institute for Biochemistry, Martinsried, Germany
DCT_1	TSDQLGYSY	Max-Planck-Institute for Biochemistry, Martinsried, Germany
DCT_2	GTYEGLLRR	Max-Planck-Institute for Biochemistry, Martinsried, Germany
$LY6K_1$	LPRVWTDANL	Max-Planck-Institute for Biochemistry, Martinsried, Germany
$LY6K_2$	KPEEKRFLL	Max-Planck-Institute for Biochemistry, Martinsried, Germany
MPO_5	NPRWDGERL	IBA GmbH, Göttingen, Germany
$PAX3_1$	SMDPVTGYQY	Max-Planck-Institute for Biochemistry, Martinsried, Germany

		IBA GmbH, Göttingen, Germany
PMEL$_1$	ALNFPGSQK	Max-Planck-Institute for Biochemistry, Martinsried, Germany
PMEL$_2$	QLRTKAWNR	Max-Planck-Institute for Biochemistry, Martinsried, Germany
PRAME$_1$	SPRRLVELAGQSL	Max-Planck-Institute for Biochemistry, Martinsried, Germany
PRAME$_2$	SPSVSQLSVL	Max-Planck-Institute for Biochemistry, Martinsried, Germany
		IBA GmbH, Göttingen, Germany
PRAME$_{2-A1}$	APSVSQLSVL	Genscript Biotech Corporation, Piscataway, USA
PRAME$_{2-A10}$	SPSVSQLSVA	Genscript Biotech Corporation, Piscataway, USA
PRAME$_{2-A2}$	SASVSQLSVL	Genscript Biotech Corporation, Piscataway, USA
PRAME$_{2-A3}$	SPAVSQLSVL	Genscript Biotech Corporation, Piscataway, USA
PRAME$_{2-A4}$	SPSASQLSVL	Genscript Biotech Corporation, Piscataway, USA
PRAME$_{2-A5}$	SPSVAQLSVL	Genscript Biotech Corporation, Piscataway, USA
PRAME$_{2-A6}$	SPSVSALSVL	Genscript Biotech Corporation, Piscataway, USA
PRAME$_{2-A7}$	SPSVSQASVL	Genscript Biotech Corporation, Piscataway, USA
PRAME$_{2-A8}$	SPSVSQLAVL	Genscript Biotech Corporation, Piscataway, USA
PRAME$_{2-A9}$	SPSVSQLSAL	Genscript Biotech Corporation, Piscataway, USA
PRAME$_{2-T1}$	TPSVSQLSVL	Genscript Biotech Corporation, Piscataway, USA
PRAME$_{2-T10}$	SPSVSQLSVT	Genscript Biotech Corporation, Piscataway, USA
PRAME$_{2-T2}$	STSVSQLSVL	Genscript Biotech Corporation, Piscataway, USA
PRAME$_{2-T3}$	SPTVSQLSVL	Genscript Biotech Corporation, Piscataway, USA
PRAME$_{2-T4}$	SPSTSQLSVL	Genscript Biotech Corporation, Piscataway, USA
PRAME$_{2-T5}$	SPSVTQLSVL	Genscript Biotech Corporation, Piscataway, USA
PRAME$_{2-T6}$	SPSVSTLSVL	Genscript Biotech Corporation, Piscataway, USA
PRAME$_{2-T7}$	SPSVSQTSVL	Genscript Biotech Corporation, Piscataway, USA
PRAME$_{2-T8}$	SPSVSQLTVL	Genscript Biotech Corporation, Piscataway, USA
PRAME$_{2-T9}$	SPSVSQLSTL	Genscript Biotech Corporation, Piscataway, USA
RAB38$_1$	LPNGKPVSV	Max-Planck-Institute for Biochemistry, Martinsried, Germany
ROPN1B$_1$	LPRIPFSTF	Max-Planck-Institute for Biochemistry, Martinsried, Germany
TYMS$_1$	KPGDFIHTL	Max-Planck-Institute for Biochemistry, Martinsried, Germany
TYMS$_2$	EPRPPHGEL	Max-Planck-Institute for Biochemistry, Martinsried, Germany
TYR$_1$	LMEKEDYHSLY	Max-Planck-Institute for Biochemistry, Martinsried, Germany
TYR$_2$	DSDPDSFQDY	Max-Planck-Institute for Biochemistry, Martinsried, Germany

Table 10: Mutation-bearing peptides and wildtype analogues

Peptide	Sequence	Company
ABCC2^{S1342F}	GRTGAGKSFL	Genscript Biotech Corporation, Piscataway, USA
ABCC2^{WT}	GRTGAGKSSL	Genscript Biotech Corporation, Piscataway, USA
AKAP6^{M1482I}	KLKLPIIMK	Genscript Biotech Corporation, Piscataway, USA
AKAP6^{WT}	KLKLPMIMK	Genscript Biotech Corporation, Piscataway, USA
GABPA^{E161K}	ETSKQVTRW	Genscript Biotech Corporation, Piscataway, USA
GABPA^{WT}	ETSEQVTRW	Genscript Biotech Corporation, Piscataway, USA
H3F3C^{T4I}	RIKQTARK	Genscript Biotech Corporation, Piscataway, USA
H3F3C^{WT}	RTKQTARK	Genscript Biotech Corporation, Piscataway, USA
MAPK3K9^{E689K}	ASWVVPIDIK	Genscript Biotech Corporation, Piscataway, USA

MAPK3K9[WT]	ASWVVPIDIE	Genscript Biotech Corporation, Piscataway, USA
NCAPG2[P333L]	KLILWRGLK	Genscript Biotech Corporation, Piscataway, USA
NCAPG2[WT]	KPILWRGLK	Genscript Biotech Corporation, Piscataway, USA
NOP16[P169L]	SPGPVKLEL	Genscript Biotech Corporation, Piscataway, USA
NOP16[WT]	SPGPVKLEP	Genscript Biotech Corporation, Piscataway, USA
RBPMS[P46L]	RLFKGYEGSLIK	Genscript Biotech Corporation, Piscataway, USA
RBPMS[WT]	RPFKGYEGSLIK	Genscript Biotech Corporation, Piscataway, USA
SEC23A[P52L]	LPIQYEPVL	Genscript Biotech Corporation, Piscataway, USA
SEC23A[WT]	PPIQYEPVL	Genscript Biotech Corporation, Piscataway, USA
SEPT2[Q125R]	YIDERFERY	Genscript Biotech Corporation, Piscataway, USA
SEPT2[WT]	YIDEQFERY	Genscript Biotech Corporation, Piscataway, USA
SYTL4[S363F]	GRIAFFLKY	Genscript Biotech Corporation, Piscataway, USA
SYTL4[WT]	GRIAFSLKY	Genscript Biotech Corporation, Piscataway, USA

Table 11: Viral control peptides

Peptide	Sequence	Company
BRLF-1$_{148-156}$	RVRAYTYSK	Genscript Biotech Corporation, Piscataway, USA
EBNA 3C$_{79-87}$	RRIYDLIEL	Genscript Biotech Corporation, Piscataway, USA
EBNA-1$_{407-417}$	HPVGEADYFEY	Genscript Biotech Corporation, Piscataway, USA
pp65$_{417-426}$	TPRVTGGGAM	AG Busch, TU München

2.1.10 Antibodies and multimers

2.1.10.1 Antibodies

Table 12: Antibodies used for flow cytometry

Antibody	Clone	Conjugation	Company
anti-human CD3	HIT3a	APC	BD Biosciences, Franklin Lakes, USA
anti-human CD3	UCHT1	PE, AF®700	BD Biosciences, Franklin Lakes, USA
anti-human CD4	RPA-T4	PE, APC-Cy™7	BD Biosciences, Franklin Lakes, USA
anti-human CD8	RPA-T8	APC, V450, APC-Cy™7	BD Biosciences, Franklin Lakes, USA
anti-human CD8	HIT8a	FITC	BD Biosciences, Franklin Lakes, USA
anti-human CD14	M5E2	PE	BD Biosciences, Franklin Lakes, USA
anti-human CD19	HIB19	APC	BD Biosciences, Franklin Lakes, USA
anti-human CD27	O323	APC	Thermo Fisher scientific, Waltham, USA
anti-human CD28	CD28.2	PE	BD Biosciences, Franklin Lakes, USA
anti-human CD45	HI30	V500	BD Biosciences, Franklin Lakes, USA
anti-human CD45RO	UCHL1	PE, AF®700	BD Biosciences, Franklin Lakes, USA
anti-human CD62L	DREG-56	PE, V450	BD Biosciences, Franklin Lakes, USA
anti-human CD80	L307.4	PE	BD Biosciences, Franklin Lakes, USA
anti-human CD83	HB15e	FITC	BD Biosciences, Franklin Lakes, USA

anti-human CD86	2331	APC	BD Biosciences, Franklin Lakes, USA
anti-human CD137	4B4-1	APC	Miltenyi Biotec GmbH, Bergisch Gladbach, Germany
anti-human CCR7 (CD197)	3D12	PE	Thermo Fisher scientific, Waltham, USA
anti-human HLA-ABC	W6/32	FITC	BioLegend Inc., San Diego, USA
anti-human HLA-DR	L243	APC	BD Biosciences, Franklin Lakes, USA
anti-IFNγ	B27	AF®700	BD Biosciences, Franklin Lakes, USA
anti-IL-2	5344,111	BV510	BD Biosciences, Franklin Lakes, USA
anti-TNFα	Mab11	V450	BD Biosciences, Franklin Lakes, USA
anti-murine TCR (αTCRmu)	H57-597	PE	BD Biosciences, Franklin Lakes, USA
Isotype	MOPC-21	FITC, PE, APC, AF®700, V450, APC-Cy^{TM}7	BD Biosciences, Franklin Lakes, USA
Isotype	X40	V500, BV510	BD Biosciences, Franklin Lakes, USA

Table 13: Antibodies used for IFNγ ELIspot

Antibody	Clone	Conjugation	Company
anti-IFNγ coating antibody	1-D1K	None	Mabtech AB, Nacka Strand, Sweden
anti-IFNγ capture mAb	7-B6-1	biotin	Mabtech AB, Nacka Strand, Sweden

2.1.10.2 Multimers

All Multimers used in this study were fluorescently labeled with Phycoerythrin (PE).

Table 14: Multimers

pMHC-Multimer	Peptide	HLA allele	Structure	Source
AKAP6^{M1482I}-pMHC	KLKLPIIMK	A0301	Tetramer	AG Busch, TU München, Germany
AKAP6^{WT}-pMHC	KLKLPMIMK	A0301	Tetramer	AG Busch, TU München, Germany
BRLF-1$_{148-156}$-pMHC	RVRAYTYSK	A0301	Tetramer	AG Busch, TU München, Germany
MPO$_2$-pMHC	TPAQLNVL	B0702	Tetramer	AG Busch, TU München, Germany
MPO$_4$-pMHC	FVDASMVY	A0101	Tetramer	AG Busch, TU München, Germany
MPO$_5$-pMHC	NPRWDGERL	B0702	Tetramer	AG Busch, TU München, Germany
NCAPG2^{P333L}-pMHC	KLILWRGLK	A0301	Tetramer	AG Busch, TU München, Germany
PAX3$_1$-pMHC	SMDPVTGYQY	A0101	Tetramer	AG Busch, TU München, Germany
PRAME$_2$-pMHC	SPSVSQLSVL	B0702	Tetramer	AG Busch, TU München, Germany
SYTL4^{S363F}-pMHC	GRIAFFLKY	B2705	Pentamer	ProImmune Ltd., Oxford, UK
SYTL4^{WT}-pMHC	GRIAFSLKY	B2705	Pentamer	ProImmune Ltd., Oxford, UK
TYR$_1$-pMHC	LMEKEDYHSLY	A0101	Tetramer	AG Busch, TU München, Germany

2.1.11 Vectors

Vector	Characteristics	Resistance	Source
pALF10A1-GaLV ("env")	Plasmid coding for viral envelope of the Gibbon ape Leukemia Virus (GaLV)	Ampicillin	Wolfgang Uckert, Berlin, (Stitz et al., 2000)
pcDNA3.1	Vector derived from pcDNA3 and designed for high-level stable and transient expression in mammalian hosts; facilitates in-vitro transcription of cloned inserts using T7 polymerase	Ampicillin	Thermo Fisher scientific, Waltham, USA
pcDNA3.1-MLV („gag-pol")	Plasmid coding for group-specific antigen and polymerases under control of the CMV promotor	Ampicillin	Wolfgang Uckert, Berlin Christopher Baum, Hannover
pMP71G$_{PRE}$	Retroviral vector containing eGFP marker under control of MPSV-LTR promotor, with PRE* element from woodchuck Hepatitis Virus.	Ampicillin	Wolfgang Uckert, Berlin, (Engels et al., 2003)
pMP71-P2A-eGFP	pMP71G$_{PRE}$ with P2A element upstream of GFP; insertion of additional SalI cutting site	Ampicillin	Cloned by Richard Klar and Martina Rami
pMP71-P2A-DsRed	pMP71G$_{PRE}$ with P2A element upstream of DsRed; insertion of additional SalI cutting site	Ampicillin	Cloned by Richard Klar
pUC57-TCR 8D4om	Cloning vector containing optimized and murinized TCR construct	Ampicillin	Genscript Biotech Corporation, Piscataway, USA

2.1.12 Primer sequences

Primers were purchased from Sigma-Aldrich Chemie GmbH, Taufkirchen, Germany as dried products and dissolved in DEPC-H$_2$O to a stock concentration of 100 µM. Sequences are depicted in 5' → 3' direction. Primers used for cloning, sequencing and determination of TCR alpha and beta chain are listed below. Primers and probes used for qPCR are specific for respective isolated TCR and remain confidential.

Table 15: Cloning and sequencing primers

Primer	Sequence	Application
PRAME_fwd	TAGCGGCCGCCACCATGGAACGAAGGCGTTTGTG	Cloning of whole antigen
PRAME_rev	TAGTCGACATTAGGCATGAAACAGGGGC	Cloning of whole antigen
PAX3_fwd	TAGCGGCCGCCACCATGACCACGCTGGCCGGCGC	Cloning of whole antigen
PAX3_rev	TAGTCGACAAAAGTCCAAGGCTTACTTT	Cloning of whole antigen
AKAP6_fwd	TAGCGGCCGCCACCATGGATGAGGGGGAAAGCAT	Cloning of mutated and wt minigene
AKAP6_rev	TAGTCGACTTCTATATTGCCACTTTTAT	Cloning of mutated and wt minigene
NOP16_fwd	TAGCGGCCGCCACCATGTCCTCGATTCTTTGCAG	Cloning of mutated and wt minigene
NOP16_rev	TAGTCGACAGAGCGGGGAGTGTGCACGT	Cloning of mutated and wt minigene
SYTL4_fwd	TAGCGGCCGCCACCATGAGTACGATCGGCAGCAT	Cloning of mutated and wt minigene

SYTL4_rev	TAGTCGACCTTGGCTTCATCAGCATAGG	Cloning of mutated and wt minigene
NCAPG2_fwd	TAGCGGCCGCCACCATGTCTCCAGTGCATTCCAA	Cloning of mutated and wt minigene
NCAPG2_rev	TAGTCGACCATGAAGGTTTGGATCC	Cloning of mutated and wt minigene
TCR 8D4a_fwd	TAGCGGCCGCCACCATGGAGTCATTCCTGGGAGG	Cloning of TCR 8D4 alpha chain
TCR 8D4a_rev	TACAATTGTCAGCTGGACCACAGCCGCA	Cloning of TCR 8D4 alpha chain
TCR 8D4b_fwd	TAGCGGCCGCCACCATGGGCTGCAGGCTCCTCTG	Cloning of TCR 8D4 beta chain
TCR 8D4b_rev	ATGAATTCCTAGCCTCTGGAATCCTTTC	Cloning of TCR 8D4 beta chain
MP71 fwd	TGAAAATTAGCTCGACAAAG	Sequencing of cloned inserts in pMP71
T7	TAATACGACTCACTATAGGG	Sequencing of cloned inserts in pcDNA3.1

Table 16: Primer for TCR repertoire

TCRAV gene segment family-specific primers			TCRBV gene segment family-specific primers		
Primer	**Sequence**	**C$_{WORK}$**	**Primer**	**Sequence**	**C$_{WORK}$**
P-5'αST	CTG TGC TAG ACA TGA GGT CT	2.5 µM	**5ßST**	AAG CAG AGA TCT CCC ACA C	5 µM
P-3'αST	CTT GCC TCT GCC GTG AAT GT	2.5 µM	**P-3ßST**	GAG GTG AAG CCA CAG TCT G	5 µM
3'T-Cα	GGT GAA TAG GCA GAC AGA CTT GTC ACT GGA	5 µM	**P-3CßII**	GAT GGC TCA AAC ACA GCG ACC TC	5 µM
Vα1	AGA GCC CAG TCT GTG ASC CAG; S=C/G	2.5 µM	**Vß1**	GCA CAA CAG TTC CCT GAC TTG GCA C	5 µM
Vα1.1	AGA GCC CAG TCR GTG ACC CAG; R=A/G	2.5 µM	**Vß2**	TCA TCA ACC ATG CAA GCC TGA CCT	2.5 µM
Vα2	GTT TGG AGC CAA CRG AAG GAG	5 µM	**Vß3**	GTC TCT AGA GAG AAG AAG GAG CGC	2.5 µM
Vα3	GGT GAA CAG TCA ACA GGG AGA	2.5 µM	**Vß4**	ACA TAT GAG AGT GGA TTT GTC ATT	2.5 µM
Vα4	TGA TGC TAA GAC CAC MCA GC	5 µM	**Vß5.1**	ATA CTT CAG TGA GAC ACA GAG AAA C	2.5 µM
Vα5	GGC CCT GAA CAT TCA GGA	2.5 µM	**Vß5.2**	TTC CCT AAC TAT AGC TCT GAG CTG; Vß5.2 + Vß5.2T 1:1 MIX	5 µM
Vα6	GGT CAC AGC TTC ACT GTG GCT A	2.5 µM	**[Vß5.2T]**	[TTC CCT AAT TAT AGC TCT GAG CTG]	2.5 µM
Vα7	ATG TTT CCA TGA AGA TGG GAG	5 µM	**Vß6.1**	GCC CAG AGT TTC TGA CTT ACT TC	2.5 µM
Vα8	TGT GGC TGC AGG TGG ACT	5 µM	**Vß6.2**	ACT CTG ASG ATC CAG CGC ACA; S=C/G	2.5 µM
Vα9	ATC TCA GTG CTT GTG ATA ATA	5 µM	**Vß6.3**	ACT CTG AAG ATC CAG CGC ACA	2.5 µM
Vα10	ACC CAG CTG CTG GAG CAG AGC CCT	5 µM	**Vß7**	CCT GAA TGC CCC AAC AGC TCT C	2.5 µM
Vα11	AGA AAG CAA GGA CCA AGT GTT	2.5 µM	**Vß8**	ATT TAC TTT AAC AAC AAC GTT CCG	2.5 µM
Vα12	CAG AAG GTA ACT CAA GCG CAG ACT	2.5 µM	**Vß8.3**	GCT TAC TTC CGC AAC CGG GCT CCT	5 µM
Vα13	GAG CCA ATT CCA CGC TGC G	2.5 µM	**Vß9**	CCT AAA TCT CCA GAC AAA GCT	2.5 µM
Vα14.1	CAG TCC CAG CCA GAG ATG TC	2.5 µM	**Vß10**	CTC CAA AAA CTC ATC CTG TAC CTT	2.5 µM
Vα14	CAG TCT CAA CCA GAG ATG TC	2.5 µM	**Vß11**	TCA ACA GTC TCC AGA ATA AGG ACG	5 µM
Vα15	GAT GTG AGC AGA GTC TTT TC	2.5 µM	**Vß12**	AAA GGA GAA GTC TCA GAT	5 µM
Vα16	TCA GCG GAA GAT CAG GTC AAC	2.5 µM	**Vß12.3**	GCA GCT GCT GAT ATT ACA GAT	2.5 µM
Vα17	GCT TAT GAG AAC ACT GCG T	2.5 µM	**Vß13**	TCG ACA AGA CCC AGG CAT GG	2.5 µM
Vα18	GCA GCT TCC CTT CCA GCA AT	2.5 µM	**Vß13.1**	CAA GGA GAA GTC CCC AAT	5 µM
Vα19	AGA ACC TGA CTG CCC AGG AA	2.5 µM	**Vß13.2**	GGT GAG GGT ACA ACT GCC	2.5 µM
Vα20	CAT CTC CAT GGA CTC ATA TGA	2.5 µM	**Vß13.5**	ATA CTG CAG GTA CCA CTG GCA	2.5 µM
Vα21	GTG ACT ATA CTA ACA GCA TGT	5 µM	**Vß14**	GTC TCT CGA AAA GAG AAG AGG AAT	2.5 µM
Vα22	TAC ACA GCC ACA GGA TAC CCT TCC	2.5 µM	**Vß15**	AGT GTC TCT CGA CAG GCA CAG GCT	5 µM
Vα23	TGA CAC AGA TTC CTG CAG CTC	2.5 µM	**Vß16**	AAA GAG TCT AAA CAG GAT GAG TCC	2.5 µM
Vα24	GAA CTG CAC TCT TCA ATG C	2.5 µM	**Vß17**	CAG ATA GTA AAT GAC TTT CAG	2.5 µM
Vα25	ATC AGA GTC CTC AAT CTA TGT TTA	2.5 µM	**Vß18**	GAT GAG TCA GGA ATG CCA AAG GAA	2.5 µM
Vα26	AGA GGG AAA GAA TCT CAC CAT AA	5 µM	**Vß19**	CAA TGC CCC AAG AAC GCA CCC TGC	2.5 µM

Vα27	ACC CTC TGT TCC TGA GCA TG	2.5 µM		**Vß20**	AGC TCT GAG GTG CCC CAG AAT CTC	2.5 µM
Vα28	CAA AGC CCT CTA TCT CTG GTT	2.5 µM		**Vß21**	AAA GGA GTA GAC TCC ACT CTC	2.5 µM
Vα29	AGG GGA AGA TGC TGT CAC CA	2.5 µM		**Vß22.1**	CAT CTC TAA TCA CTT ATA CT	5 µM
Vα30	GAG GGA GAG AGT AGC AGT	2.5 µM		**Vß22.2**	AAG TGA TCT TGC GCT GTG TCC CCA	2.5 µM
Vα31	TCG GAG GGA GCA TCT GTG ACT A	2.5 µM		**Vß22.3**	CTC AGA GAA GTC TGA AAT ATT CG	2.5 µM
Vα32	CAA ATT CCT CAG TAC CAG CA	2.5 µM		**Vß23**	GCA GGG TCC AGG TCA GGA CCC CCA	2.5 µM
				Vß24	ATC CAG GAG GCC GAA CAC TTC T	5 µM

Table 17: Primers for degenerated TCR beta repertoire

Primer	Sequence	c_{WORK}
Primer VP1	GCIITKTIYTGGTAYMGACA	10 µM
Primer VP2	CTITKTWTTGGTAYCIKCAG	10 µM
Primer VP3	ATCTTTATTGGTATCGACGT	10 µM
Primer VP4	ATGTTTACTGGTATCATAAG	10 µM
Primer CP1	GCACCTCCTTCCCATTCAC	10 µM

Table 18: Primers for SYBR Fast-based real-time PCR

Primer	Sequence
PRAME_rt_fwd	CTGCGTAGACTCCTCCTCTC
PRAME_rt_rev	GACACTTAGCTGACTGACGC
PAX3_rt_fwd	CGTCAGTGAGTTCCATCAGC
PAX3_rt_rev	TTCTCTCAAAAGCACGCTCC
GAPDH_rt_fwd	GAGTCAACGGATTTGGTCGT
GAPDH_rt_rev	TTGATTTTGGAGGGATCTCG
HMBS_rt_fwd	AGGATGGGCAACTGTACCTG
HMBS_rt_rev	TCGTGGAATGTTAACGAGCAG
HPRT1_rt_fwd	AAGCTTGCTGGTGAAAAGGAA
HPRT1_rt_rev	AAGCAGATGGCCACAGAACT

2.1.13 Software and web-based tools

Table 19: Software tools

Software	Application	Company
CloneManager 7, version 7.03	In-silico cloning	Scientific & Educational Software, Denver, USA
EndNote™ X5	Citation management	Thomson Reuters, New York City, USA
FlowJo v7.6.5	Flow cytometry analysis	Tree Star, Ashland, USA
Graphpad Prism v6	Data processing and analysis	GraphPad Software, Inc., La Jolla, USA
Immunospot software 5.4.0.1	ELIspot analyses	CTL-Europe, Bonn, Germany
Microsoft Office (Word, Excel, Powerpoint), 2010	Data processing and presentation	Microsoft Corporation, Redmond, USA

| Sequencher v5.0 | Sequence alignment | GeneCodes Corporation, Ann Arbor, USA |
| StepOne Software v2.3 | Processing of real-time PCR data | Life Technologies Corporation, USA |

Table 20: Web-based tools

Tool	Application	Homepage
BioGPS	Antigen expression analysis	http://biogps.org/
Cancer-Testis Database	Target antigen selection	http://www.cta.lncc.br/
Catalogue of somatic mutations in cancer (COSMIC)	Search for previously identified mutations	http://cancer.sanger.ac.uk/cosmic
CBS Prediction Servers (NetMHCpan 2.8, NetMHC 4.0 and others)	In-silico epitope prediction	http://www.cbs.dtu.dk/services/NetMHC/
EMBOSS needle	Protein sequence alignment	http://www.ebi.ac.uk/Tools/psa/emboss_needle/
Ensembl GRCh38.78	Sequence extraction from reference genome	http://www.ensembl.org/index.html
Genevestigator	Antigen expression analysis	https://genevestigator.com/
Human Protein Atlas	Protein expression analysis	http://www.proteinatlas.org/
IMGT	TCR sequence identification	http://www.imgt.org/
NCBI Basic Local Alignment Search Tool (BLAST)	TCR reconstruction; Primer blast	https://blast.ncbi.nlm.nih.gov/Blast.cgi
Oncomine	Antigen expression analyses in cancer tissues	https://www.oncomine.org/resource/login.html
Primer3	Primer and probe design	http://bioinfo.ut.ee/primer3/
SYFPEITHI	In-silico epitope prediction	http://www.syfpeithi.de/
UCSC Genome Browser Gateway (BLAT)	Antigen expression analysis	http://genome-euro.ucsc.edu

2.2 Methods

2.2.1 Cell culture

Processing and cultivation of cells was performed under sterile conditions. Work with human blood samples, EBV-transformed cells and retroviruses was done according to S2 safety guidelines.

2.2.1.1 Isolation and cultivation of primary cells

Peripheral blood mononuclear cells (PBMC) were isolated from whole blood or leukapheresis products using Ficoll gradient density centrifugation. Therefore, 15 ml of Ficoll solution was prepared in 50 ml falcons each. Whole blood was diluted with RPMI in a ratio of 1-2:1 and leukapheresis product in a ratio of 4-5:1, respectively. 35 ml of each mixture were carefully overlaid on the Ficoll solution avoiding disturbance of both solutions. After centrifugation for 25 min at 880 g with reduced acceleration (grade 4 of 9) and no brake, leukocyte layer was carefully removed with a 10-ml serological pipet. Cell suspensions were pooled and washed twice with RPMI. Purified PBMC were then used for further downstream applications.

Primary tumor tissue was obtained from the pathology department after surgical resection for the isolation of tumor cells and tumor-infiltrating lymphocytes (TIL). TIL were extracted from tumor fragments by cultivation of minced tumor pieces on γ-irradiated feeder cells (30 Gy, ^{137}CS) in TCM supplemented with 1000 U/ml IL-2 and 30 ng/ml OKT3. Medium was exchanged twice a week with fresh TCM supplemented with 300 U/ml IL-2. TIL were grown for 2-3 week and cryopreserved until use. Another part of the fresh tumor was used for direct coculture. Therefore, tumor tissue was digested as described previously (R. F. Wang, 2009) with slight modifications. Briefly, tissue was minced into small pieces (< 3mm^3) and incubated with tumor digestion medium (Table 7) for 3-4 hours with 1400 rpm at 37°C on a Thermomixer Compact. Cell suspension was then transferred to a 15ml falcon, washed three times with RPMI and resuspended in TCM for coculture experiments.

2.2.1.2 Cultivation of cell lines

Suspension cell lines were cultivated in cRPMI and adherent cell lines were cultivated in cDMEM, if not indicated otherwise. Cell lines were split twice a week or if medium color indicated high cell density. Adherent cell lines were washed with PBS and detached from the flask bottom by incubation with Trypsine/EDTA for 2-3 min at 37°C, followed by addition of medium. After centrifugation, cells were resuspended in cRPMI or cDMEM, respectively. T293 and RD114 were split by clapping the flask carefully to mechanically detach the cells. Cell lines were regularly checked under the light microscope and tested for the absence of mycoplasma infection using *Venor GeM mycoplasma detection kit* according to the manufacturer's instructions.

2.2.1.3 Freezing, thawing and counting of cells

Viable cells were cryopreserved after centrifugation and discard of supernatant by resuspending them in 1ml freezing medium per aliquot. Cyro tubes were placed in a NALGENE Cryo 1°C Freezing Container at -80°C and transferred the next day to the vaporous phase of liquid nitrogen for long-term storage.

For re-cultivation, frozen cell-media suspensions were quickly thawed by adding small amounts of RPMI and transferring thawed material directly to a prepared falcon with 10 ml RPMI. Residual DMSO was removed by centrifugation at 500 g for 5 min and resuspending the cells in appropriate cell culture medium.

Cells were counted using a Neubauer counting chamber. Therefore, 10 µl of cell suspension was diluted with 10-40 µl Trypane blue (or higher in cases of leukapheresis). Cells were counted in 16 quarters of each corner and cell concentration was calculated using the following formula:

$$c_{cells} \text{ [Mio/ml]} = \text{[counter number of cells in all 4 corners]}/4 * \text{dilution factor} * 10\,000 / 10^6$$

2.2.1.4 Generation of EBV-transformed lymphoblastoid cell lines

The in-vitro transformation of B cells was performed with Epstein Barr Virus (EBV) to generate immortalized lymphoblastoid cell lines (LCL) was performed according to standard procedures. Therefore, EBV-supernatant was produced by harvesting supernatants of cell line ATCC-1A2 (ATCC) and freezing supernatant three times. Aliquots of 2 ml were then stored at -80°C until use. For the transformation of B cells, 8-10 Mio fresh or thawed PBMC were washed, resuspended in 8 ml cRPMI (20% ΔFCS) supplemented with 2 µg/ml Cyclosporin A. Cell suspension was distributed in two T25 flasks and 1ml of thawed EBV supernatant was added to each flask. After one week, medium was changed by removing 2.5 ml of supernatant and adding cRPMI supplemented with 20% ΔFCS and 1 µg/ml Cyclosporin A. Medium was changed twice a week with fresh cRPMI + 20% ΔFCS + 1 µg/ml Cyclosporin A, until cell accumulations were visible characteristic for successful transformation (usually after four to six weeks). B-cell origin was phenotypically confirmed by flow cytometry, cells were further expanded to sufficient numbers and cryopreserved until use.

2.2.2 In-vitro stimulation of T-cells

2.2.2.1 Priming of naïve T cells in an HLA-matched setting

Dendritic cells (DC) were generated as previously described (Klar et al., 2014) with slight modifications. Briefly, 100-150 Mio PBMC were washed, resuspended in pre-warmed DC medium and allowed for adherence in an 80cm^2 flask for 1.5 hours in the incubator at 37°C. Non-adherent cells were then carefully removed by rinsing the opposite site with pre-warmed RPMI for three times and cultivating adherent cells with DC medium supplemented with 20 ng/ml IL-4 and 100 ng/ml GM-CSF for 48 hours. For induction of maturation, a cytokine cocktail containing TNF-α (c_{END} = 10 ng/ml), IL-1β (10 ng/ml), IFN-γ (5000 U/ml), PGE$_2$ (250 ng/ml), CL075 (1 µg/ml), GM-CSF (100 ng/ml) und IL-4 (20 ng/ml) was added. The next day, DC were harvested by rinsing the flask with PBS + 1% ΔHS and collecting remaining cells with a cell scraper. DC phenotype was analyzed by flow cytometry. For in-

vitro stimulation, DC were pulsed with 0.1 µM or 1 µM peptide for 2 h at 37°C, washed and γ-irradiated with 30 Gy.

Naïve CD8^{+} T cells were isolated from PBMC in two subsequent steps. First, CD8^{+} T cells were isolated using *CD8 untouched isolation kit* (Invitrogen) according to the manufacturer's instructions. The obtained population was incubated with CD45RO- and CD57-microbeads for 15 min at 4°C in a MACS rotator. After washing, cells were resuspended in 500 µl Isolation buffer and depleted for CD45RO^{+} and CD57^{+} cells by adding the cell suspension on a *LD column* (Miltenyi) followed by 3x washing with 1ml Isolation buffer. The collected flow-through containing the CD8+ naïve T-cell fraction was phenotypically characterized by flow cytometry.

T cells and DC were coincubated at an effector-to-target ratio of 10:1 in TCM + 30 ng/ml IL-21. After 3 days, IL-7 and IL-15 were added in a concentration of 5 ng/ml. Medium change was performed with TCM supplemented with IL-7 and IL-15 every 2-3 days.

2.2.2.2 Naïve T-cell stimulation in a single HLA-mismatched setting

DC were differentiated and matured as described (2.2.2.1). 24 hours after maturation, adherent cells were harvested, washed two times with OptiMEM and counted. 2-3 Mio cells were resuspended in 200 µl ice-cold OptiMEM, transferred to an Electroporation Cuvettes and incubated for 3 min on ice. DC were then electroporated with 40 µg in-vitro transcribed HLA-eGFP RNA (2.2.3.10) using an exponential protocol and 300 µF, 300 V on a *Gene Pulser Xcell Electroporation System* (Bio-Rad). Immediately after electroporation, 800 µl pre-warmed DC medium was added, cells were carefully transferred to a tissue culture-treated 6-well plated (V_{END} = 2 ml) and incubated over night at 37°C.

Allo-depletion of T cells was performed after overnight co-incubation with γ-irradiated antigen-negative targets and subsequent depletion of CD137^{+} T cells. Up to 10 Mio T cells were resuspended in 40 µl Isolation buffer and stained with 10 µl αCD137-APC antibody for 10 min at 4°C. After washing and resuspension in 80 µl Isolation buffer, 20 µl of anti-APC-microbeads were added to the cell suspension and incubated for 15 min at 4°C. Labeled cells were washed, resuspendend in 500 µl buffer and applied on a LD column followed by rinsing the column with 2x 1 ml buffer. The unlabeled flow through was collected as the allo-depleted fraction.

T cells and DC were coincubated in TCM supplemented with 30 ng/ml IL-21 at an effector-to-target ratio of 10:1. After 3 days, IL-7 and IL-15 were added (c_{END} = 5 ng/ml). Medium was changed with TCM supplemented with IL-7 and IL-15 every 2-3 days.

2.2.2.3 Accelerated cocultured DC culture

For stimulation and expansion of T cells in mixed cocultures, a modified protocol of a previously reported stimulation procedure (Martinuzzi et al., 2011) was established. Therefore, 0.3–0.5 Mio PBMC per well were cultivated in AIM-V supplemented with 100 ng/ml IL-4 and 100 ng/ml GM-CSF in a flat-bottom 96-well plate. After 24 hours, peptide (c_{END} = 1 µM), Poly-I:C (20 µg/ml) and IL-7 (0.5 ng/ml) were added to each well. After 24 hours of incubation, cells were washed twice with AIM-V, transferred to a previously coated ELIspot plate (2.2.4.6) and cultured overnight without any movement of the plate in the incubator. Afterwards, cells were harvested by careful resuspension several times on the ELIspot plate and transferred to a new round-bottom 96-well plate. After 2 days, medium was exchanged with TCM supplemented with IL-7 and IL-15 (5 ng/ml each), followed by IL-7 and IL-15 addition every 2-3 days. Cells were split and expanded as indicated by cell density and medium color. Figure 1 gives an overview of the stimulation procedure and time points for assessment of functional reactivity.
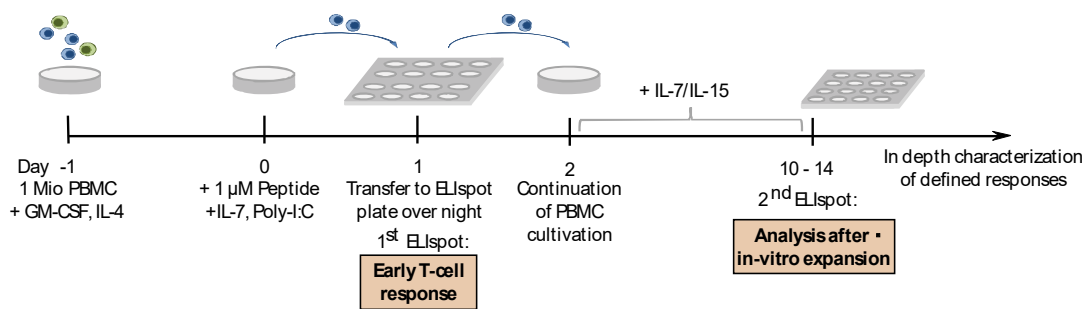
Figure 1: Schematic overview of PBMC stimulation and analysis in mixed cocultures

2.2.2.4 Clonality analysis of T cells by limiting dilution

For determination of T-cell responses on a clonal level and subsequent TCR isolation, expanded T-cell lines were diluted to a final concentration of 0.5 to 1 cells per well and plated on γ-irradiated Feeder PBMC (50 000/well) in TCM with 50 U/ml IL-2 and 30 ng/ml OKT-3. IL-2 was added twice a week to a final concentration of 50 U/ml. T-cell clones were screened for specific reactivity after nine to twelve days using one half of cell suspension. One quarter was used for RNA isolation and remaining cells were re-stimulated with Feeder PBMC for further expansion as described previously.

2.2.3 Molecular biology methods

2.2.3.1 Isolation of RNA and DNA

RNA from T cells, cell lines and PBMC was isolated using TRIzol reagent. Cell pellets were dissolved in 200 µl (T-cell clones and lines) or 1000 µl (PBMC and cell lines) TRIzol and vortexed thoroughly. In case of small amounts below 200 000 cells, yeast t-RNA was added to the TRIzol-cell-mixture. 40 µl or 200 µl 1 Bromo-3-choloro-propan was added, well vortexed and incubated for 10 min at RT. After centrifugation for 15 min at 12000 rpm, the clear upper phase containing RNA was transferred to a new 1.5 ml tube containing 100 µl or 500 µl Isopropanol. The solution was incubated over night at -20°C and centrifuged for 20 min at 12000 rpm, 4°C. Supernatant was discarded and the pellet was washed with 500 µl or 1000 µl 75% v/v Ethanol. To remove any residual Ethanol, a second centrifugation for 5 min, 12000 rpm, 4°C was performed and the supernatant was discarded. Pellet was air-dried and then dissolved in 15 to 50 µl DEPC-H_2O.

To obtain RNA from snap-frozen tumor material, tissue was first minced and sheared with *QIAshredder Homogenizer* (Qiagen) according to the manufacturer's instructions. RNA was isolated using *RNeasy mini kit* (Qiagen) according to the manufacturer's instructions and eluted in 20 µl DEPC-H_2O.

Genomic DNA (gDNA) from tumor tissue or PBMC was extracted with DNA blood and tissue kit (Qiagen) according to the manufacturer's instructions. DNA was eluted with 20 – 50 µl DEPC- H_2O.

Extraction yield after each isolation procedure was measured with *NanoDrop ND-1000*.

2.2.3.2 Reverse transcription PCR

Isolated RNA (2.2.3.1) was used for Reverse transcription (RT) into complementary DNA (cDNA) with *AffinityScript Multiple Temperature cDNA Synthesis Kit* (Agilent Technologies) with slight modifications. Therefore, 500 -1000 ng RNA were diluted in DEPC-H_2O to a total volume of 13.5 µl. 1µl of oligo(dT) (c_{STOCK} = 500 µg/ml) was added and annealing was performed for 5 min at 65°C and cooled down for 10 min at RT. 2 µl of Affinity Script Buffer, 2 µl dNTP (c_{STOCK} = 10 mM each) and 1 µl Affinity Script Reverse Transcriptase were added to the mixture and incubated for 1 hour at 47.5°C followed by 15 min at 70°C for heat-inactivation of the Transcriptase. cDNA was stored at -20°C until use.

2.2.3.3 PCR for cloning of desired constructs

cDNA from cell lines or primary human material was used as template for the amplification of different genes or minigenes. KOD Hot Start DNA Polymerase Kit (Merck) was used for PCR and reaction mix was prepared as follows (Table 21).

Table 21: Reaction mix for standard PCR using KOD polymerase.

Reagent	c_{STOCK}	c_{END}	Volume
10x KOD Buffer	10x	1x	10 µl
MgSO4	25 mM	1.5 mM	6 µl
dNTP	2 mM each	0.2 mM each	10 µl
5' fwd Primer	10 µM	300 pM	3 µl
3' rev Primer	10 µM	300 pM	3 µl
cDNA			2 µl
KOD Polymerase	10^3 U/ml	2 U / 100 µl	2 µl
DEPC-H_2O			64 µl
V_{END}			100 µl

The resulting mixture was split into two PCR reaction tubes (50 µl each) and amplification was performed on a Thermocycler using the following program (Table 22):

Table 22: PCR program using KOD polymerase

Step	Temperature	Time	Cycles
1	94°C	2 min	
2	97°C	30 s	
3	57°C	30 s	35 (step 2-4)
4	72°C	1 min 30 s	
5	72°C	10 min	
6	4°C	pause	

2.2.3.4 TCR repertoire PCR

TCR alpha and beta chains of specific T-cell clones were detected by PCR with primer pairs covering all possible variable alpha and beta segments. Variable primers were used as listed in (Table 16) and PCR reactions for alpha and beta repertoire were prepared accordingly (Table 23) using *HotStarTaq Plus MasterMix Kit* (Qiagen). Degenerated TCR beta repertoire was performed as previously described (Zhou et al., 2006). For each clone, two reaction mixtures were prepared as depicted in Table 24 using respective primers (Table 17). PCR of all described TCR primer combinations was performed on a Thermocycler using the program listed in Table 25.

Table 23: Reaction mix for TCR alpha and beta repertoire

Reagent	Description	Volume
HotStar MasterMix		12.5 µl
P-5'aST / P-5'bST	Primer fwd constant region	1.5 µl
P-3'aST / P-3'bST	Primer rev constant region	1.5 µl
3'-a const / CbII	Primer rev variable fragment	2 µl
Vax	Primer fwd variable fragment	3 µl
cDNA		0.55 µl
Coral load		2.5 µl
DEPC H2O		1.45 µl
V_{END}		25 µl

Table 24: Reaction mix for degenerated TCR beta repertoire

Reagent	Tube I	Tube II
HotStar MasterMix	12.5 µl	12.5 µl
Primer VP1	5 µl	-
Primer VP2	-	5 µl
Primer VP3	-	1 µl
Primer VP4	-	1 µl
Primer CP1	1 µl	1 µl
cDNA	0.5 µl	0.5 µl
Coral load	2.5 µl	2.5 µl
DEPC H2O	1.45 µl	1.45 µl
V_{END}	25 µl	25 µl

Table 25: PCR Program for TCR repertoire

Step	Temperature	Time	Cycles
1	95°C	15 min	
2	94°C	1 min	
3	54°C	1 min	35 (step 2-4)
4	72°C	1 min	
5	72°C	10 min	
6	4°C	pause	

2.2.3.5 Gel electrophoresis and purification

Success of amplification and correct length of amplified products was determined by gel electrophoresis. 1-1.5% agarose gels were prepared by adding 1.5 – 2.25 mg agarose to 150 ml of 1x TAE buffer followed by heating until the agarose was completely dissolved. Ethidium bromide was added (c_{END} = 0.53 µg/ml) and the liquid agarose was poured into a gel tray with appropriate combs. 20 µl 6x loading buffer were added to respective samples. When the gel was hardened, prepared samples and 6 µl of 100-bp or 1 kb DNA ladder were loaded into the pockets and electrophoresis was performed for 30-40 min with 100 V in 1x TAE buffer using a *Compact M Horizontal Gel Electrophoresis Apparatus* (Biometra). DNA-Bands were visualized with *BioDocAnalyze Gel documentation system* (Biometra) and PCR products with correct length were cut out and purified using *Nucleospin Gel and PCR Cleanup kit* (Macherey-Nagel) according to the manufacturer's instructions. PCR products were eluted with 20 µl of DEPC- H_2O and concentration was determined using NanoDrop ND-1000.

2.2.3.6 Reconstruction of TCR alpha and beta chain

Purified PCR products of TCR fragments derived from distinct bands were sent for Sanger sequencing to MWG Eurofins (Ebersberg, Germany). Obtained sequences were analyzed using IMGT vQuest (Table 20) for identification of CDR3 regions and determination of alpha and beta variable segments. The remaining sequences of variable and constant regions that were not captured by sequencing were deducted from human reference genomes using ensemble genome browser. Primer were designed according to the reconstructed sequence and TCR were amplified from cDNA (2.2.3.3) derived from respective T-cell clone.

2.2.3.7 Restriction digest

Purified PCR products and backbone vectors were digested with restriction enzymes NotI and SalI or NotI and EcoRI depending on the cloning strategy. Reaction mix was set up according to the following table (Table 26).

Table 26: Reaction set-up for restriction digest

Reagent	c_{STOCK}	Vector	Insert
Vector DNA / PCR product	1 µg/µl / various	15 µl	20 µl
Buffer O	10x	10 µl	10 µl
NotI	10 U/µl	2 µl	2 µl
EcoRI or SalI	10 U/µl	2 µl	2 µl
DEPC-H_2O	-	71 µl	66 µl
V_{END}		100 µl	100 µl

Digestion was performed for 2 hours at 37°C, followed by heat-inactivation at 65°C for 15 min. Cut vectors were run on a gel and bands with expected size were excised and purified (2.2.3.5). Digested PCR products were directly purified using *Nucleospin Gel and PCR Cleanup kit* (Macherey-Nagel).

2.2.3.8 Ligation and Transformation

Ligation of cut and purified products was performed with T4 ligase. Amounts of inserts and respective vectors were calculated with regard to their length according to the following formula:

V(insert) = n * 1 µl [V(vector)] * c(vector)/c(insert) * [insert length in bp]/ [vector length in bp]

The molar ratio (n) of insert to vector was chosen between 3 and 10. Reaction mix was set up according to Table 27 and ligation was performed for 16 hours at 16°C, followed by heat-inactivation for 15 min at 65°C.

Table 27: Reaction mix for ligation

Reagent	Volume
Insert	[*variable*]
Vektor	1 µl
T4 Buffer 10x	1 µl
T4 Ligase	1 µl
DEPC-H_2O	[*variable*]
V_{END}	10 µl

For clonal amplification of ligated vector constructs, ligation products were transformed into NEB5a competent E.coli. An aliquot of E.coli was quickly thawed and split into two reaction tubes. 2 µl of ligation product was added and the mixture was incubated for 30 min on ice. Heat-shock transformation was performed for 30 s at 42°C followed by 5 min incubation on ice. 475 µl of S.O.C. medium was added and transformed bacteria were shaked for 1 hour at 330 rpm and 37°C. Different dilutions of cell suspensions were dispersed on LB-agar plates supplemented with Ampicillin (100 µg/ml) and grown over night at 37°C. Grown colonies were picked and expanded for DNA vector purification by growing them over night in 3 ml LB medium (+ 100 µg/ml Ampicillin).

2.2.3.9 DNA vector purification

Amplified DNA vectors were purified from 1.5 ml bacterial suspension using *JETSTAR™ 2.0 Plasmid Purification Kit* (Genomed) according to the manufacturer's instructions. Control digest of 1 µg of purified vector was performed as described above (2.2.3.7), analyzed by gel electrophoresis (2.2.3.5) and vector constructs exhibiting correct fragment length were send for Sanger sequencing to MWG

Eurofins (Ebersberg, Germany). If the expected sequence was confirmed, re-transformation of purified vectors was performed using 100 ng for heat-shock transformation into E.coli (2.2.3.8). After over-night cultivation, two to three bacterial colonies were picked and grown as separate starting cultures in 3 ml LB medium (+ 100 µg/ml Ampicillin) for 6-8 hours at 37°C. 500 µl of one well-grown culture was diluted in 250 ml LB medium and grown over night at 37°C for large-scale amplification. Vector products were then purified from bacterial cultures using either *JETSTAR™ 2.0 Plasmid Purification Kit* (Genomed) in case of antigen- or HLA-expression vectors or *NucleoBond® Xtra Maxi EF* (Macherey Nagel) for endotoxin-free plasmid preparation of TCR constructs according to the manufacturer's instructions. Extraction yield was analyzed using *NanoDrop-1000* and purified DNA vectors were stored at -20°C until use.

2.2.3.10 In-vitro transcription of HLA-ivt RNA

HLA-P2A-eGFP constructs were in-vitro transcribed using *mMESSAGE mMACHINE® T7 Transcription Kit* (Thermo Fisher scientific) according to the manufacturer's instructions. Afterwards, polyadenylation was performed with *Ambion™ Poly(A) Tailing Kit* (Thermo Fisher scientific) as recommended by the manufacturer. Yield was measured with *NanoDrop ND-1000* and in-vitro transcribed RNA was stored at -80°C until use.

2.2.3.11 Optimization of TCR constructs

For an improved surface expression and improved pairing of TCR alpha and beta chain, an optimized tandem gene sequence was constructed: The TCR beta chain was linked with a P2A element to the alpha chain (Leisegang et al., 2008) and human TRAC and TRBC regions were replaced by their murine counterparts (Cohen, Zhao, Zheng, Rosenberg, & Morgan, 2006). An additional cysteine bond was inserted into the tandem construct by exchange of amino acids Serine on position S212C and Threonine at position T545C, respectively. Codon-optimization for expression in human cells was performed to optimize expression in human lymphocytes (Scholten et al., 2006), which was conducted by Genscript according to in-house algorithms. The optimized construct was then synthesized by Genscript and cloned into the expression vector pMP71 using the restriction sites NotI and EcoRI. The complete sequence of TCR 8D4om is listed in the appendix (6.3).

2.2.3.12 Quantitative real-time PCR

Primers used for determination of antigen expression and primer and probes specific for variable regions of TCR beta chains were designed using Primer3 (Table 20).

Expression patterns of PRAME and PAX3 transcripts were assessed with semi-quantitative real-time PCR using *KAPA SYBR® Fast qPCR Master Mix* (PeqLab / VWR). Reverse transcribed cDNA from different cell lines or primary tissue using *Human total RNA Master Panel II* (Clontech) was used as

template for the determination of relative expression of antigens of interest in relation to the mean of three different housekeeping genes (GAPDH, HMBS, HPRT1).

Table 28: Reaction mix for real-time PCR using SYBR Fast

Reagent	c_{END}	Volume
Sybr Fast	1x	5 µl
DEPC-H$_2$O	-	1.5 µl
Primer fwd (c_{WORK} = 3 µM)	200 nM	0.65 µl
Primer rev (c_{WORK} = 3 µM)	200 nM	0.65 µl
ROX high	1x	0.2 µl
cDNA		2 µl
V_{END}		10 µl

Real-time quantitative PCR was performed on a *StepOnePlus* (Applied Biosystems) using the following program (Table 29):

Table 29: Program for template quantification using SYBR-fast-based real-time PCR

Stage	Step	Temperature	Time	Cycles	Ramp rate	Acquisition
Holding	1	50°C	2 min			
	2	95°C	3 min			
Cycling	1	95°C	3 s	40		
	2	65°C	30 s			
Melt Curve	1	95°C	15 s			
	2	65°C	15 s		+ 0.3°C	Step and Hold
	3	95°C	15 s			

Expression values were normalized to the mean of GAPDH, HMBS and HPRT1 using the ΔΔCT Method (Livak & Schmittgen, 2001).

Expression analyses of TCR were conducted with dual-labeled hybridization probes using *KAPA PROBE FAST qPCR Kit* (PeqLab / VWR). The reaction mix was set up as described in Table 30 and 5-10 ng/condition of reverse transcribed RNA or 10-50 ng/ condition of gDNA were used. Amplification was performed using standard program (Table 31). Serial dilutions of cloned vectors were used as a standard curve to quantify absolute numbers of detected molecules (Whelan, Russell, & Whelan, 2003).

Table 30: Reaction mix for expression analysis using dual-labeled hybridization probes

Reagent	c_{END}	Volume
KAPA Probe	1x	10 µl
DEPC-H$_2$O	-	x µl
Primer fwd (c_{WORK} = 10 µM)	300 nM	0.6 µl
Primer rev (c_{WORK} = 10 µM)	300 nM	0.6 µl
Probe	250 nM	0.5 µl
ROX high	1x	0.4 µl
cDNA / gDNA		x µl
V_{END}		20 µl

Table 31: PCR program using dual-labeled hybridization probes

Stage	Step	Temperature	Time	Cycles
Holding	1	95°C	3 min	
Cycling	1	95°C	3 s	40
	2	60°C	20 s	

2.2.4 Flow Cytometry and analyses of T-cell specificity

2.2.4.1 Staining of surface markers

Cells were washed with FACS buffer and blocked with 100% ΔHS for 10 min at 4°C. After washing with FACS buffer, 1.5 µl of each surface marker and 1 µl 7-AAD (c_{END} = 0.5 mg/ml) were added followed by incubation of 20-30 min on ice in the dark. Cells were washed with 1 ml FACS buffer, fixed with 1% PFA and stored at 4°C in the dark until measurement. Acquisition was performed on a *LSRII* (BD Biosciences) and results were analyzed using FlowJo v7.6.5 software (TreeStar).

2.2.4.2 Pentamer and Tetramer staining

Multimer staining was performedaccording to current recommendations and protocols of the CIMT Immunoguiding Program[3]. Briefly, cells were blocked with ΔHS and washed as described in (2.2.4.1.). Tetramers were prepared by diluting 1 µl of Tetramer solution in 250 µl Multimer staining buffer and centrifuged for 5 min at 14000 g to pellet undesired aggregates. Supernatant containing soluble pMHC-Tetramer complexes were collected carefully and 50 µl were added to the cell suspension in a 1:1 dilution. Pentamer dilutions were performed in Multimer staining buffer as recommended by the manufacturer. Cells were incubated with Tetramer or Pentamer solution for 25 min on ice in the

---

[3] http://www.cimt.eu/workgroups/cip

dark. Surface antibodies and reagents for life-dead discrimination were added followed by incubation for additional 20 min on ice.

For sorting of multimer-positive cells, staining procedure was performed as described above with the exception of adding Propidium Iodide (c_{END} = 1 µg/ml) instead of 7-AAD for life-dead discrimination. Cell sort was performed on a *FACSAria III* (BD Biosciences).

2.2.4.3 Co-cultures of effector and target cells

For functional analysis, effector T cells were washed, resuspended in TCM and counted. Cell concentrations between 10 000 and 100 0000 cells/well were plated in 100 µl/well in a round-bottom 96-well plate. For peptide-dependent analyses, target cells were pulsed in AIM-V for 2 hours at 37°C with 1 µM peptide, if not indicated otherwise. Cell lines with endogenous antigen expression were used without any specific pre-treatment. After washing, cells were resuspended in TCM and added in appropriate effector-to-target (E:T) ratios as indicated. Coculture experiments were performed in triplicates except for some experiments using rare patient or T-cell clone material. In these cases, duplicates were analyzed as indicated.

2.2.4.4 Intracellular cytokine staining

Combinatorial cytokine production was assessed using intracellular cytokine staining. Therefore, co-cultures of 50 000-100 000 T cells with target cells in an E:T of 1:1 were incubated for 1 hour at 37°C. To inhibit intracellular protein transport, brefeldin A was added followed by incubation of four hours at 37°C. Afterwards, co-cultures were sealed with Parafilm, stored over night at 4°C, transferred the next day to FACS tubes and washed with FACS-azide buffer. Cells were blocked with ΔHS and, for exclusion of dead cells, stained with EMA (c_{END} = 4 µg/ml). Therefore, cells were incubated 10 min on ice in the dark followed by 10 min on ice under strong light exposure to induce photolysis of EMA and covalent binding to DNA of cells with compromised membranes. Antibodies for staining of surface markers were added as described (2.2.4.1) and incubated for 20 min on ice in the dark. After washing with FACS-azide buffer, intracellular staining was performed with *eBioscience™ Intracellular Fixation & Permeabilization Buffer Set* (Thermo Fisher scientific) according to the manufacturer's instructions with slight modifications. Cells were fixated by adding 100 µl of IC Fixation buffer, vortexed and incubated for 20 min on ice in the dark. 1 ml of 1x Perm Buffer was added, cells were centrifuged and vortexed shortly. Again, 1 ml 1x Perm Buffer was added, and after centrifugation and removal of supernatant, cells were incubated with 1.5 µl of antibodies against intracellular proteins for 20 min incubation on ice. After washing the cells with 1 ml Perm Buffer and 1ml FACS-azide buffer, they were stored at 4°C until measurement.

2.2.4.5   FACS-based cytotoxicity

Cocultures were set up as described above (2.2.4.3) using 50000 target and 50000 effector cells. After 20-24 hours, cell mixtures were stained with surface markers and 7-AAD (2.2.4.1). For absolute quantification of remaining target cells, *AccuCheck COUNTING BEADS* (Thermo Fisher scientific) were added before measurement. Target cell lysis was calculated using the following formula:

$$percentage\ of\ lysed\ cells = (1 - \frac{absolute\ number\ of\ remaining\ targets}{mean\ of\ untreated\ targets}) * 100$$

2.2.4.6   IFN-γ ELIspot

Low frequencies of antigen-specific T cells were determined by IFNγ ELIspot assay. Therefore, ELISpot plates MAHAS4510 (Merck) were coated with IFNγ capture antibody 1-D1K (c_{END}=10µg/ml in PBS) and incubated over night at 4°C. The next day, coated plates were washed four times with PBS including 10 min incubation at RT between each washing step, followed by blocking of uncoated areas on the plate with TCM for 45 min at 37°C. For determination of early T-cell responses (2.2.2.3), stimulated PBMC were resuspended well, directly transferred to blocked plates and incubated over night at 37°C. For assessment of reactivity of expanded T-cell lines (2.2.2.1, 2.2.2.3), 20 000 – 40 000 effector cells were coincubated with 20 000 peptide-pulsed target cells on the blocked plate and incubated for 72 hours at 37°C. PMA (c_{END} = 1 µg/ml) and Ionomycin (2 µg/ml) were used as a positive control. After incubation, 150 µl of supernatant was removed and stored at -20°C for further analyses. Cells were either used for further cultivation by adding 150 µl/well AIM-V careful resuspension and transfer of the cell suspension to a new round-bottom 96-well plate (in case of analysis of early time-point T-cell responses, 2.2.2.3) or otherwise discarded. ELIspot plates were washed six times with washing buffer. Secondary anti-IFNγ antibody 7-B6-1-Biotin was diluted in PBS + 0.5% BSA to a final concentration of 2 µg/ml and 100 µl was added to each well followed by incubation for two hours at RT. After six washing steps with washing buffer, HRP-complex solution was added followed by one hour incubation in the dark. ELIspot plates were then washed two times with washing buffer and two times with PBS. 5 µl of 50% H_2O_2 were added to 10 ml of AEC buffer before pipetting 100 µl to each well. The reaction was incubated in the dark until the positive control became visible (after 2-8 min). The reaction was then stopped with running tap water and plates were dried in towels and stored in the dark until analysis. Read-out was performed on an ImmunoSpot S6 Ultra-V Analyzer using Immunospot software 5.4.0.1 (CTL-Europe, Bonn, Germany).

2.2.4.7   Analysis of IFNγ, and IL-2 secretion by ELISA

Cocultures of effector and target cells were set up using 10 000 cells from each fraction (E:T = 1:1) if not indicated otherwise. After 20-24 hours, 150 µl of cell culture supernatant was removed for the determination of cytokine release using *BD OptEIA™ Human IFN-γ* or *IL-2 ELISA Set* (BD Bioscience)

following manufacturer's recommendations with slight modifications. Briefly, ELISA plates were coated with IFNγ or IL-2 capture antibody dissolved in Coating buffer (1:250) and incubated over night at 4°C. The next day, plates were washed three times with washing buffer followed by the addition blocking solution and incubation of one hour at room temperature. IFNγ or IL-2 standards were freshly prepared by dissolving stock solutions in TCM to a concentration of 1000 pg/ml or 500 pg/ml and performing five serial 1:1 dilutions and one blank. Plates were washed three times and 50 µl of supernatants or standard dilutions were added and incubated for one hour at room temperature. After washing plates five times, detection solution was pipetted containing Detection antibody (IFNγ: 1:250, IL-2: 1:500) and Enzyme Conjugate (1:250) dissolved in blocking solution. After incubation for one hour at room temperature in the dark, plates were washed seven times. For substrate reaction, solution A and B from *BD OptEIA™ TMB Substrate Reagent Set* (BD Biosciences) were mixed in a ratio of 1:1 and 100 µl substrate solution was added per well. Plates were incubated at RT in the dark for 10-20 min, until the standard curve becomes completely visible and the reaction was stopped by adding 50 µl of sulfuric acid. Intensity of enzymatic reaction was measured with an absorbance at 450 nm and a reference of 570 nm with *Sunrise^TM absorbance reader* (Tecan).

2.2.4.8 Enrichment of peptide-specific T cells by CD137$^+$ selection

T-cells were cocultured with γ-irradiated (100 Gy) peptide-pulsed target cells for 20-24 hours to induce antigen-specific upregulation of CD137 on the cell surface. T cells were then labeled using anti-CD137 antibody and microbeads (Miltenyi Biotec) as described (2.2.2.2). For the isolation procedure, labeled cell suspension was applied on a LS-column and flow-through was only collected for control of sorting results using flow cytometry. After rinsing the column with 2x 1ml Isolation buffer, magnetically labeled T cells were eluted from the column by adding 1 ml Isolation buffer and flushing through the liquid quickly with a stamp. Isolated T cells were then centrifuged, resuspended in TCM and expanded as lines or clones (2.2.2.4).

2.2.5 Retroviral gene transfer

2.2.5.1 Production of virus particles

For production of retroviral supernatant, T293 or RD114 cells were used as viral packaging cell line. 0.2-0.3 Mio cells per well were seeded in 3 ml/well cDMEM on a tissue-culture treated six-well plate and allowed for adherence for at least eight hours. The transfection solution for each construct was prepared in 200 µl DMEM by adding 9 µl (or 3 µl) TransIT, vortexing and incubating 20 min at RT. 1 µg of retroviral vector and 1 µg of both packaging plasmids, gag-pol and env (not required for RD114), were added to the transfection solution and dispersed carefully with the pipet tip. The mixture was

incubated for 30 min at RT and then added dropwise on the plated packaging cell line and incubated for 48 hours at 37°C.

2.2.5.2 Transduction of PBMC and cell lines

Non-tissue culture treated 24-well plates were coated with 400 µl/well with RetroNectin diluted to a final concentration of 12.5 µg/ml. Plates were sealed with Parafilm, incubated overnight at 4°C and blocked with PBS + 2% BSA for 30 min at 37°C. Wells were washed twice with PBS + 2.5 % v/v HEPES and stored at 4°C until use.

PBMC were isolated from peripheral blood withdrawals of healthy donors as described above (2.2.1.1) and activated in TCM with 30 ng/ml OKT3 and 50 U/ml IL-2 for 48 hours. On the day of first transduction, activated PBMC were harvested and 1 Mio cells per condition were plated on RetroNectin-coated and blocked 24-well plates in 1ml TCM per well supplemented with IL-2 (c_{END} = 100 U/ml), HEPES (c_{END} = 5 mM) and Protamine sulfate (c_{END} = 4 µg/ml) with all endconcentrations calculated in relation to V_{END} = 2 ml/well (cell suspension + retroviral supernatant).

Suspension cell lines were washed and 0.3 – 0.5 Mio cells per condition were seeded in 1 ml cRPMI on RetroNectin-coated and blocked 24-well plates with addition of HEPES and Protamine sulfate as described above.

Adherent cell lines were plated on the evening before on tissue-culture treated 6-well plates in a density of 0.1 -0.3 Mio cells/well. The next day, cells were checked for proper adherence and 1 ml/well of fresh medium was added supplemented with HEPES and Protamine sulfate as described above.

Retroviral supernatant was harvested and filtered through a 0.45 µm filter. Remaining supernatant was kept on the packaging cell lines for the second transduction. 1 ml of virus-supernatant was added to each well containing the cell suspension and spininfection was performed at 820 g for 90 min at 32°C without break. After incubation for 24 hours at 37°C, the cells from each condition were harvested, washed and seeded onto two wells of a new RetroNectin-coated and blocked 24-well plate. Adherent cells were kept on the original plate. New media supplemented with IL-2, Protaminsulfat and HEPES and retroviral supernatants were prepared for each condition as described above and second transduction was conducted equally to the first. After 24 hours, cells were washed and resuspended in respective culture medium. PBMC were expanded in TCM supplemented with 5 ng/ml IL-7 and 5 ng/ml IL-15.

3 Results

3.1 Workflow for the diversified immunogenicity assessment of HLA ligands presented on primary melanoma tissue

In total, the immunopeptiome of 25 melanoma samples was analyzed by mass spectrometry (MS). Immunoprecipitation of human leukocyte antigen (HLA)-bound ligands from native tumor tissue from melanoma patients and measurement of peptide ligands was performed by Michal Bassani-Sternberg (Max-Plank Institute of Biochemistry, Martinsried). Detailed descriptions of the results regarding mass spectrometry analyses are reported in the related publication (Bassani-Sternberg et al., 2016). The immunogenic potential for a selection of identified ligands was assessed by the interrogation of different TCR repertoires (Figure 2).

Due to the measurement of patient samples at different time points, immunopeptidomic results of five patients were initially available. Within the first part of the project, identified HLA ligands were filtered, ranked and synthesized for the investigation of peptide-specific responses within the allogeneic repertoire of healthy donors (Figure 2A).

In the later course of this study, five patients were selected due to their interesting clinical course for additional exome sequencing of tumor tissues and respective PBMC. Analysis was performed in cooperation with AG Rad (IInd Medical Department) and resulted in the determination of tumor-derived mutations specific for each patient's tumor. Using these individual mutations as a template for the construction of a patient-tailored database, previously analyzed mass spectra were mined again for the presence of HLA ligands containing tumor-specific mutations. As a second part of this thesis, identified ligands were subjected to analysis of immune responses within patient material as well as in HLA-matched healthy donor-derived T cells (Figure 2B).
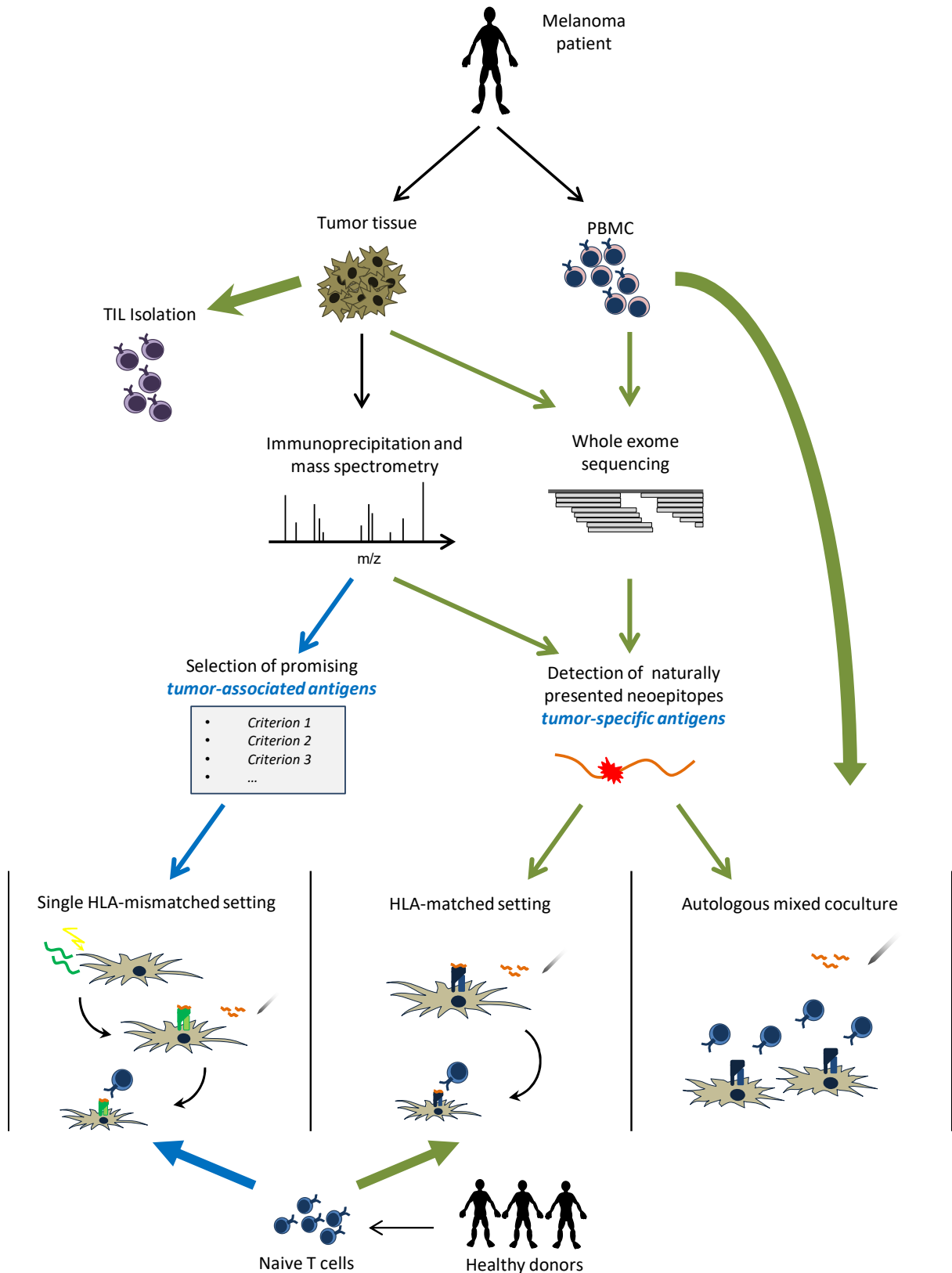
Figure 2: Overview of epitope identification and T-cell stimulation.
(A) Non-mutated peptide ligands were identified, and a selection was used for in-vitro stimulation in an HLA-mismatched setting (blue arrows). (B) Exome-sequencing was integrated into the workflow and immunogenicity of identified mutated peptides was determined using patient-derived material and PBMC from HLA-matched healthy donors (green arrows).

3.2 Immune responses against tumor-associated antigens

3.2.1 Selection of potential target antigen candidates

First patients to be analyzed were Mel3, Mel4, Mel5, Mel8 and Mel12. A workflow was established to select the most promising tumor associated antigen (TAA) candidates as depicted in Table 32.

Table 32: Workflow for priorization of non-mutated eluted HLA ligands

Criteria for selection process	Reference
1. Select peptides with 8-11 amino acid length	
⇓	
2. Genotyping of patients' HLA alleles	
⇓	
3. Focus on most frequent HLA alleles	http://www.allelefrequencies.net/
⇓	
4. Screen antigens for previously described tumor- and melanoma associated antigens and CTA	Andersen R.S. et al. Cancer Res 2012 Cancer-Testis Database, http://www.cta.lncc.br/
⇓	
5. In silico assessment of RNA and protein expression	Open source online databases: BioGPS, BLAT, Genesapiens, Genevestigator, Oncomine, Human Protein Atlas, The Cancer Genome Atlas
⇓	
6. Antigen-specific literature search	PubMed
⇓	
7. Confirmation of HLA restriction of selected ligands derived from potential antigen candidates	NetMHCpan 2.8 HLA facts book (Steve Marsh) Syfpeithi

As most frequent HLA types present in our patient cohort, we focused on HLA-A0101 (27.7% phenotype frequency in German population), -A0201 (49.9%), -A0301 (28.6%) and -B0702 (24.5%).[4] Application of this workflow led to the selection of 21 promising peptide candidates (Table 33).

---

[4] http://www.allelefrequencies.net

Table 33: Naturally presented non-mutated HLA ligands selected for in-vitro stimulation

Name	Peptide	Gene	Patient sample	HLA allele (prediction)	Prediction[5] nM; %rank; bindLevel	Prediction score[6]
ATAD2$_1$	KPPISKKKAVL	ATAD2	Mel12	HLA-B*07:02	515.19; 1.20; WB	-[7]
ATAD2$_2$	SVYENGLSQK	ATAD2	Mel8	HLA-A*03:01	15.58; 0.05; SB	32
CASC5$_1$	HVSKERIQQSL	CASC5	Mel8	HLA-B*07:02	0.096; 17679.28; -	-[7]
CCDC110$_1$	QTDPDVHRNGKY	CCDC110	Mel3/8	HLA-A*01:01	236.12; 0.25; SB	-[7]
CDK4$_1$	KARDPHSGHFVAL	CDK4	Mel8	HLA-B*07:02	529.61; 1.20; WB	-[7]
CTAG1A$_1$	TPMEAELARRSL	CTAG1A	Mel8	HLA-B*07:02	11.90; 0.05; SB	-[7]
DCT$_1$	TSDQLGYSY	DCT	Mel8	HLA-A*01:01	4.77; 0.01; SB	31
DCT$_2$	GTYEGLLRR	DCT	Mel8	HLA-A*03:01	174.86; 0.70; WB	14
LY6K$_1$	LPRVWTDANL	LY6K	Mel8	HLA-B*07:02	16.20; 0.08; SB	23
LY6K$_2$	KPEEKRFLL	LY6K	Mel8	HLA-B*07:02	75.83; 0.40; SB	22
PAX3$_1$	SMDPVTGYQY	PAX3	Mel8	HLA-A*01:01	21.65; 0.04; SB	27
PMEL$_1$	ALNFPGSQK	PMEL	Mel4	HLA-A*03:01	12.28; 0.03; SB	32
PMEL$_2$	QLRTKAWNR	PMEL	Mel3	HLA-A*03:01	1201.56; 2.50; -	23
PRAME$_1$	SPRRLVELAGQSL	PRAME	Mel8	HLA-B*07:02	17.25; 0.08; SB	-[7]
PRAME$_2$	SPSVSQLSVL	PRAME	Mel8	HLA-B*07:02	61.18; 0.30; SB	23
RAB38$_1$	LPNGKPVSV	RAB38	Mel4	HLA-B*07:02	182.07; 0.70; WB	20
ROPN1B$_1$	LPRIPFSTF	ROPN1B	Mel8	HLA-B*07:02	10.03; 0.04; SB	22
TYMS$_1$	KPGDFIHTL	TYMS	Mel8	HLA-B*07:02	173.89; 0.60; WB	22
TYMS$_2$	EPRPPHGEL	TYMS	Mel8	HLA-B*07:02	7.69; 0.02; SB	27
TYR$_1$	LMEKEDYHSLY	TYR	Mel4/12	HLA-A*01:01	134.09; 0.17; SB	25
TYR$_2$	DSDPDSFQDY	TYR	Mel4/8/12	HLA-A*01:01	47.04; 0.08; SB	30

3.2.2 Immunogenicity assessment within the healthy donor-derived HLA-mismatched T-cell repertoire

To test the immunogenic potential of selected peptide ligands, in-vitro stimulations were conducted with naïve T cells from HLA-matched and mismatched healthy donors (HD). Of note, no PBMC from those patients were available for extensive in-vitro analyses. Table 34 gives an overview over performed stimulation assays. In-vitro stimulations in the allogeneic setting using T cells from HD2 were performed by Tanja Koch and are described in detail in her bachelor's thesis. In some cases, stimulation approaches were conducted using a fraction of allo-depleted T cells in parallel to naïve T cells (2.2.2.2) (marked in dark grey).

---

[5] NetMHC 4.0, http://www.cbs.dtu.dk/services/NetMHC
[6] SYFPEITHI, http://www.syfpeithi.de/
[7] No prediction available

Table 34: Overview of in-vitro stimulations of HD derived T cells with TAA

Name	HD1	HD2	HD3	HD4
ATAD2$_1$			X	
ATAD2$_2$				
CASC5$_1$			X	
CCDC110$_1$	X X		X	X
CDK4$_1$			X	
CTAG1A$_1$			X	
DCT$_1$	X		X	
CDT$_2$				
LY6K$_1$			X	
LY6K$_2$			X	
PAX3$_1$	X X		X	X
PMEL$_1$				
PMEL$_2$				
PRAME$_1$			X	
PRAME$_2$		X[8] X[8]	X	
RAB38$_1$			X	
ROPN1B$_1$			X	
TYMS$_1$			X	
TYMS$_2$			X	
TYR$_1$	X X		X	X
TYR$_2$	X		X	

For only very few candidates, we detected peptide-specific reactivities in functional screenings after in-vitro stimulations. For those interesting ligands, multimers were produced in cooperation with Prof. Busch, Institute of Microbiology (listed in Table 14) and used for assessment of multimer-binding T-cell frequencies and sorting of specific T cells from expanded T-cell lines. In one T-cell line from HD2, which was stimulated and expanded by Tanja Koch, a clear multimer-positive population could be observed (Figure 3). Notably, this population was only detected within the naïve T-cell repertoire, but not within the allo-depleted fraction.

---

[8] *In vitro stimulations conducted by Tanja Koch*
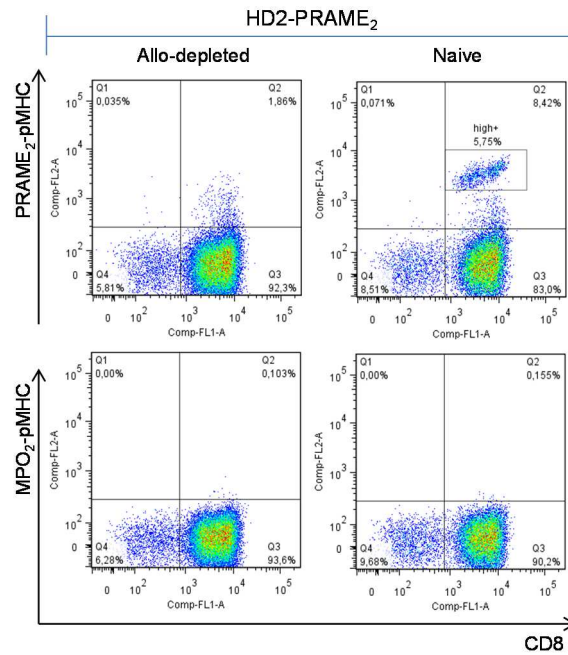
Figure 3: Multimer staining of T-cell line HD2-PRAME$_2$ after in-vitro priming and expansion.

After in vitro priming and expansion of T cells from HD4, specific binding of the PAX3$_1$-pMHC multimer was detected in a T-cell line that was depleted for allo-reactive cells against HLA-A0101 and afterwards stimulated with TYR$_1$ peptide (Figure 4). However, the T-cell fraction stimulated with the PAX3$_1$ ligand did not show enrichment of specific T cells despite all stimulation steps were performed in parallel and naïve T cells were used from the same time point of blood withdrawal of HD4. Repetition of the multimer staining confirmed these observation and rendered mistakes during staining procedure highly unlikely. As those cells binding PAX3$_1$-pMHC appeared as a very distinct population, the specificity of PAX3$_1$-directed T cells within T-cell line HD4-TYR$_1$ was analyzed more in detail.
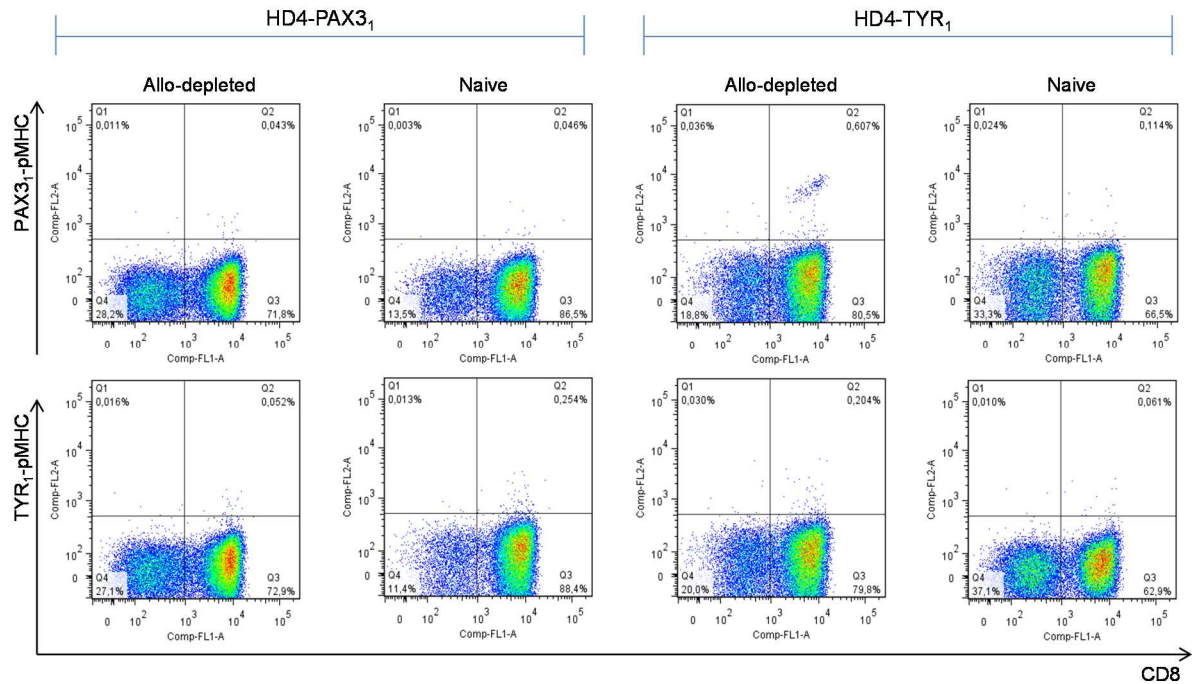
Figure 4: Multimer staining of T-cell lines HD4-PAX3$_1$ and HD4-TYR$_1$.
After in-vitro stimulation and expansion, T-cell lines were stained with multimers PAX3$_1$-pMHC and TYR$_1$-pMHC. Gating was performed on 7-AAD negative events.

3.2.3 Expression pattern of PRAME and PAX3 in healthy and diseased tissue

For the assessment of a defined antigen recognition pattern, both antigens PRAME and PAX3 were cloned into MP71-P2A-DsRed (2.2.3). Antigen-negative cell lines were retrovirally transduced with these vectors and transduction efficiency was confirmed by DsRed expression analyzed by flow cytometry. Transduced cell lines were cloned by limiting dilution and antigen expressing cells were selected based on homogenous high DsRed-positivity.

In addition to the above described in-silico assessment of antigen expression levels, detailed expression analysis of PRAME and PAX3 were conducted with RNA from primary healthy tissues and cell lines. Semi-quantitative real-time PCR confirmed preferential expression of PRAME and PAX3 in a selection of different cell lines and a comparably low expression in a panel of healthy tissue-derived cDNA (Figure 5).
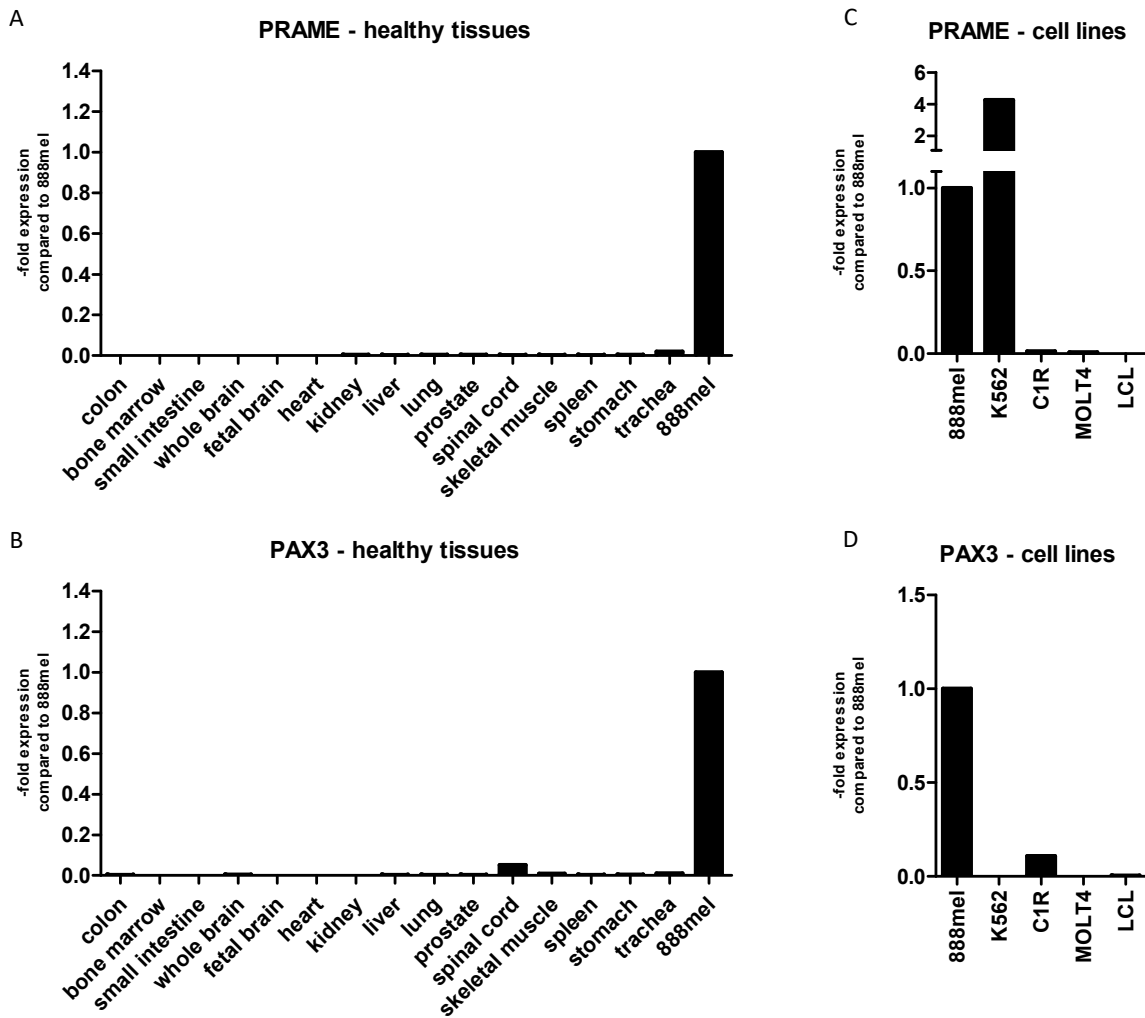
Figure 5: Expression pattern of tumor-associated antigens PRAME and PAX3 in healthy and diseased tissue.
Relative expression was determined by semi-quantitative real-time PCR normalized to housekeeping genes GAPDH, HPRT1 and HMBS. Expression levels of genes of interest were calculated in relation to the mean of expression in 888mel. A, B: Antigen expression in a panel of healthy tissues; C, D: Expression of PRAME and PAX3 in selected cell lines.

3.2.4 Allo-derived T-cell clones against PRAME and PAX3

T-cell lines HD2-PRAME$_2$ and HD4-TYR$_1$ were enriched for observed specificities using multimers PRAME$_2$-pMHC and PAX3$_1$-pMHC, respectively. A part of the sorted T cells was directly cloned on feeder cells by limiting dilution and remaining cells were expanded as cell line 2.2.2.4. T-cell clones were screened for specific reactivity against T2 cells transduced with respective HLA restriction element. The majority of T-cell clones isolated from PRAME$_2$–pMHC multimer sort recognized the relevant peptide, but not irrelevant control (Figure 3A). Clones derived from T-cell line HD4-TYR$_1$ were in general less reactive. However several clones displayed specific reactivity only against PAX3$_1$, but not the irrelevant TYR$_1$ peptide ligand (Figure 3B).
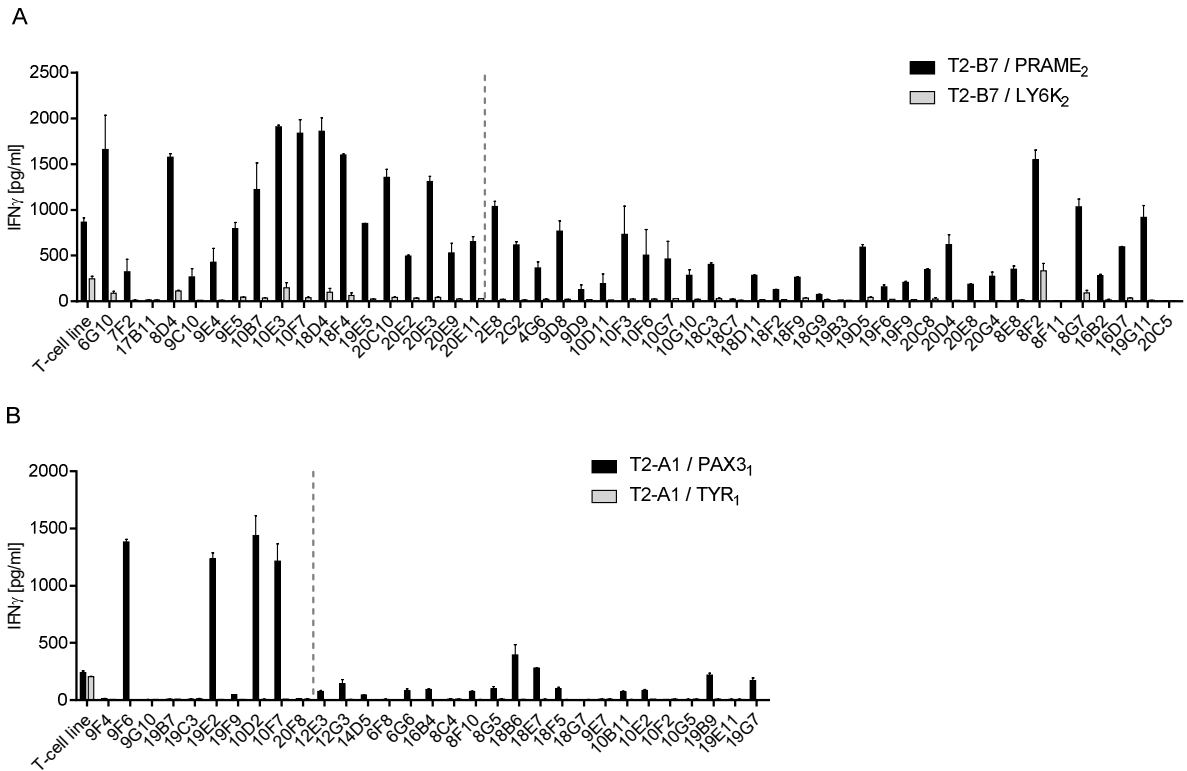
Figure 6: Screening of expanded T-cell clones for specific IFNγ release against peptide-pulsed T2 cells.
A: Line and clones directed against T2-B7 cells pulsed either with the relevant epitope $PRAME_2$; or with a control peptide ($LY6K_2$) B: IFNγ release of T-cell line and clones against T2-A1 cells presenting $PAX3_1$ or TYR_1.

Selected T-cell clones were further expanded and stained with specific or control tetramers as indicated (Figure 7). All analyzed clones showed a homogenous population positive only for the multimer of interest reflecting the observations for the initially expanded T-cell lines.
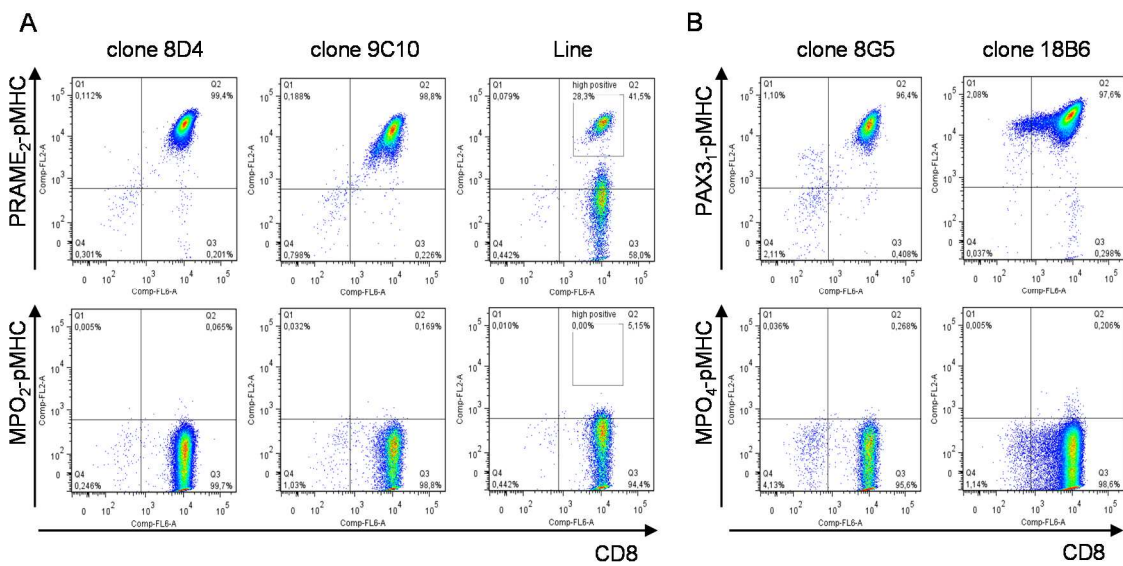
Figure 7: Staining of expanded T-cell clones with $PRAME_2$-pMHC or $PAX3_1$-pMHC.
(A) T-cell clones 8D4 and 9C10 and T-cell line HD2-$PRAME_2$-sort were stained with $PRAME_2$-pMHC or a control multimer. (B) PAX_3-reactive T-cell clones 8G5 and 18B6 stained with respective relevant or control multimer. Cells were gated on 7-AAD negative events and singlets.

Expanded T-cell clones 8G5 and 18B6, which showed recognition only of the $PAX3_1$ ligand in the initial screening, were further characterized regarding their functional reactivity (Figure 8). Detailed analyses revealed substantial reactivity against K562 and LCL (Figure 8A, B) although no PAX3-expression was detected by real-time PCR (Figure 5). Additionally, in contrast to the initial screening analysis, peptide-specific responses could not be reproduced, even not with excessive concentrations of peptide pulsed on target cells (Figure 8C, D). Therefore, isolation and characterization of this TCR was not further pursued.
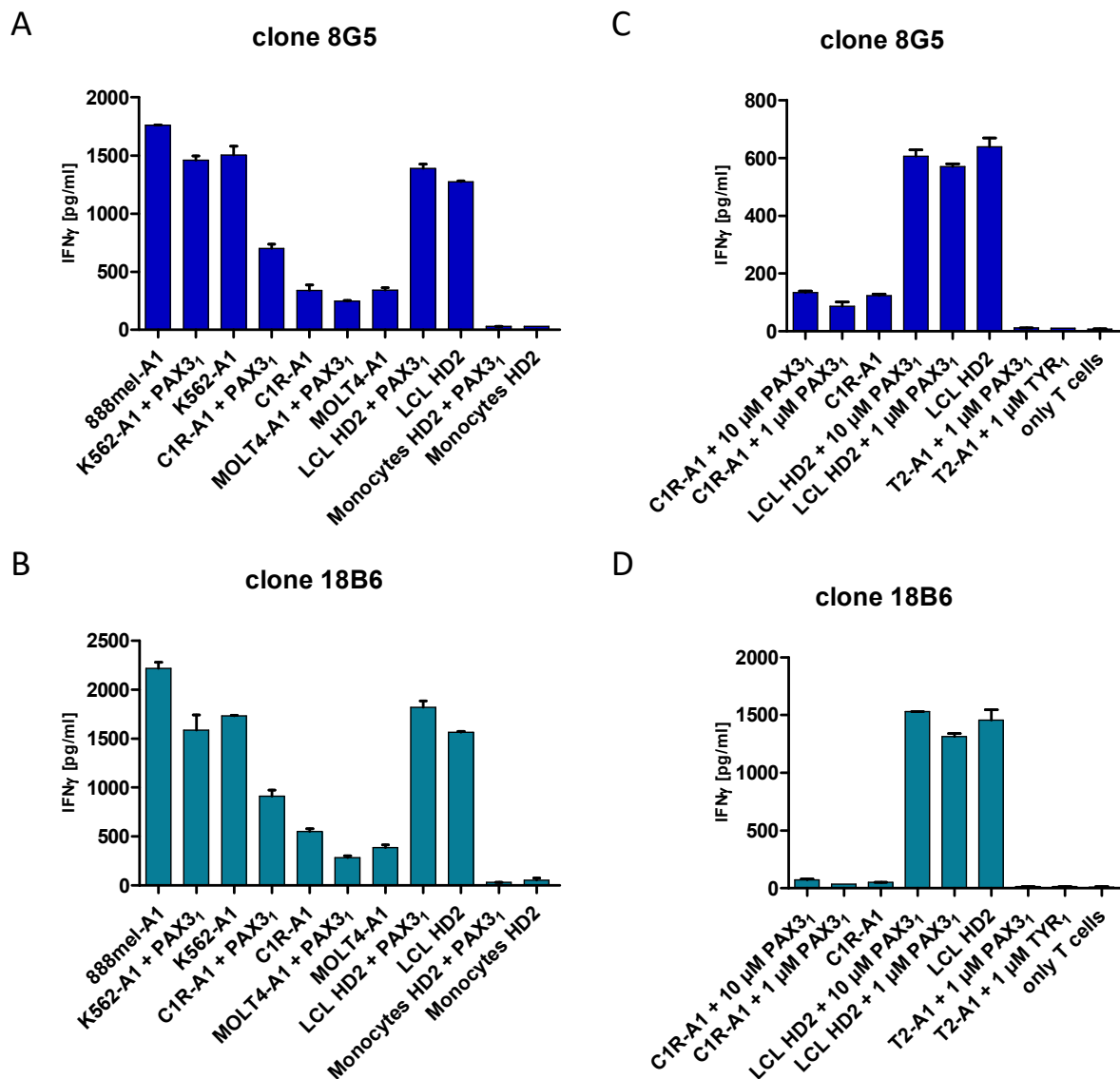
Figure 8: Analysis of tumor-and peptide-specific reactivity pattern of T-cell clones 8G5 and 18B6.
T-cell clones derived from the $PAX3_1$-pMHC sorted fraction were coincubated with different cell lines for analysis of antigen-specific IFNγ production (A, B). To assess peptide-specific recognition, effector cells were coincubated with target cells pulsed with different concentrations of the relevant HLA ligand (C, D).

The PRAME$_2$-specific T-cell clone 8D4 continued stable in-vitro expansion and showed strong peptide-specific IFNγ release (Figure 7). Therefore, this clone was used for detailed investigation of antigen-specific reactivity. 888mel and K562 transduced with the relevant restriction element and high endogenous PRAME expression (Figure 5) elicited strong reactivity, whereas cell lines with low to undetectable antigen expression, such as LCL, MOLT4-B7 and C1R-B7 cells merely evoked any IFNγ release (Figure 9A). Coincubation with peptide-pulsed target cells (Figure 9B) elicited only minor responses compared to the initial screening procedure, but it was unclear whether this was due to dampened functional capacity of the T-cell clone as a potential consequence of cellular exhaustion.
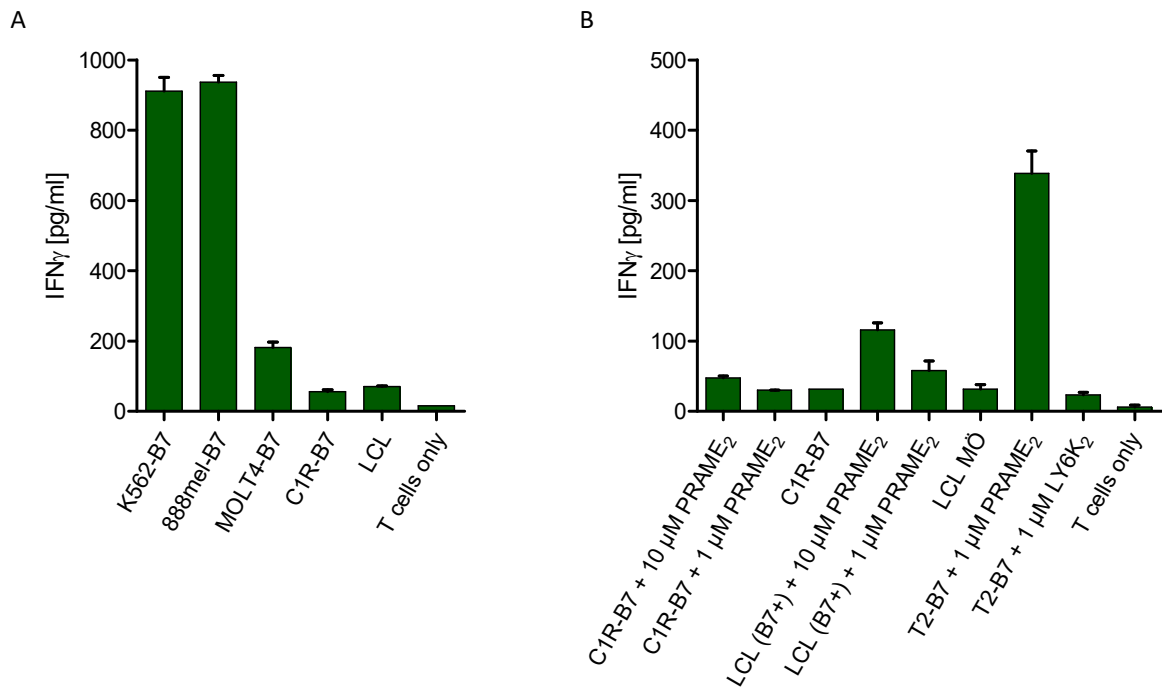
Figure 9: Reactivity pattern of T-cell clone 8D4.
Cocultures of effector cells with target cells lines with or without endogenous PRAME-expression (A) and peptide-pulsed targets (B). Analysis was performed in duplicates and IFNγ release was assessed by ELISA.

Due to reduced proliferation of T-cell clone 8D4, variable regions of TCR alpha and beta chains were determined by TCR repertoire PCR (2.2.3.4). Gel electrophoresis and sequencing of amplified products revealed specific bands for Va5/8 and Vb9, respectively. Table 35 shows detailed sequence information of isolated TCR chains.

Table 35: Sequence characteristics of PRAME$_2$-directed TCR 8D4

TCR	TRAV	TRAJ	CDR3α	TRBV	TRBJ	TRBD	CDR3β
8D4	6*02	22*01	CARPFFSGSARQLTF	3-1*01	2-2*01	D2*01	CASSQERSGVTGELFF

3.2.5 Functional characterization of TCR 8D4om

To further elucidate reactivity of PRAME$_2$-specific TCR 8D4, the optimized version TCR 8D4om was in silico constructed and synthesized (2.2.3.11). After cloning into pMP71, the optimized TCR construct was retrovirally transferred into human PBMC (2.2.5.2). TCR 2.5D6om was used as a control for TCR expression and functionality of each transduction. This TCR recognizes the HLA-B0702-restricted peptide ligand MPO$_5$ and has been isolated and characterized thoroughly by Richard Klar (Klar et al., 2014).

Binding of αTCRmu antibody was used as a correlate for expression of optimized TCR constructs (Mall et al., 2016; Weigand et al., 2012). Flow cytometry analysis revealed comparable transduction rates of both TCR (Figure 10). Specific multimer binding indicated correct pairing of introduced alpha and beta chain for each construct, as TCR 8D4om-transduced T cells only bound the PRAME$_2$-pMHC multimer, but not MPO$_5$-pMHC multimer. Vice versa, TCR 2.5D6om-transgenic cells only stained positive for MPO$_5$-pMHC, but did not bind PRAME$_2$-pMHC.

For the assessment of functional avidity of TCR 8D4om, effector cells were coincubated with titrated concentration of PRAME$_2$ ligand pulsed on T2-B7 (**Figure 11**). As expected, the relevant peptide elicited IFNγ release in a dose-dependent manner. However, substantial background reactivity was observed against T2 cells pulsed with the control peptide MPO$_5$. In comparison, TCR 2.5D6om-transduced cells showed a clear reactivity pattern and non-transduced T cells lacked any IFNγ secretion ruling out unspecific or allo-reactivity of respective PBMC used for transduction (**Figure 10**).

To further elucidate single determinants of peptide-dependent recognition, variants of the PRAME-2 ligand were synthesized containing substitutions at each single amino acid position either with Alanine or Threonine (Figure 12). Coincubation of TCR 8D4om-transduced T cells with T2-B7 pulsed with different peptide variants revealed a decreased recognition, if position 2 and position 7 were exchanged with irrelevant amino acids. However, all target cells evoked IFNγ secretion of TCR 8D4om-transgenic cells in contrast to TCR 2.5D6om-transduced or non-transduced cells, which showed a very clear profile against the same target cells. Again, this analysis indicated a relative unspecific activation of TCR 8D4om, pointing towards a rather HLA- than peptide-dependent reactivity.
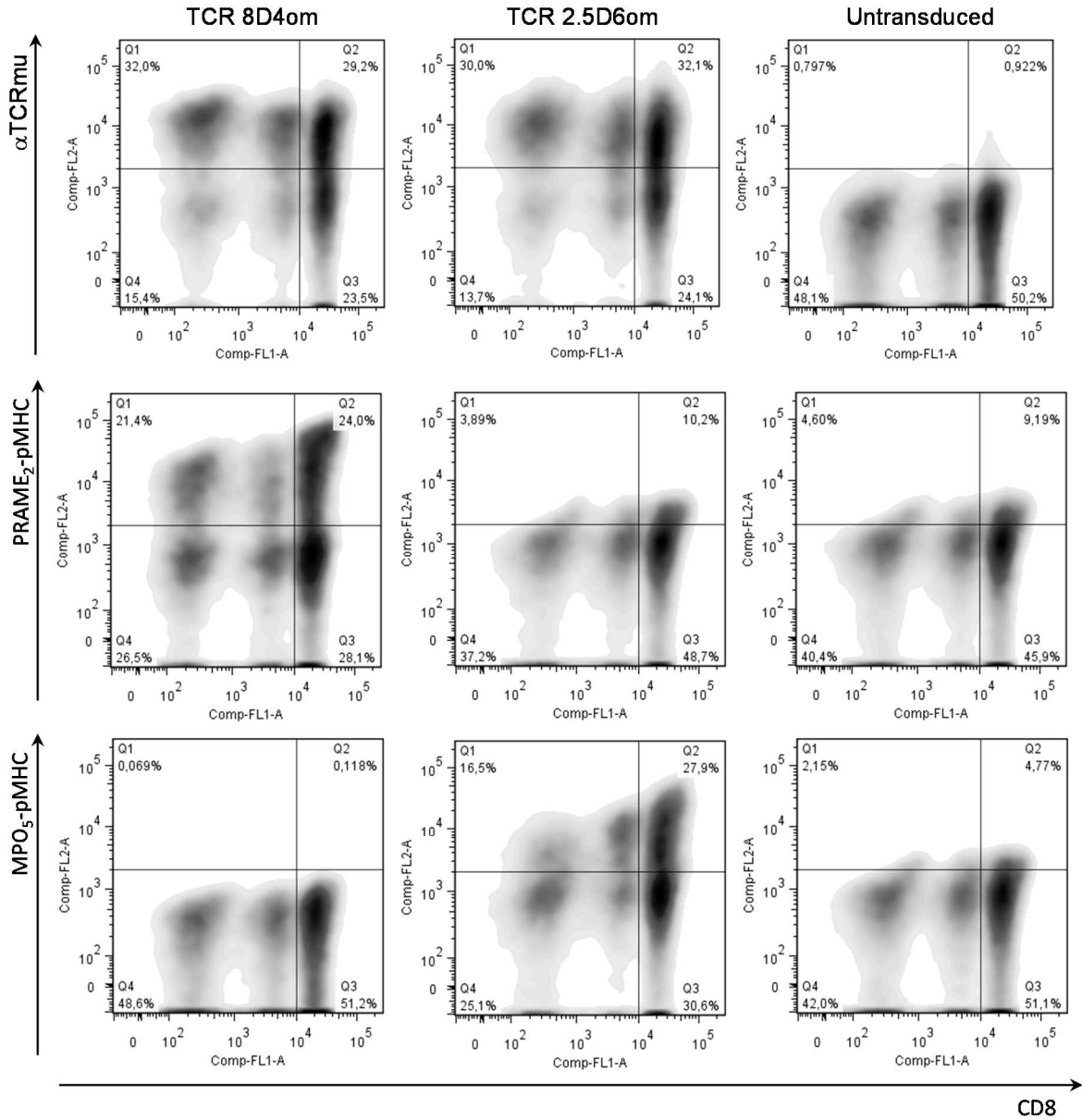
Figure 10: Expression analysis of transduced TCR constructs.
Cells were stained with αTCRmu or multimers PRAME$_2$-pMHC and MPO$_5$-pMHC and specific binding was assessed by flow cytometry. Cells were gated on 7-AAD negative events.
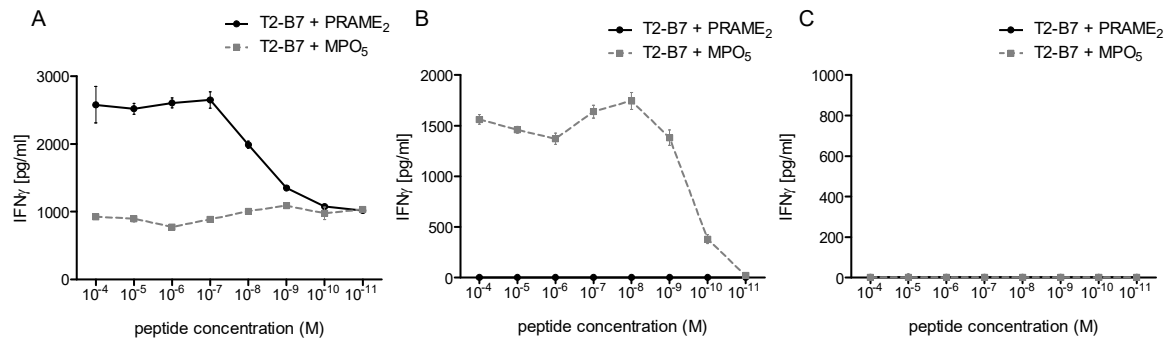
Figure 11: Peptide titration of PRAME$_2$.
IFNγ secretion of PBMC transduced with TCR 8D4om (A) or TCR 2.5D6om (B) or non-transduced PBMC (C) was assessed upon coculture with T2-B7 cells pulsed with titrated concentrations of PRAME$_2$ or MPO$_5$. Analysis was performed in triplicates and cytokine concentration was determined by ELISA.
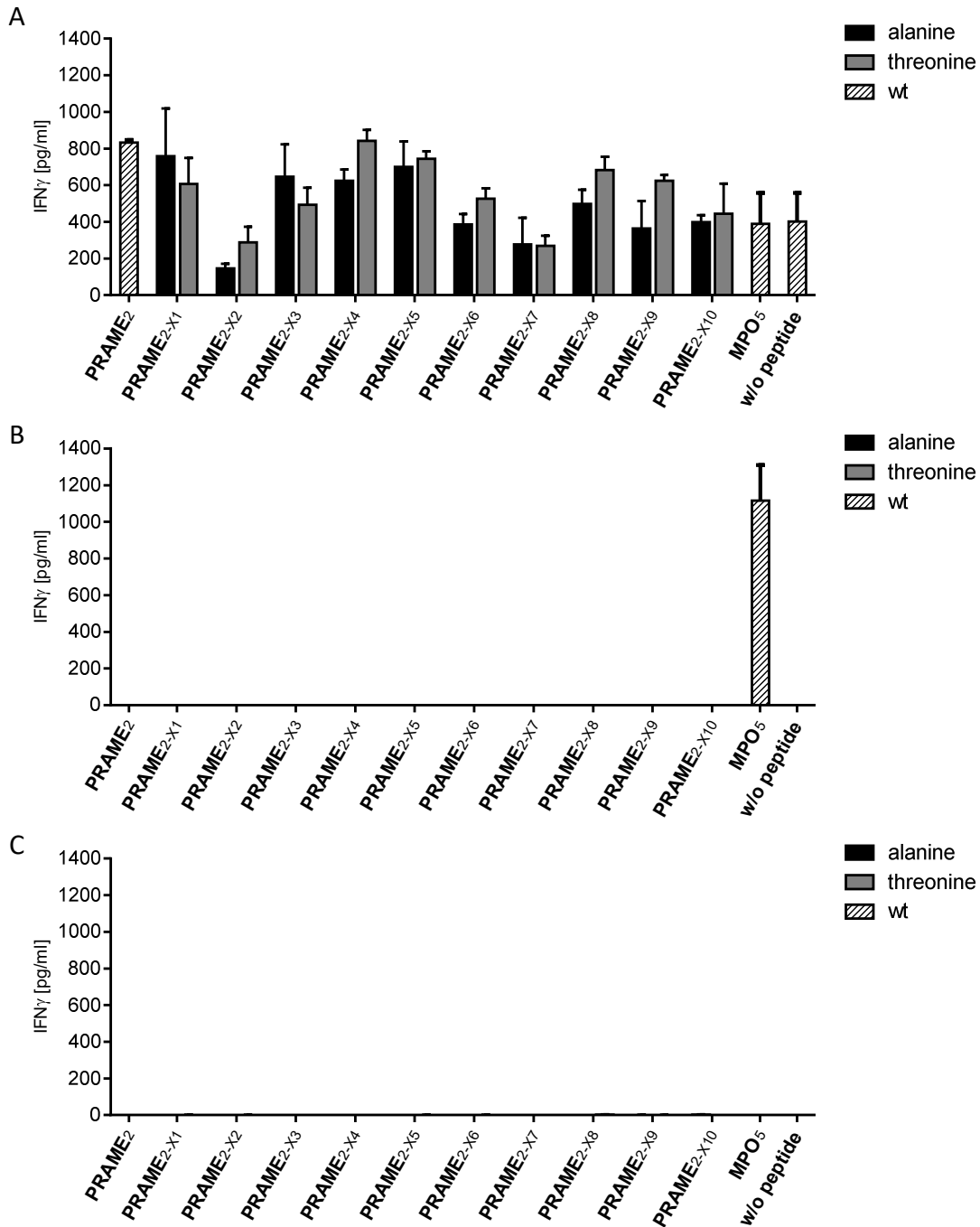
Figure 12: Reactivity scan of TCR 8D4om transduced cells against peptide variants of PRAME$_2$.
PBMC transduced with TCR 8D4om (A) or 2.5D6om (B) were coincubated with T2-B7 cells pulsed with variants of PRAME$_2$ containing amino acid exchanges with Alanine or Threonine as indicated (marked as an X). Non-transduced PBMC from the same donor were used as control (C). Analysis was performed in triplicates and IFNγ release was determined by ELISA.

TCR 8D4om-transgenic PBMC were further analyzed with regard to their capability to recognize target cells expressing the antigen of interest, i.e. PRAME. Therefore, transduced effector cells were incubated with a panel of different cell lines (Figure 12Figure 2). As expected, K562-B7 and 888mel-B7 were efficiently recognized by TCR 8D4om and additional peptide-pulsing of 888mel-B7 did not increase specific IFNγ response indicating maximal stimulation by unpulsed 888mel (Figure 13A). Reactivity against peptide-pulsed T2 cells revealed preferential activation by PRAME$_2$-presenting

targets despite a substantial reactivity against T2-B7 pulsed with MPO$_5$. Coincubation of effector cells with antigen-transduced LCL and ML2-B7 did not show a marked difference between PRAME-negative and -positive cell lines (Figure 13B).
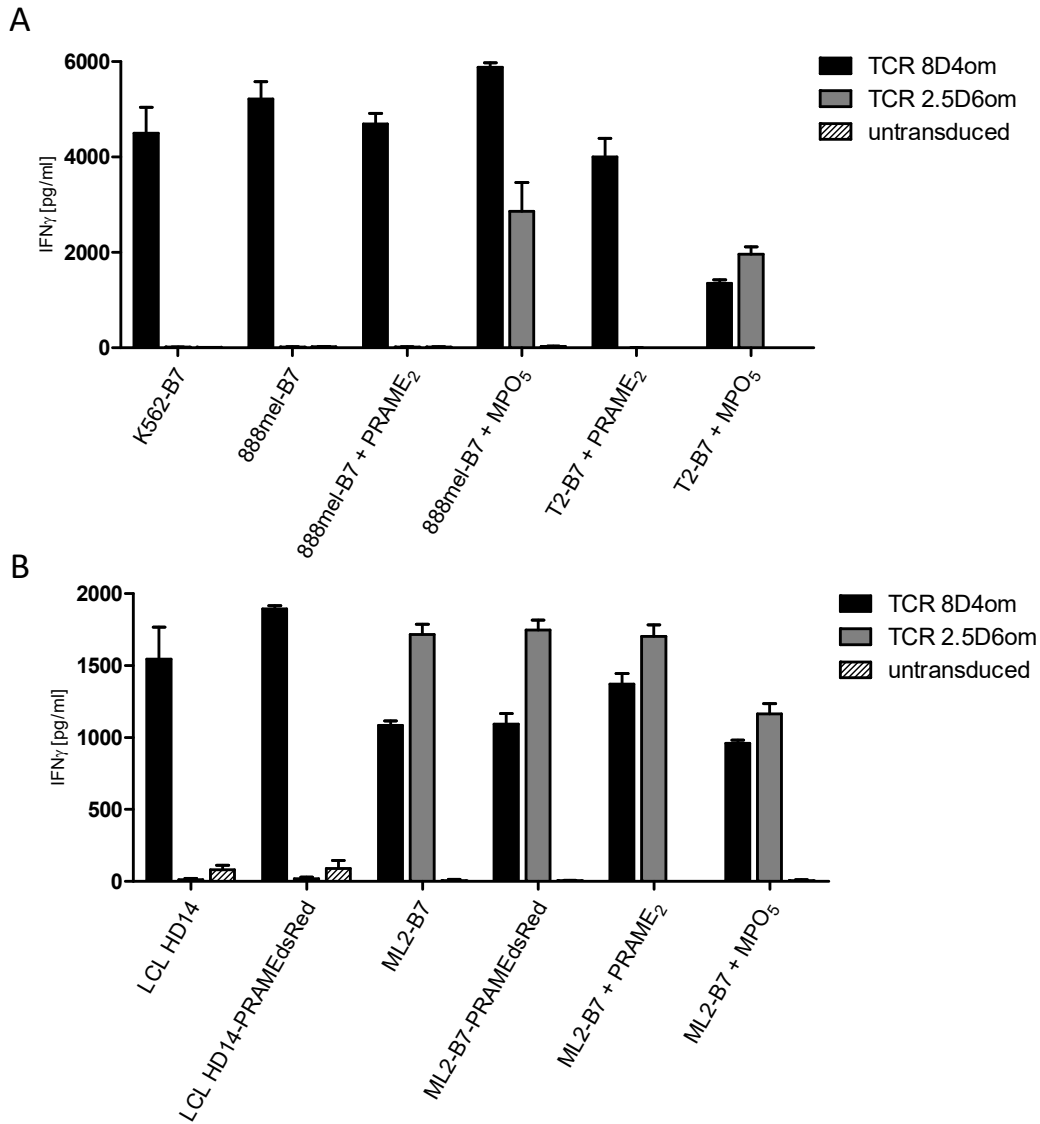
Figure 13: Recognition profile of TCR 8D4om-transduced T cells against different cell lines.
TCR-transgenic T cells were incubated with naturally PRAME-expressing target cells (A) or antigen-transduced cell lines (B). Peptide-pulsed conditions were included for confirmation peptide-specific reactivity and MPO-expressing ML2-B7 were used as positive control for endogenous target processing and presenting of peptide MPO$_5$ to TCR 2.5D6om.

For the assessment of potential fratricide of transduced effector T cells, TCR 8D4om was retrovirally transduced in PBMC obtained from an HLA-B0702 positive and negative healthy donor (Figure 14). Cell counts after transduction revealed mere expansion of TCR 8D4om-transduced HLA-B0702+ effector cells (Figure 14A), whereas PBMC derived from the HLA-B0702 negative donor proliferated comparably in direct comparison of all conditions (Figure 14B). Functional analysis TCR 8D4om transduced PBMC showed a clear reduction in IFNγ release upon specific stimulation when compared to reactivity of HLA-B0702 negative donor cells (Figure 14C, D).
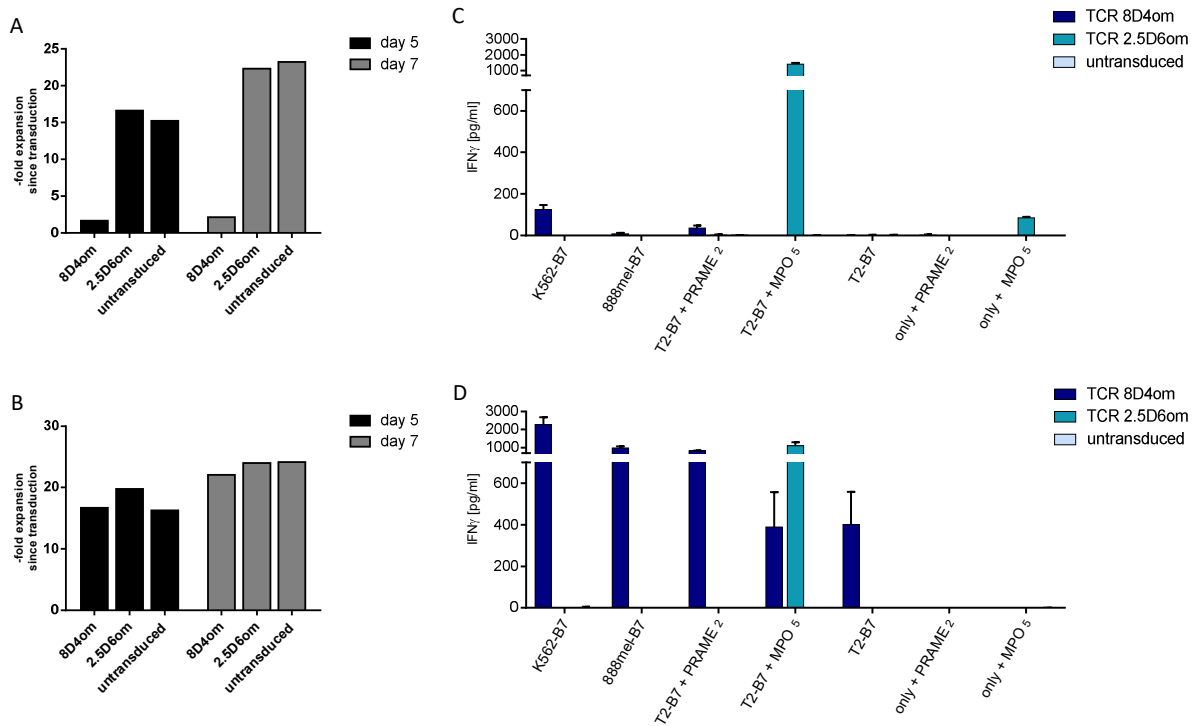
Figure 14: Analysis of TCR 8D4om-transduced T cells from an HLA-B0702 positive and negative donor.
(A) Proliferation of HLA-B0702 positive PBMC transduced with TCR 8D4om, 2.5D6om and non-transduced control was determined five and seven days after second transduction. (B) Proliferation of transduced cells from an HLA-B0702 negative donor. (C-D) IFNγ release of HLA-B0702 (C) positive or negative (D) transduced cells was analyzed upon stimulation with different target cells. Cocultures were performed in triplicates and IFNγ concentrations in supernatants were determined by ELISA.

Altogether, these results displayed an unexpected reactivity pattern of TCR 8D4om including undesired cross reactivity. Thus, this TCR was not further characterized.

3.3 Immune responses against mutated antigens

3.3.1 Identification of naturally presented mutated peptide ligands on primary tumor tissue by mass spectrometry

In order to explore the presence of mutated HLA ligands within the analyzed mass spectra, whole exome sequencing (WES) was performed in cooperation with AG Rad and used as patient-tailored database (3.1). Five patients, Mel5, Mel8, Mel12, Mel15 and Mel16, were selected for WES due to their clinical course (6.2) and availability of patient material. Performance of WES on healthy and diseased tissue resulted in the detection of eleven different mutated ligands in three patients (Table 36). Mass spectra of all mutated ligands were confirmed by production and mass spectrometric analysis of synthesized peptides.

Table 36: Mutated ligands naturally presented on primary melanoma tissue and detected by mass spectrometry

Mutated peptide	Sequence (Position)	a.a Alt	HLA allele Predicted affinity (nM; %rank; bind Level)	Patient	FDR	Reads Tumor Ref:Alt	Reads PBMC Ref:Alt
SYTL4^{S363F}	GRIAFFLKY	S363F	HLA-B* 27:05 (18.43 ; 0.6 ; SB)	Mel15	1%	29:9	51:1
RBPMS^{P46L}	RLFKGYEGSLIK	P46L	HLA-A* 03:01 (29.2 ; 0.15 ; SB)	Mel15	1%	63:18	122:0
SEC23A^{P52L}	LPIQYEPVL	P52L	HLA-B* 35:03 (436.2 ; 0.01 ; SB)	Mel15	1%	36:9	34:0
H3F3C^{T4I}	RIKQTARK	T4I	HLA-A* 03:01 (1614 ; 3.0 ; --)	Mel15	5%	48:6	63:0
NCAPG2^{P333L}	KLILWRGLK	P333L	HLA-A* 03:01 (32.6 ; 0.15 ; SB)	Mel15	1%	130:23	107:1
AKAP6^{M1482I}	KLKLPIIMK	M1482I	HLA-A* 03:01 (23.3 ; 0.1 ; SB)	Mel15	1%	56:20	108:0
MAPK3K9^{E689K}	ASWVVPIDIK	E689K	HLA-A* 03:01 (400.9 ; 1.2 ; WB)	Mel15	5%	24:6	41:0
ABCC2^{S1342F}	GRTGAGKSFL	S1342F	HLA-B* 27:05 (192.9 ; 0.7 ; WB)	Mel15	5%	27:10	50:0
NOP16^{P169L}	SPGPVKLEL	P169L	HLA-B* 07:02 (26.3 ; 0.12 ; SB)	Mel8	5%	80:11	90:0
GABPA^{E161K}	ETSKQVTRW	E161K	HLA-A* 25:01 (3231.1 ; 0.40 ; SB)	Mel5	5%	17:22	87:0
SEPT2^{Q125R}	YIDERFERY	Q125R	HLA-A* 01:01 (6.0 ; 0.01 ; SB)	Mel5	5%	107:77	148:0

3.3.2 Immune responses in patient Mel15

Patient Mel15 showed up with an interesting clinical course, as he responded well to Ipilimumab therapy in 11/2013 except for one abdominal metastasis. This tumor lesion was resected and analyzed by mass spectrometry resulting in the detection of eight mutated ligands (Table 36). Blood withdrawals were taken 532, 546, 740, 796 and 839 days after first Ipilimumab application and were analyzed for specific T-cell reactivity (Figure 15).
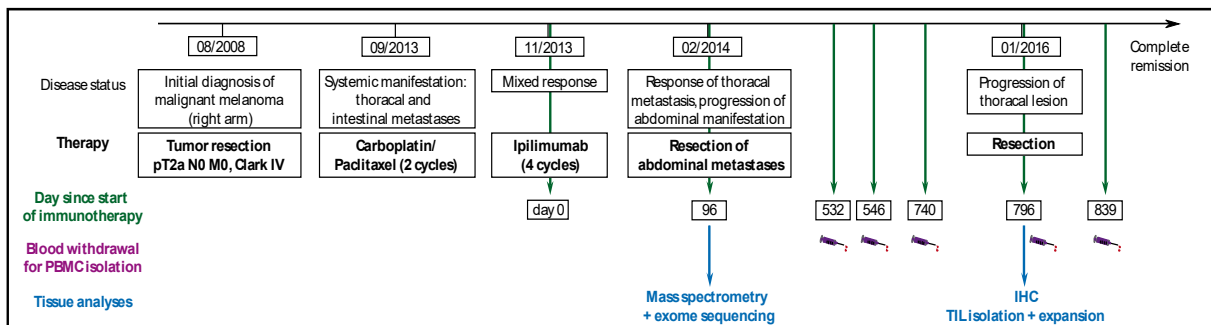
Figure 15: Clinical course of patient Mel15 and time points of sample collection.

Therefore, PBMC were stimulated in a mixed co-culture using the accelerated-coculture DC approach (2.2.2.3). Responses against mutated peptide ligands were assessed at an early time point (2 days after peptide addition) and at a second time point after in-vitro expansion (Figure 1). Analysis of an early T-cell response two days after peptide-specific in-vitro stimulation resulted in the detection of responses against epitopes SYTL4^{S363F} in several blood samples as shown by ELIspot analysis (Figure 16).
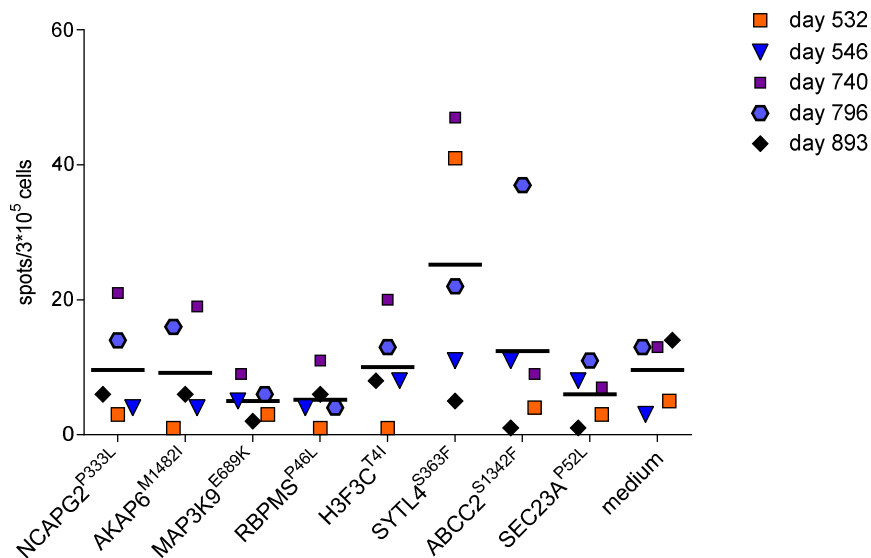
Figure 16: Early immune responses of peptide-stimulated PBMC.
Cytokine release of patient-derived PBMC from different blood withdrawals was analyzed two days after peptide addition by IFNγ ELIspot.

Ten to 14 days after peptide-specific in-vitro stimulation, expanded T-cell lines were analyzed again for specific reactivity by coculture with targets cells bearing respective HLA restriction element and pulsed with relevant mutated or irrelevant peptides. Responses against NCAPG2^{P333L} and SYTL4^{S363F} were repeatedly observed in samples from different time points of blood withdrawal, whereas no significant responses could be detected for the other mutated peptides (Figure 17). In total, two out of eight mutated ligands elicited immune responses after stimulation using the accelerated-cocultured DC approach.
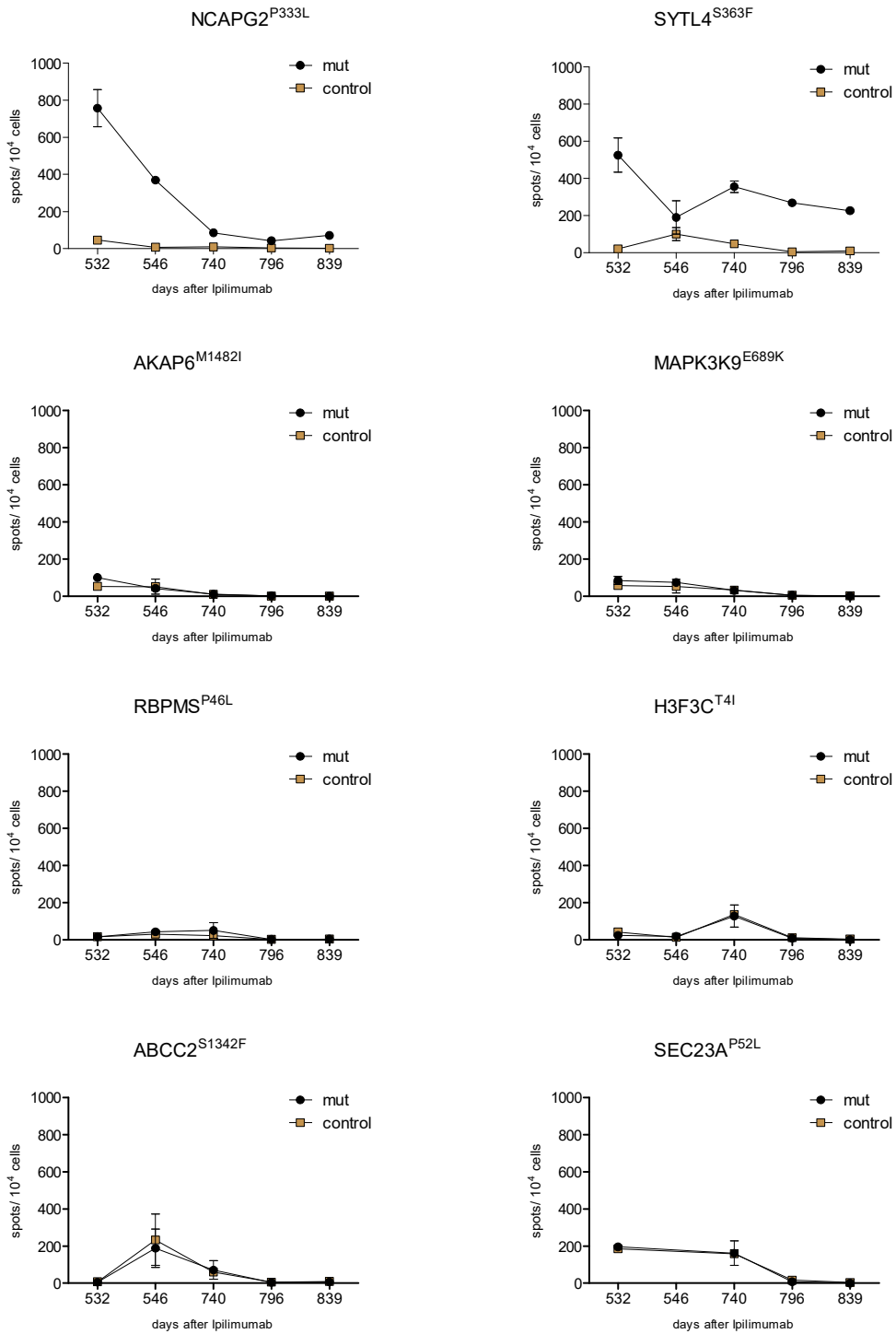
Figure 17: IFN-γ release of expanded T-cell lines derived from different time points of blood withdrawal against target cells pulsed with respective mutated peptide ligands.

After in-vitro expansion, pre-stimulated T-cell lines were coincubated with target cells expressing respective HLA restriction element and pulsed with the relevant mutated peptide or an irrelevant control peptide. IFNγ release was analyzed by ELIspot and cocultures were performed in duplicates.

For analysis of multifunctionality, NCAPG2^{P333L} and SYTL4^{S363F}-stimulated T-cell lines from bloodwithdrawals of day 546 and 740 were analyzed for the secretion of multiple cytokines upon stimulation with peptide-pulsed target cells. A distinct population of neoepitope-reactive T cells was detected in both T-cell lines (**Figure 18**).
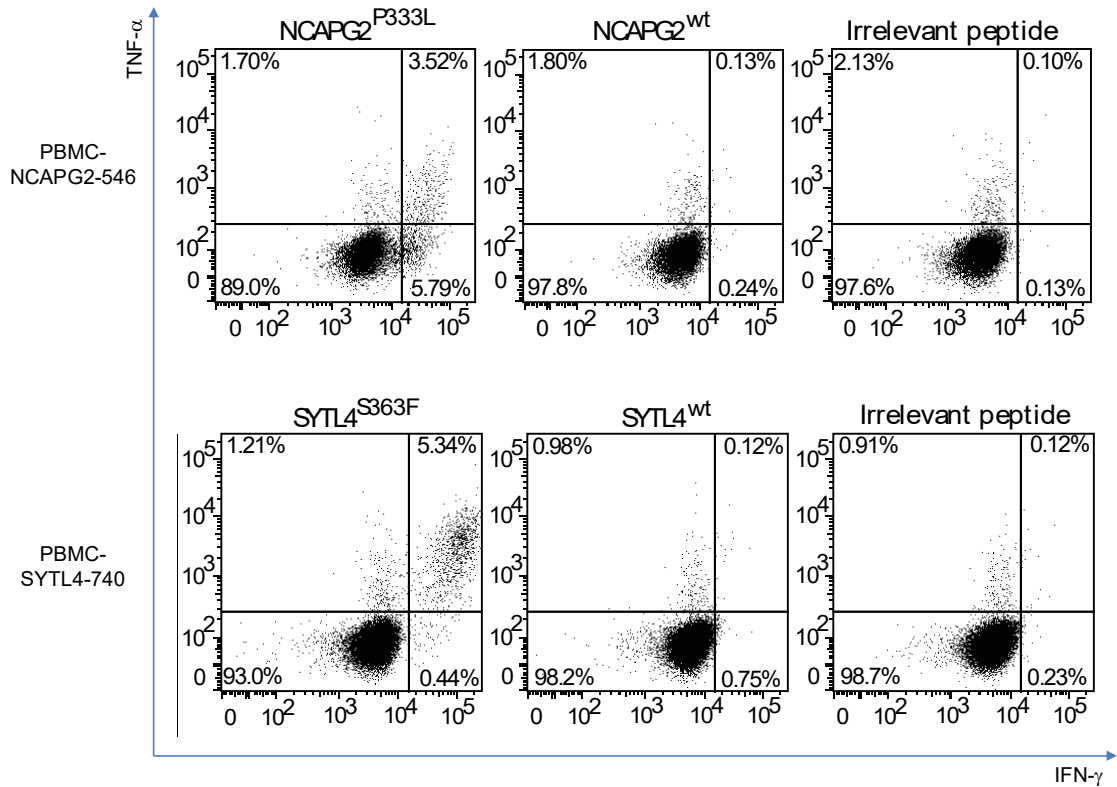
Figure 18: Dual cytokine production of expanded T-cell lines PBMC NCAPG2-546 and PBMC-SYTL4-740.
Effector cells were coincubated with peptide-pulsed target cells and analyzed for production of IFNγ and TNFα by intracellular staining of cytokines and flow cytometric analysis. Cells were gated on EMA negative and CD8 positive cells.

As a correlate to peptide-specific reactivity, multimer staining of line PBMC-NCAPG2-546 revealed a proportion of 14.2% of viable cells binding NCAPG2^{P333L}-pMHC multimer (Figure 19).
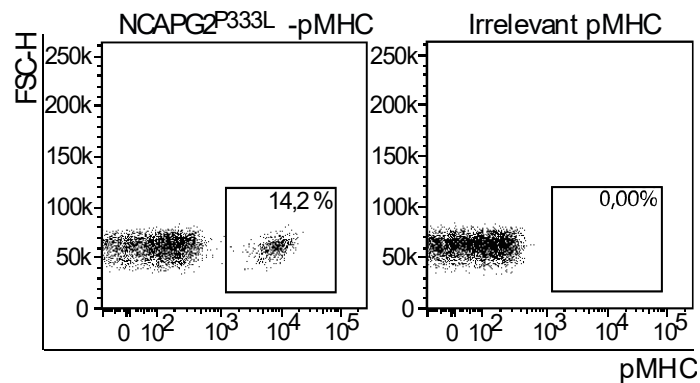
Figure 19: Multimer staining of T-cell line PBMC-NCAPG2-546.
Cells were gated on 7-AAD negative events.

Due to progression of one residual lung metastasis of patient Mel15 until 12/2015, this singular lesion was resected (Figure 15). Tumor tissue that was not used for diagnostic purposes was processed as described above (2.2.1.1). For analysis of in-vitro recognition of freshly isolated tumor tissue, digested or minced tumor material was coincubated either with freshly isolated PBMC or with T-cell line PBMC-SYLT4-740 (Figure 20). IFNγ secretion was observed when T cells pre-stimulated with SYTL4^{S363F} were used, but not after coincubation of PBMC with cut or digested tumor tissue, indicating tumor recognition only by the peptide-stimulated T-cell line.
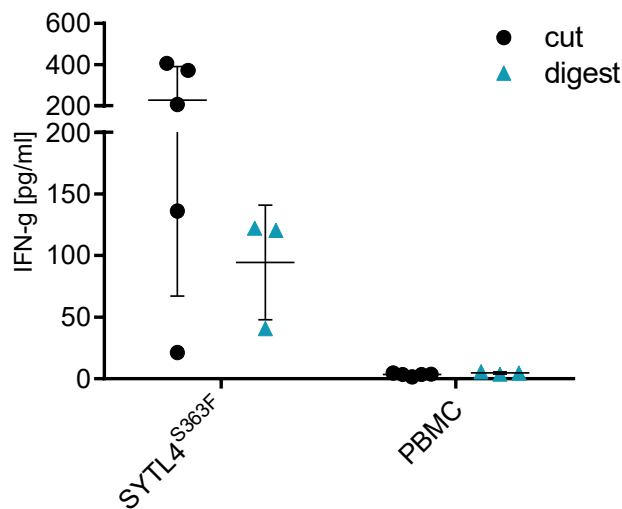
Figure 20: Coincubation of fresh tumor material with T-cell line PBMC-SYTL4-740.
IFNγ secretion of peptide-stimulated and expanded line PBMC-SYTL4-740 on co-culture with cut (5 wells) or digested (3 wells) fresh tumor material for 36 hours. Non-stimulated PBMC from Mel15 (day 796) served as controls.

Tumor material from the resected lung metastasis was analyzed with regard to the persistence of respective mutation on the genomic and transcriptomic level. PCR products derived from tumor cDNA and gDNA contained the mutated version containing thymine instead of cytosine (Figure 21). As a control, the altered base could not be detected in PBMC from Mel15.

G G C A G G A T T G C C T T T T C C C T G A A G T A T
                                 T

G   R   I   A   F   S   L   K   Y
G   R   I   A   F   F   L   K   Y
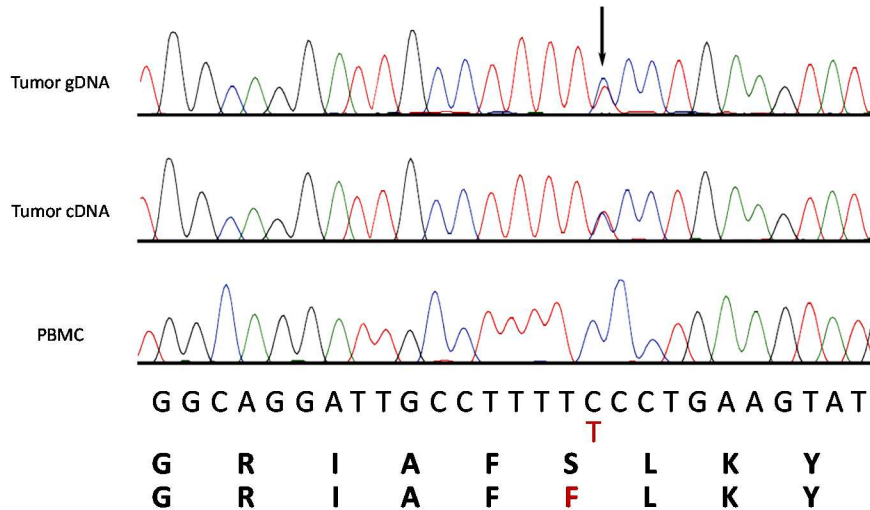
Figure 21: Sanger sequencing of the SYTL4-coding region in tumor-derived gDNA and cDNA.
Reverse transcribed PBMC from patient Mel15 served as control. Black arrow marks the mutation C>T.

In parallel to analyses of tumor material, tumor-infiltrating lymphocytes (TIL) were isolated from the lung metastasis and in-vitro expanded (2.2.1.1). After 18 days, TIL were harvested and expression of different T-lymphocyte markers was assessed by flow cytometry (Figure 22). After expansion, CD3$^+$CD45$^+$ lymphocytes were predominantly CD8$^+$ (67.6%) and CD8$^+$ T cells were largely CD27$^+$CD28$^+$. ELIspot analysis of expanded TIL against different target cells pulsed with all mutated peptide ligands, which have been detected in the first metastasis (Table 36), revealed reactivity against the SYTL4^{S363F} epitope but not against other mutated ligands (Figure 23).
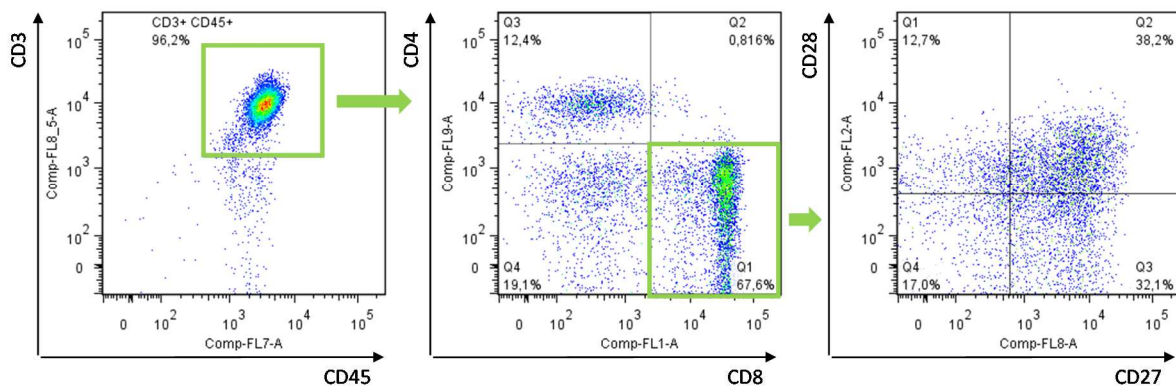
Figure 22: Surface staining of TIL after in vitro expansion.
Cells were phenotyped using T-cell and activation markers. Gating was performed on 7-AAD negative events.
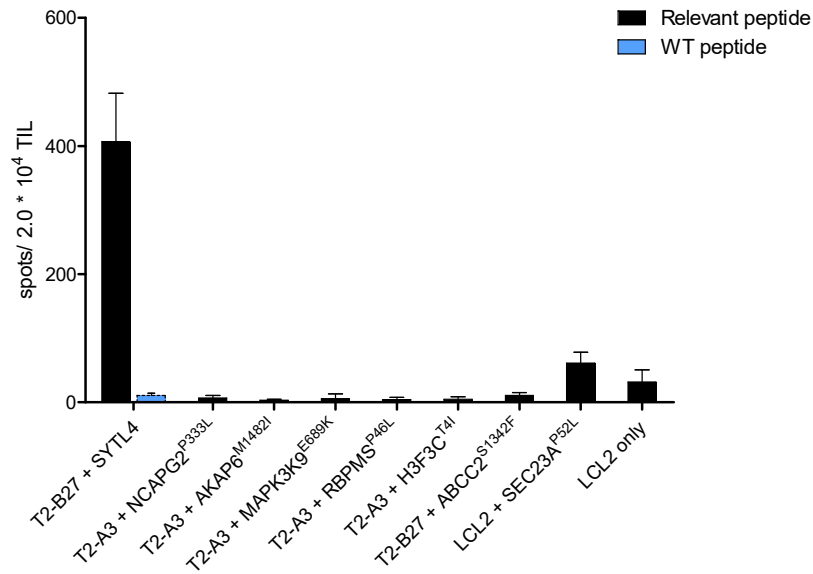
Figure 23: IFNγ release upon stimulation of expanded TIL with peptide-pulsed target cells.
TIL were incubated with target cells expressing respective HLA restriction element and pulsed with mutated peptides. SYTL4^WT peptide was included as control ligand for neoepitope SYTL4^S363F. Analysis was performed in duplicates and reactivity was assessed by IFNγ ELIspot.

Intracellular cytokine staining upon stimulation with peptide-pulsed LCL or T2-B27 cells showed a proportion of 4.38 % and 3.67 % of T cells producing both cytokines, IFN-γ and TNF-α, in response to mutated SYTL4^S363F ligand (Figure 24), indicating multifunctional reactivity of mutation-specific T cells. In contrast, only background cytokine production was observed for target cells pulsed with wild-type or irrelevant peptide.
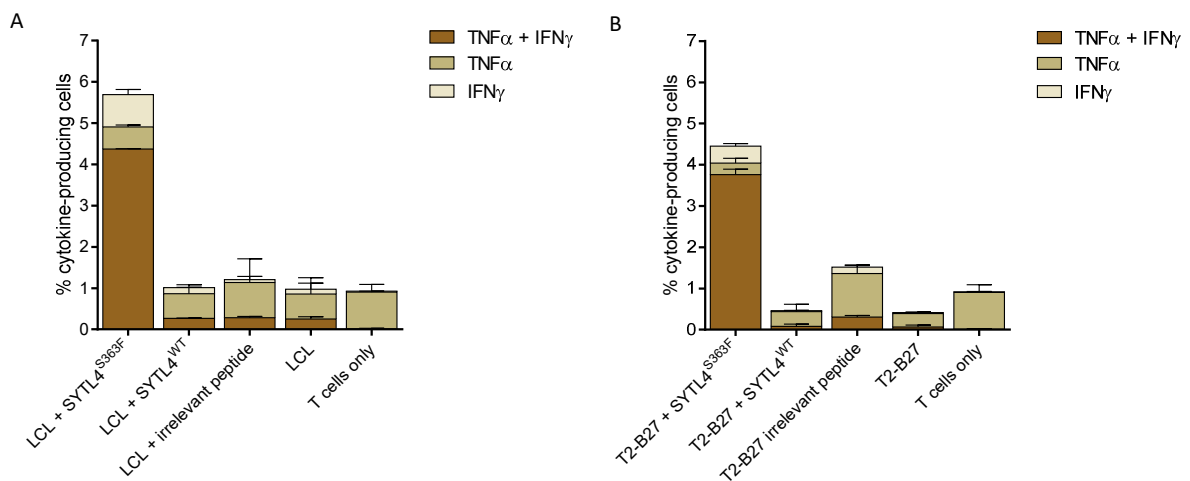
Figure 24: Cytokine production of TIL after stimulation with peptide-pulsed HLA-B2705 positive targets.
TIL were coincubated either with LCL1 (A) or T2-B27 (B) pulsed with SYTL4^S363F, SYTL4^WT or an irrelevant HLA-B2705-binding peptide. For the analysis of specific cytokine production, intracellular staining of TNFα and IFNγ was performed. Cells were gated on 7-AAD negative and CD8 positive events.

3.3.3 TCR repertoire diversity within neoantigen-specific T cells

To further investigate observed neoantigen-specific responses, expanded T-cell lines were sorted and cloned by limiting dilution. SYTL4^{S363F}-specific TIL were enriched for CD137-upregulated cells after coincubation with peptide-pulsed target cells (2.2.4.8). After expansion of cloned T cells, functional screening revealed peptide-specific reactivity in 27 of 63 analyzed clones (Figure 25).
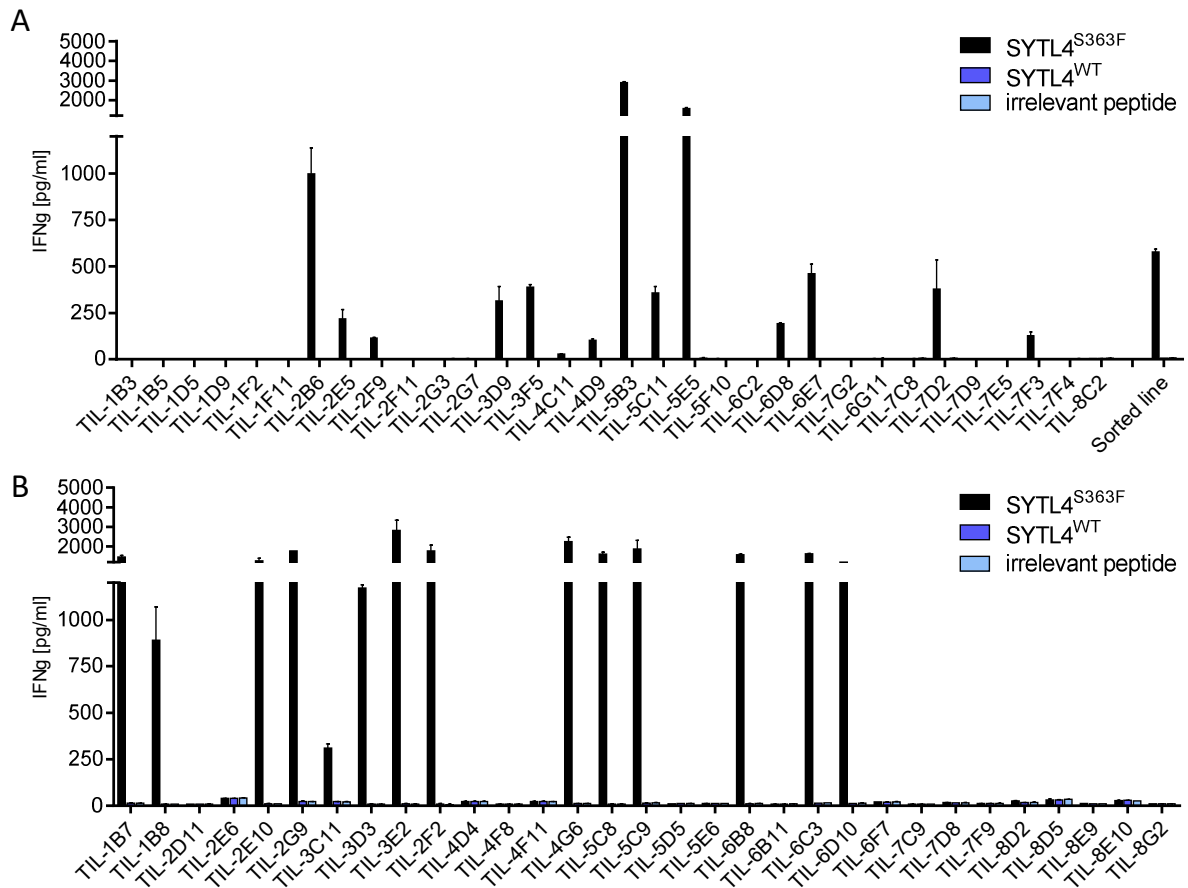
Figure 25: Functional screening of SYTL4^{3S63F} peptide-specific T-cell clones from expanded TIL.
Upon sufficient proliferation for functional assessment, 32 (A) and 31 (B) clones were coincubated with peptide-pulsed T2-B27 target cells and IFNγ–release was determined by ELISA. Analysis was performed in duplicates.

T-cell lines PBMC-NCAPG2-546 and PBMC-SYTL4-740 were sorted and cloned, resulting in detection of four reactive T-cell clones against NCAPG2^{P333L} and three clones against SYTL4^{S363F} (Figure 26).
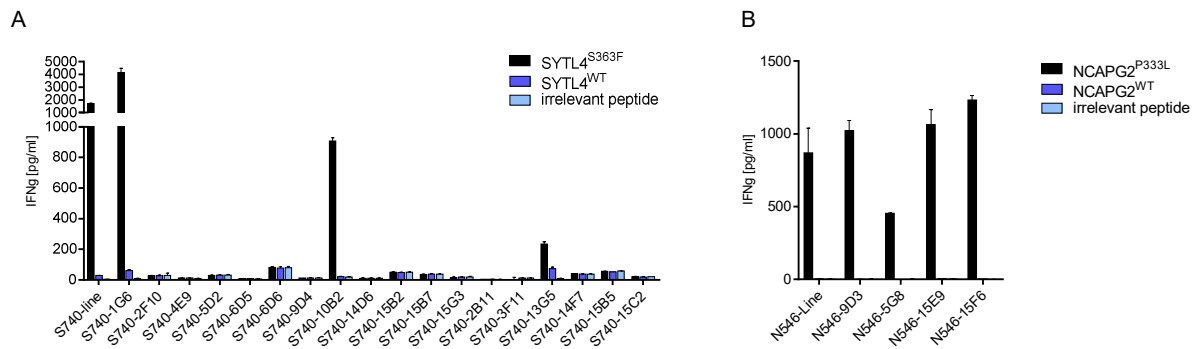
Figure 26: Reactivity T-cell clones derived from PBMC-stimulated cell lines against SYTL4^{S363F} and NCAPG2^{P333L}.
(A) Clones derived from T-cell line PBMC-SYTL4-740 were analyzed for immune responses against T2-B27 cells pulsed with SYTL4^{S363F}, SYTL4^{WT} or an irrelevant peptide. (B) Screening of IFNγ -release of T-cell clones derived from PBMC-NCAPG2-546 upon stimulation with peptide-pulsed T2-A3.

Of all clones exhibiting peptide-specific reactivity, mRNA was isolated and whole TCR repertoire was initially performed for selected clones (TIL-4D9; S740-1G6, S740-10B2 and S740-13G5; N546-9D3). TCR chains of remaining T-cell clones were detected by amplification with expected variable primer or using degenerated TCR primers (2.2.3.4) leading to the identification of six distinct pairs of TCR alpha and beta chains directed against SYLT4^{S363F} deriving either from TIL or peripheral blood cells (PBCs) of Mel15 and one TCR against NCAPG2^{P333L} (Table 37).

Table 37: Characteristics of T-cell clones directed against SYTL4^{S363F}

TCR	TRAV	TRBV	Number of clones
SYTL4-TIL1	38-2/DV8*01	TRBV7-8*01/*03	25
SYTL4-TIL2	35*02	TRBV27*01	1
SYTL4-TIL3	25*01	TRBV7-3*01	1[9]
SYTL4-PBC1	9-2*01/*02	TRBV6-2*01/6-3*01	2
SYTL4-PBC2	8-3*01	TRBV12-3	1
SYTL4-PBC3	12-3*01	TRBV9*01/9*02	1[10]
NCAPG2-PBC1	12-2*02	TRBV15*02	4

A few clones continued in-vitro proliferation and were therefore analyzed in detail with regard to their epitope-specific recognition. T-cell clones TIL-7D2 and TIL-2F9 were coincubated with LCL transduced with the mutated, wild-type or an irrelevant minigene to assess their reactivity against endogenously processed epitopes (Figure 27).

---

[9] Detected as second TCR alpha + beta chain pair in "clone" TIL-5B3 next to TCR SYTL4-TIL1
[10] Detected as second TCR alpha + beta chain pair in "clone" TIL-13G5 next to TCR SYTL4-PBC1

A

B
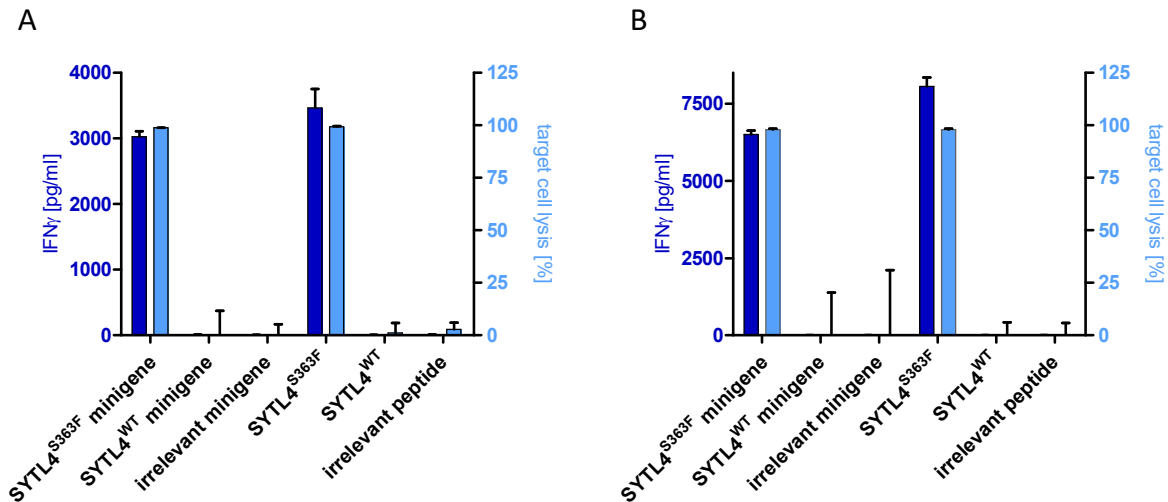
Figure 27: Cytotoxic T-cell response of TIL-derived clones against SYLT4^{S363F}.
T-cell clones TIL-7D2 (A) and TIL-2F9 (B) were coincubated with peptide-pulsed or minigene-transduced LCL1. IFNγ release (left y-axis) was assessed by ELISA and lysis of target cells (right axis) was determined by flow cytometry in relation to cocultures of T cells with LCL without any additional target presentation.

Pentamers were used for the determination of specific multimer binding (Figure 28). Staining with different dilutions was performed to determine the optimal concentration. With respect to an optimal staining intensity of specific versus unspecific population, 2.5 µl Pentamer showed best staining pattern. However, T-cell clone TIL-7D2 bound the SYTL4^{WT}-pMHC Pentamer as well and several repetitions (n = 3) showed the same results. Of note, control staining with an HLA-B2705 positive donor did not reveal unspecific binding of either Pentamer.

The identified TCR single chains were in silico reconstructed and cloned together with Yinshui Chang as focus of his Master's thesis. Functional analysis of cloned constructs revealed expected reactivity of SYTL4-TIL1, -TIL2, -PBC1, -PBC2 and NCAPG2-PBC1, but no functionality using cloned TCR constructs SYTL4-TIL3 and -PBC3. Further characterization of optimized constructs is currently ongoing.
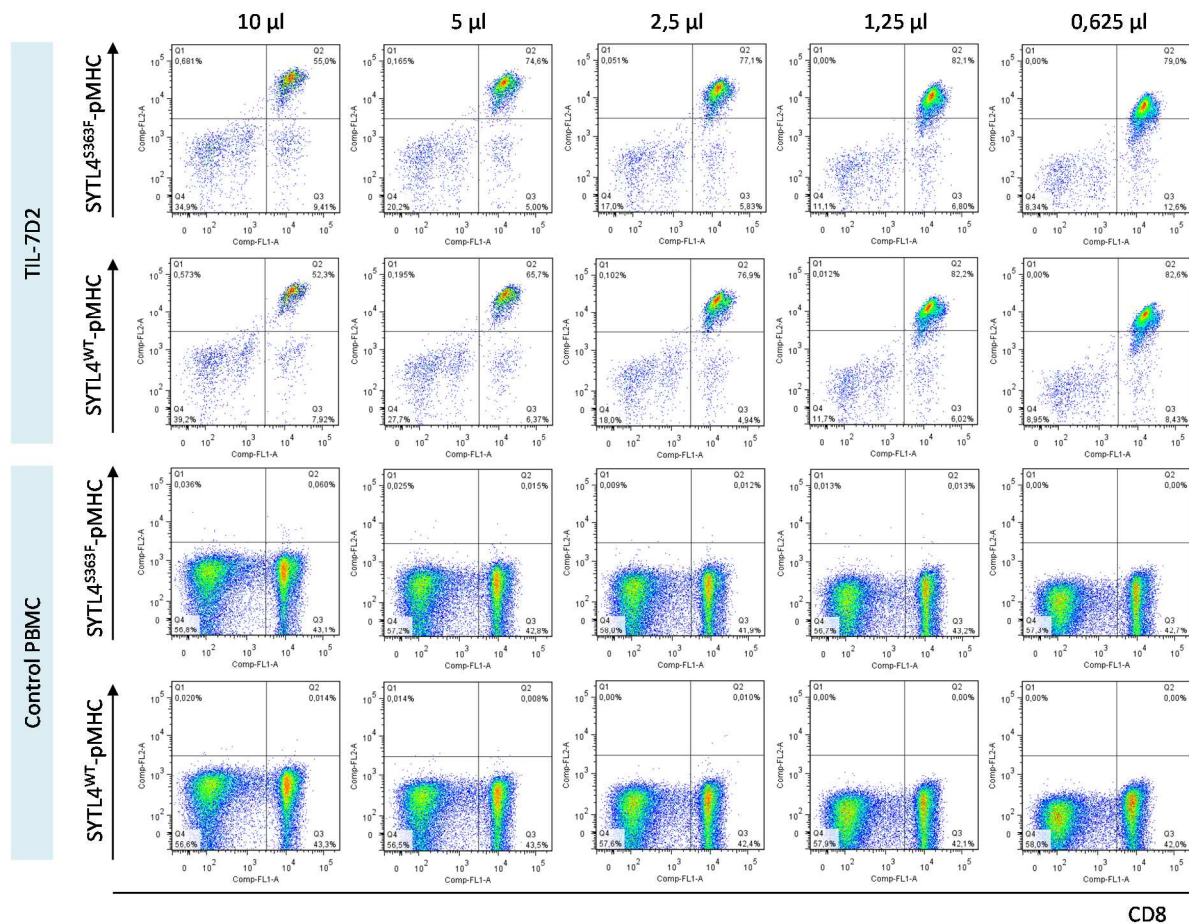
Figure 28: Pentamer staining of T-cell clone TIL-7D2.
Titrated concentrations of Pentamers exhibiting the mutated or wild type ligand were used. PBMC from an HLA-B2705 positive healthy donor served as negative control. Cells were gated on 7-AAD negative and CD3 positive events.

3.3.4 Monitoring of TCR frequencies using quantitative real-time PCR

To monitor presence and frequency of each individual TCR, a quantitative PCR specific for CDR3 regions of all constructs of interest was established. TCR beta chains cloned into MP71-eGFP (by Yinshui Chang) were used as standard curves to calculate the number of copies of specific TCR reads in comparison to total reads of the TCR beta constant region. The efficiency of each CDR3-specific probe was compared to the amplification of the control fragment spanning the TCR beta constant region (Figure 29).

Sensitivity of the applied protocol was determined with primer and probes specific for TCR SYTL4-TIL1 due to the availability of sufficient clone material for further analysis. To determine the technical limit of detection, cDNA derived from T-cell clone TIL-5C11, which expresses TCR SYTL4-TIL1, was diluted in cDNA from an unrelated donor and subjected to quantitative PCR (Figure 30).
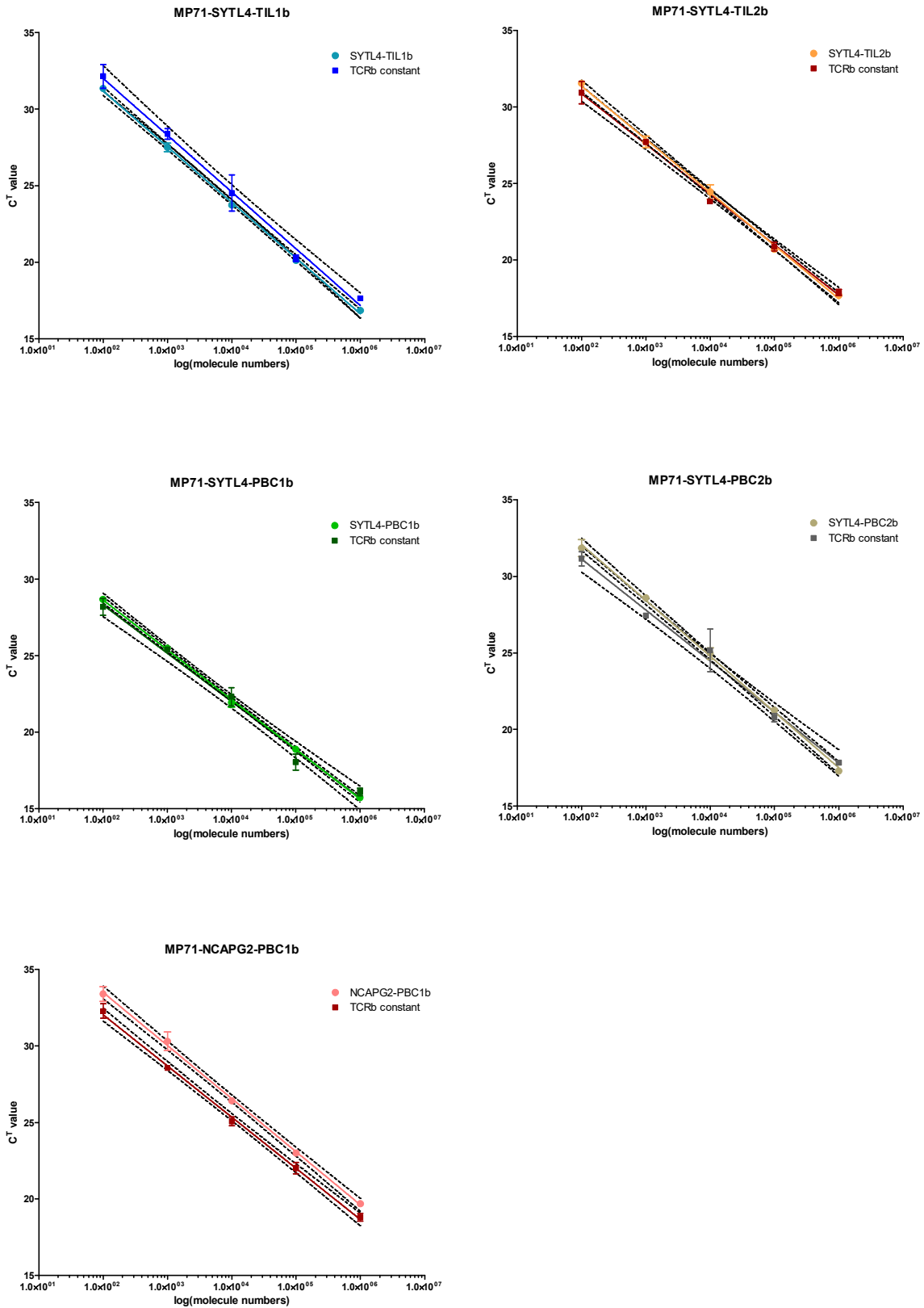
Figure 29: Dilution series of control vectors for absolute TCR quantification.
Cloned vectors of each TCR beta construct were diluted and quantification was performed with each specific primer and probe combination in comparison to the amplification of the constant region (TCRb constant). X-Axis: calculated number of molecules per well, y-axis: C_T value. Analysis was performed in duplicates.
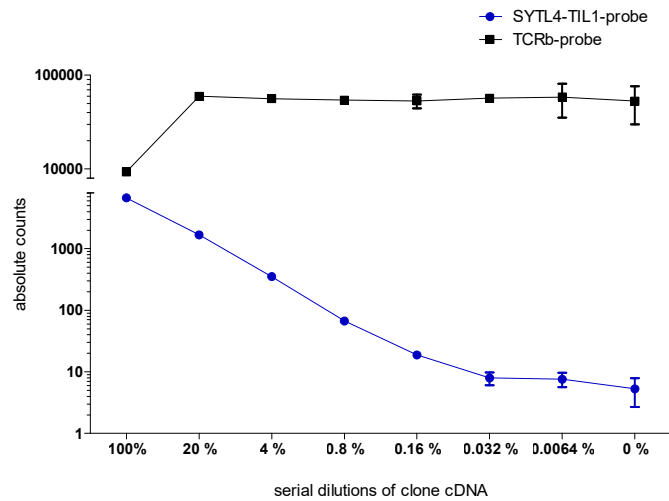
Figure 30: Detection of serial dilutions of cDNA from T-cell clone 5C11 expressing SYTL4-TIL1.
Serial five-fold dilutions were performed ranging from 20% to 0.0064% of specific clone-derived cDNA in relation to cDNA from control PBMC (HD1). Absolute numbers of templates were quantified according to a serial vector dilution run in parallel.

Next, variations in the initial isolation procedure were taken into consideration by performing several cell mixtures of T-cell clone TIL-7D2 (expressing SYTL4-TIL1 as well) as shown in Table 38. Mixtures were prepared twice and one series was used for RNA isolation with TRIzol reagent and gDNA from the second series was obtained as described (2.2.3.1). Quantification of specific TCR reads was performed for both, gDNA and cDNA (Figure 31).

Table 38: Cell mixtures containing serial dilutions of clone TIL-7D2

Cell mix	PBMC HD1	TIL-7D2	Percentage
1	1 Mio	100000	9,09091
2	1 Mio	50000	4,76190
3	1 Mio	10000	0,99010
4	1 Mio	5000	0,49751
5	1 Mio	1000	0,09990
6	1 Mio	500	0,04998
7	1 Mio	100	0,01000
8	1 Mio	50	0,00500
9	1 Mio	10	0,00100
10	1 Mio	5	0,00050
11	1 Mio	1	0,00010
12	1 Mio	0	0,00000
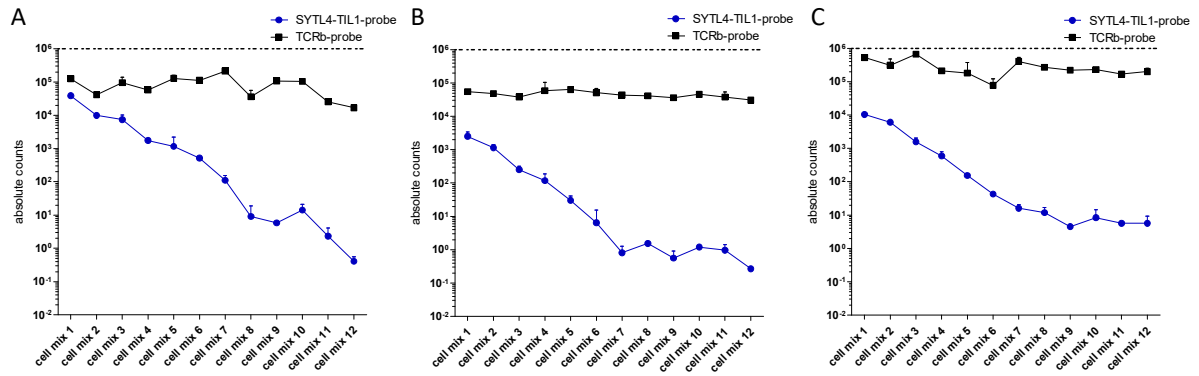
Figure 31: Detection of TCR SYTL4-TIL1 in cDNA and gDNA of cell mixtures.
A: cDNA, each well contained 5 ng of reverse transcribed RNA; B: gDNA, 10 ng/well; C: gDNA: 50 ng/well. TCR templates in different cell mixtures were quantified according to the vector standard curve run in parallel.

PBMC samples from different blood withdrawals were analyzed for the presence and frequency of previously isolated TCR with proven specificity (Figure 32). As expected, transcripts of TCR SYTL4-PBC1 and -PBC2 were detected in expanded T-cell lines from day 740. Apparently, TCR SYTL4-TIL2, originally isolated from expanded TIL was detected in this cell line as well, but was not identified among cloned T cells (Figure 26). All TCR of interest were also detected in stimulated T-cell lines from other time points of blood withdrawal (Figure 32A-D), which however were not analyzed on a clonal level. Regarding expanded TIL, amplification of all TCR chains was detected within the analyzed cDNA (Figure 32E-H). Due to the very limited amount of all material, analysis was only performed once.
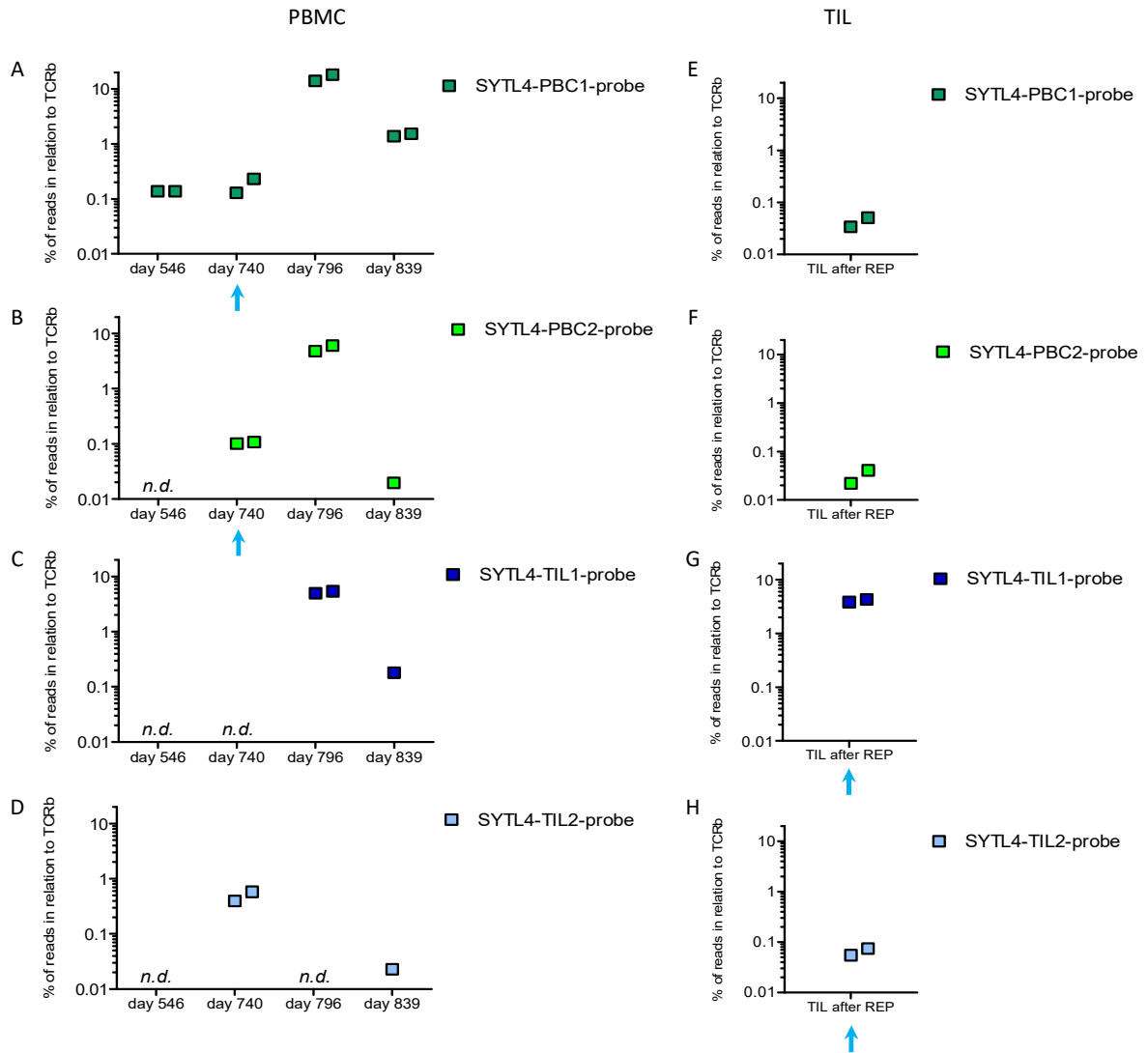
Figure 32: Detection of specific TCR sequences in peptide-stimulated PBMC and expanded TIL.
Quantitative real-time PCR was performed using cDNA from PBMC (A-D) or TIL (E-H) from patient Mel15 for the detection of all for identified TCR with confirmed specificity for SYTL4^{S363F}. A-D: Analysis of TCR frequencies in cDNA derived from peptide-stimulate expanded T-cell lines corresponding to analyzed lines at different time points of blood withdrawal (Figure 17). E-H: TCR frequencies in detected cDNA from TIL after in-vitro expansion (REP). All reads were calculated in relation to amplified products of the TCRβ constant region (TCRb). Blue arrows mark those conditions from which respective TCR were originally isolated; n.d.: not detected.

3.3.5 Stimulation of HLA-matched healthy donor-derived T cells with mutated ligands

For the assessment of the immunogenic capacity of identified peptides within HLA-matched healthy donors, respective HLA ligands were used for in-vitro stimulation of HD-derived naïve T cells as described (2.2.2.1). Table 39 gives an overview of all performed stimulations. T cells were used from healthy donors with matching HLA as predicted for each peptide. HLA types of all analyzed donors are listed in Table 2.

Table 39: Summary of in-vitro stimulations performed with HD-derived naive T cells

	HD1	HD5	HD6[11]	HD7	HD8	HD9	HD10	HD11	HD12	HD13
NCAPG2^{P333L}	X	X	X X		X	X	X			
AKAP6^{M1482I}	X	X	X X		X	X	X			
MAPK3K9^{E689K}	X		X			X	X			
SEC23A^{P52L}			X X	X						
RBPMS^{P46L}	X		X			X	X			
NOP16^{P169L}	X X	X			X	X			X	
GABPA^{E161K}										X
SEPT2^{Q125R}								X		
SYTL4^{S363F}							X			
H3F3C^{T4I}	X		X			X	X			
ABCC2^{S1342F}							X			

In two of 39 performed stimulation conditions, specific reactivity was observed against mutated peptides, NOP16^{P169L} and AKAP6^{M1482I} (Figure 33). Regarding NOP16, the T-cell line could not be further expanded. To confirm this observed immune response, a second approach of T-cell in-vitro priming from the same donor and time point of blood withdrawal was performed using cryopreserved PBMC from the same leukapheresis of HD1 as used for the initial stimulation procedure. However, previously observed reactivities could not be reproduced.

---

[11] This donor is named HD1 in the related publication
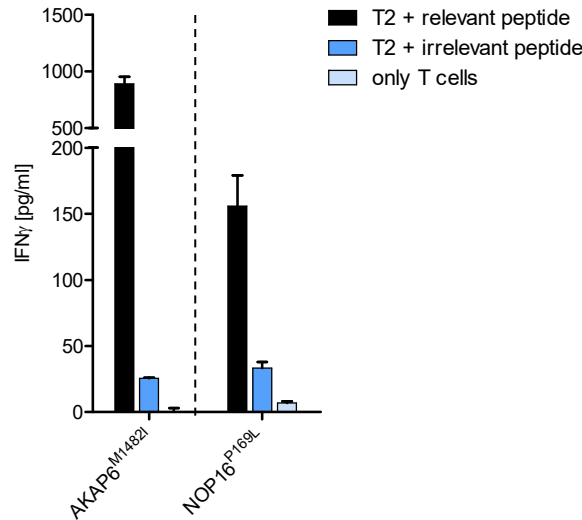
Figure 33: Immune responses of HD6- and HD1-derived T cells against AKAP6[M1482I] and NOP16[P169L].
Expanded T-cell lines were screened for specific reactivity against peptide-pulsed T2-A3 (AKAP6) or T2-B7 cells by IFNγ secretion. Analysis was performed in duplicates.

For the AKAP6[M1482I]-specific immune reactivity, T-cell line HD6-AKAP6 could be expanded to sufficient cell numbers for deeper analysis as described in the following section.

3.3.6 Expansion and characterization of AKAP6[M1482I] -specific T-cell line HD6-AKAP6

Multimer staining of the expanded T-cell line HD6-AKAP6 revealed specific binding only of the mutated, but not the wild type pMHC complex (Figure 34).
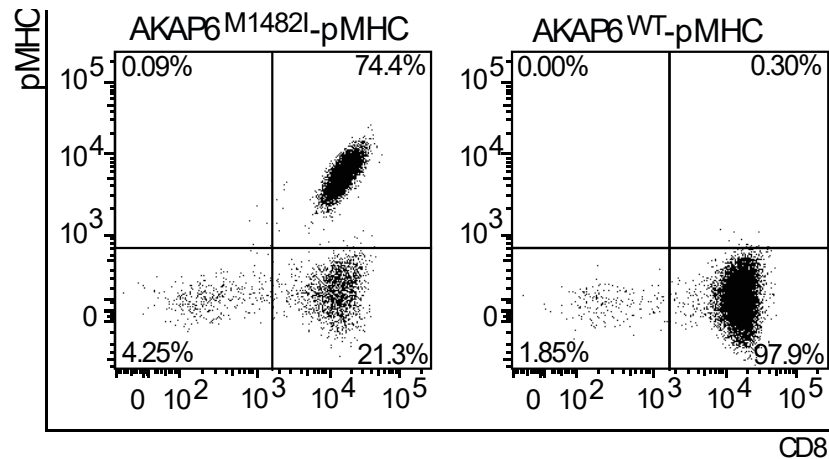
Figure 34: Multimer staining of T-cell line HD6-AKAP6.
Binding of T cells to multimers exhibiting either the mutated or the wild type AKAP6-derived epitope was analyzed by flow cytometry. Cells were gated on 7-AAD negative events.

To elucidate the functional avidity of AKAP6[M1482I]-specific T cells within T-cell line HD6-AKAP6, cells were co-incubated with T2-A3 pulsed with titrated concentrations of mutated AKAP6 ligand or its wildtype counterpart (Figure 34). Thereby, not only reactivity against the mutated, but also against the wild type peptide ligand was observed. EC_{50} was calculated as a measure for half-maximal

reactivity and amounted to 106.4 nM for AKAP6^{M1482I} and 1.678 µM for AKAP6^{WT} revealing an approximately ten-fold higher functional avidity against the neoepitope compared to the wild-type peptide.
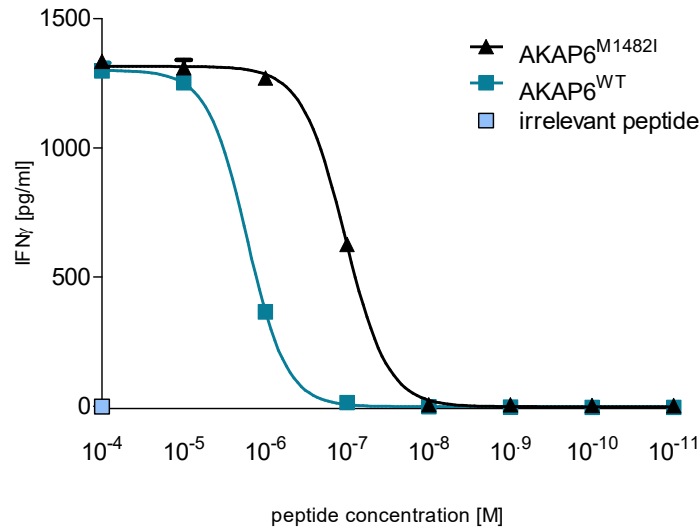
Figure 35: Functional avidity of T-cell line HD6-AKAP6.
IFNγ release was determined after coincubation with titrated concentrations of AKAP6^{M1482I} and its non-mutated counterpart using T2-A3 as targets.

The functional discrepancy between reactivity against the mutated and non-mutated peptide ligand was further confirmed by analysis of CD137 upregulation measured 24 hours after specific stimulation (Figure 36). Percentages of CD137$^+$CD8$^+$ T cells differed substantially between the neoepitope (87.6 %, MFI: 8143 in Q2) and its wild type counterpart (46.9 %, MFI: 5010 in Q2).
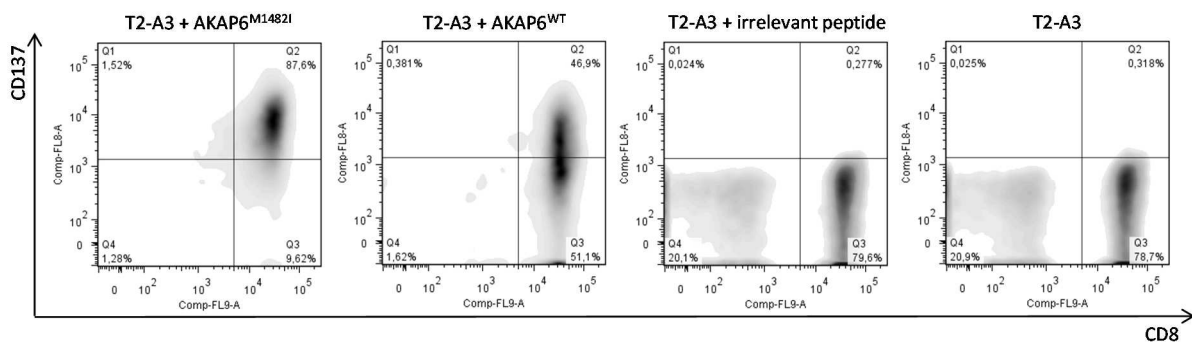
Figure 36: CD137 upregulation of cell line HD6-AKAP6 upon peptide-specific stimulation.
CD137 expression of stimulated T cells was analyzed 24 hours after coincubation with peptide-pulsed T2-A3. Effector cells were pre-gated for 7-AAD negative and CD3 positive events.

Reactivity against endogenously processed epitopes was confirmed by analysis of target cells transduced with minigenes coding for respective HLA ligand (Figure 37).
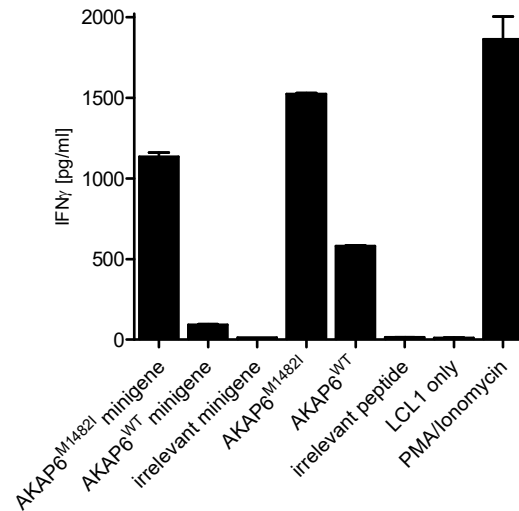
Figure 37: Recognition of endogenously processed epitope by T-cell line HD6-AKAP6.
IFNγ release of expanded T-cell line after coculture with LCL1 either transduced with different minigene constructs or pulsed with peptides.

Within this first analysis of minigene reactivity, 58.4% of LCL1-AKAP6^{M1482I}-minigene and 61.5% of LCL1-AKAP6^{WT} -minigene were DsRed positive. Therefore, only a part of coincubated targets actually expressed the minigene and respective epitope. Target cells were cloned for subsequent analysis and only target cell clones with a high, homogenous DsRed expression were used for further co-culture experiments.

T-cell line HD6-AKAP6 was further investigated for production of TNFα, IFNγ and IL-2 upon cocultivation with different target cells. Intracellular cytokine staining with peptide-pulsed or minigene-transduced LCL revealed distinct differences of quality regarding recognition of ligands of interest (Figure 38). Target cells presenting the mutated ligand, produced by minigene-expression or by exogenous peptide pulsing, elicited the highest amounts of produced cytokines. These effects were visible for the overall percentage of cytokine-producing T cells (56% and 49% after co-culture with AKAP6^{M1482I} minigene and AKAP6^{M1482I} peptide) as well as the fractions of effectors producing two or all three cytokines in parallel. Again, response against the wild-type minigene and peptide was observed as well, whereas to a lower extent, as 28% and 22% of T cells were stained positive after coculture with AKAP6^{WT} minigene or AKAP6^{WT} peptide, respectively.
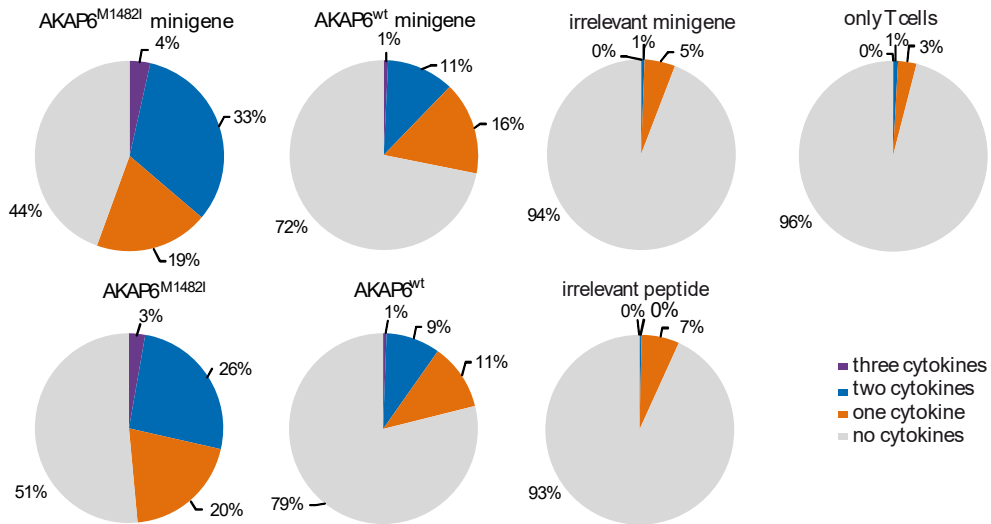
Figure 38: Multi-cytokine release of T-cell line HD6-AKAP6.
Percentage of T-cells producing combinations of IFNγ, TNFα and IL-2 was analyzed upon stimulation with minigene-transduced or peptide-pulsed LCL1. Cytokine production was assessed by flow cytometry and cells were gated on ethidium monoazide bromide-negative and CD8 positive events.

The capacity to lyse specific target cells was determined by flow cytometry-based cytotoxicity assay (2.2.4.5). Target cells presenting the mutated ligand AKAP6^{M1482I} were recognized and eliminated efficiently (Figure 39). Again, reactivity against the wild type counterpart was observed and lytic activity even appeared to be more notable as compared to IFN-γ release.
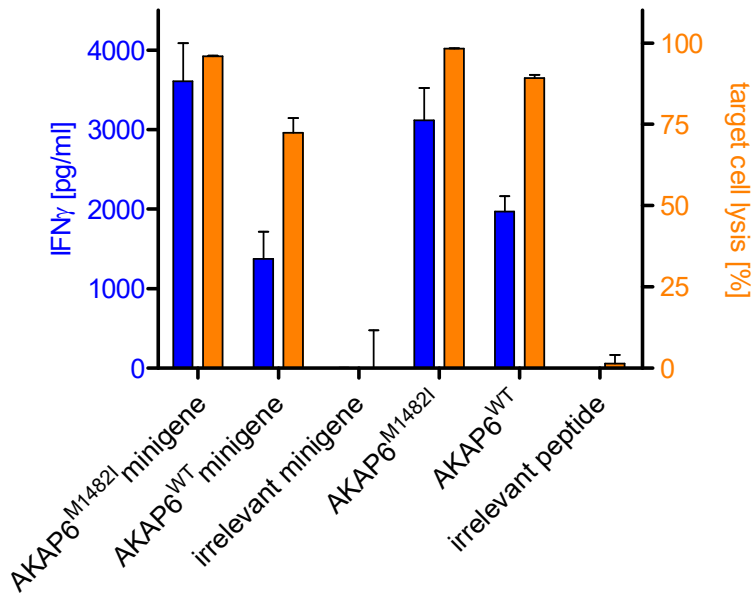
Figure 39: Cytolytic capacity of T-cell line HD6-AKAP6 upon specific stimulation.
T-cell line HD6-AKAP6 was coincubated with peptide-pulsed and minigene-transduced LCL1 in triplicates with analysis of IFNγ secretion (left Y-axis) and target-cell lysis (right Y-axis).

Functional reactivity of T-cell line HD6-AKAP6 declined over time, therefore T cells were sorted and directly cloned by limiting dilution (2.2.2.4). Only few clones grew and screening of those clones was performed by coincubation with T2-A3 pulsed with mutated, wild type or irrelevant peptide (Figure 40).
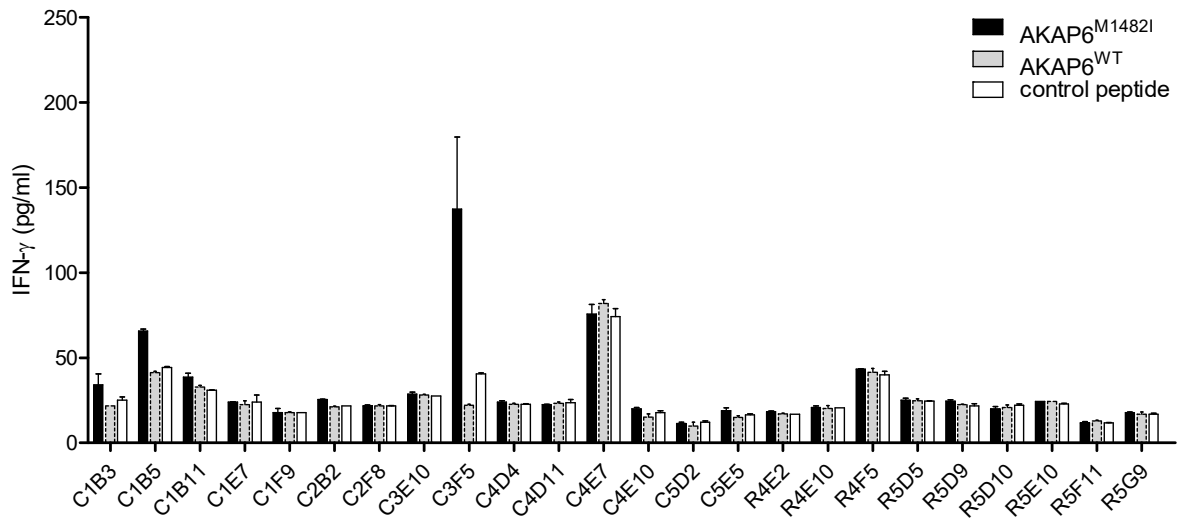
Figure 40: Screening of T-cell clones derived from line HD6-AKAP6 for specific reactivity against peptide AKAP6^{M1482I}.
T2-A3 were pulsed with AKAP6^{M1482I}, AKAP6^{WT} or control peptide and served as target cells for coincubation of expanded T-cell clones. Analysis of specific IFNγ release was performed in duplicates.

Only one clone, C3F5, showed a distinct response against the mutated ligand. mRNA was isolated and TCR repertoire analysis resulted in isolation of each, one single alpha and beta chain. This mutation-specific healthy donor-derived TCR HD6-AKAP6 was in-silico optimized and synthesized by Biocat (Heidelberg, Germany). Further functional analysis is currently ongoing (06/2017).

4 Discussion

4.1 Potential and limitations of detection of immune responses against tumor-associated antigens

4.1.1 Single-HLA mismatched stimulation resulted in detection of multimer-binding T cells with partial antigen specificity

The utilization of immune responses against so-called tumor-associated antigens (TAA) has proven to bear a great potential for cancer immunotherapy (Johnson et al., 2009; Robbins et al., 2015). After in-vitro stimulation of naïve T cells from an HLA-mismatched donor with melanoma-derived peptides, a multimer-binding population could be identified for two epitopes, $PRAME_2$ and $PAX3_1$, based on distinct binding of the relevant multimer and lack of binding to control multimer containing an irrelevant peptide binding to the same HLA restriction element. Initial functional screenings regarding both epitopes displayed a promising reactivity pattern; therefore these two specificities were analyzed in detail.

The $PAX3_1$-pMHC multimer binding population was detected within T-cell line $HD4$-TYR_1, which was originally stimulated with ligand TYR_1. One reason might be the unintended addition of the wrong peptide within the priming procedure. Another reason may rely in the dendritic cells (DC) that were used for stimulation, as PAX3 expression is reported also in DC. After a more detailed analysis of functional reactivity against different target cells with or without endogenous PAX3 expression, a clear pattern of antigen-specific recognition could not be detected. Besides, presentation of $PAX3_1$ in healthy dendritic cells may lead to undesired recognition of healthy cells and therefore bear the high risk of on-target off-tumor toxicity. If respective TCR would have been isolated and further investigated, analysis of functional avidity would have ad information on the capacity to recognize and lyse PAX3-expressing tumor cells. However, characterization of expanded T-cell clones showed undesired reactivities and thereby did not advocate further analysis. In contrast, PAX3-specific T cells have been previously described as potent actors against tumors in a murine model and a DC-based PAX3 peptide vaccination has proven to be safe (Himoudi et al., 2007). Thus, taking PAX3 as a target candidate for clinical translation into consideration would require an even more detailed, critical exploitation of antigen expression. Moreover, selection of low-avidity T cells might circumvent undesired targeting of healthy tissues expressing low amounts of antigen.

The selection process was based on multimer-sorting, which is a well-established method for the identification and enrichment of antigen-specific T cells (Altman et al., 1996; Davis, Altman, & Newell,

2011; Moris, Teichgraber, Gauthier, Buhring, & Rammensee, 2001). Although isolated T-cell clones confirmed specific binding only of the relevant multimer, functional analysis could not support a clear peptide- and antigen specific reactivity. Based on selection of the source antigen and the T-cell pool of interest, functional enrichment of T cells via CD137 upregulation or IFN-γ capture after specific stimulation with antigen-presenting target cells might serve as an alternative strategy for the isolation of tumor-specific T cells (Wolfl et al., 2007).

4.1.2 Allo-derived T cells demanding extensive safety analyses

Regarding PRAME$_2$, TCR 8D4 was isolated from a peptide-specific T-cell clone, optimized and further characterized with regard to its functional avidity and reactivity pattern against various target cells. Thereby, substantial background reactivity was detected against target cells bearing the HLA-B0702 restriction element but lacking endogenous expression of the antigen of interest determined by real-time PCR. The absence of RNA expression of respective source antigen serves as the basis for the assumption of the absence of the antigen-derived HLA peptide. The relative peptide-independence of the isolated TCR was also demonstrated by the alanine and threonine scan, as mostly exchange of position 2 and 7 led to a decreased reactivity against peptide-pulsed targets, but all analyzed variants elicited IFNγ release. A possible reason for this kind of cross-reactivity might be a higher dependence of TCR 8D4 on the HLA- rather than on peptide-mediated activation. In addition, PBMC from an HLA-B0702-positive donor transduced with TCR 8D4om showed a clear reduction of proliferation and compromised functionality compared to transduced cells from an HLA-B0702 negative donor. These results indicate fratricide amongst transduced effector cells, a phenomenon that has been observed in previous examples of TCR isolated from the allogeneic repertoire (Kirschner et al., 2016; Leisegang et al., 2010). However, whether lymphocytes actually expressed the PRAME$_2$ epitope on their surface or whether the compromised functionality of TCR-transgenic cells was rather due to the observed crossreactivity of TCR 8D4om, was not further investigated. The observed cross-reactivity rules out any potential for clinical application, as several examples within the history of TCR-transgenic adoptive immunotherapy may lead to strong immune responses in the host, including cytokine storm or severe cytotoxic responses against healthy tissues resulting in several cases to therapy related deaths (Linette et al., 2013; Morgan et al., 2013; van den Berg et al., 2015). The detection of PRAME-specific T cells within the allogeneic repertoire was recently performed in PBMC samples from patients suffering from Graft-versus-Host disease (GvHD) after HLA-mismatched stem-cell transplantation (Amir et al., 2011). However, T-cell clones isolated within this study reacted against mature DC and kidney epithelial cells emphasizing the high need of a thorough characterization of potential target antigens.

Other previous examples have shown that it is in principle possible to successfully isolate peptide-specific TCR from the allogeneic repertoire (Simpson et al., 2011). Therefore, the number of donors analyzed and stimulation approaches in our study might be too low for a comprehensive analysis of the immunogenic potential of all selected ligands. Current studies aim at an early selection time point to decide whether an isolated TCR might be suitable or not. Specificity and selectivity of TCR with pursued clinical application is still the major hurdle currently limiting a broader application of adoptive therapies with TCR-engineered T cells. In future investigations, limitations of capacity can be faced throughout the further automatization of screening methods, on the level of antigen presentation, such as the expression of multiple relevant antigens in parallel as pursued by the tandem-minigene approach (Tran, Robbins, & Rosenberg, 2017), as well as on the level of T-cell selection, for example TCR gene capture (Linnemann et al., 2013) or combinatorial multimer staining and sorting (Bentzen et al., 2016). This may lead to far higher chances to successfully isolate peptide-specific T-cell receptors from the HLA-mismatched repertoire against tumor-associated antigens. However, as all currently available screening methods require intensive investigations of effector cells and TCR; further developments and inventions of high-throughput analyses are urgently needed.

4.1.3 Optimization of peptide selection process

The proposed workflow displays one possible strategy next to several well-educated workflows, which were developed and published in meantime. Several aspects should be taken into consideration for further optimization of the proposed selection strategy. Throughout the implementation of large datasets from MS immunopeptidomics, prediction algorithms will be further optimized (Abelin et al., 2017; Bassani-Sternberg & Gfeller, 2016). This may lead to a reduction of bias still persistent in most of the established in-silico prediction tools, which is partially caused by training data resulting from in-vitro proteasomal digest or binding data of synthetic peptides. Besides, measurement of more samples may reveal distinct areas within a protein with preferential expression on different HLA molecules possibly due to various determinants in proteasomal processing. Such "hot spots" as a source for frequently presented HLA ligands have been detected in the gp100 protein in the later course of this project (Bassani-Sternberg et al., 2016). Peptide ligands derived from these hot-spots are likely to be presented in different patients and may thereby present attractive targets across different HLA types. In addition, implementation of alternative strategies into the established selection process, such as focusing on differential expression patterns, may narrow down the list of potential target candidates to such peptides suitable for a broad application. This includes individual tumor-specific target structures such as differentiation antigens but also distinct proteins or protein families with overexpression in tumor-subsets. Moreover, assessment

and integration of a patient-specific antigen expression profile may provide a more accurate picture of suitable target candidates for individual patients, as heterogeneous expression has been described for several promising antigens (Zajac et al., 2017).

4.2 Immunogenic potential of mutated peptide ligands

Mutation-spanning epitopes have proven to be involved in immune-mediated tumor recognition and rejection as recently reviewed (Schumacher & Schreiber, 2015). Within the herein deducted analysis, reactivity against naturally presented mutated HLA ligands was observed in PBMC and TIL of one patient as well as among PBMC-derived T cells from healthy donors.

4.2.1 Patient Mel15 as a role model for immune responsiveness

Three out of five patients were found to present mutated HLA ligands on the surface of their tumor cells, with one patient bearing eight different mutated peptides. Out of these eight peptides, two of them repeatedly elicited reactivity in autologous T cells at different time points during the patient's clinical course. Taking this high "hit rate" of truly immunogenic neoepitopes identified by mass spectrometry into consideration, the proposed workflow gives rise to the hope of a more efficient identification of mutated ligands with actual presentation and immunogenicity. In contrast, approaches using reverse immunology achieved a comparably low yield of neoantigens with proven T-cell reactivity (Table 1). Detailed characterization of observed immune responses against NCAPG2^{P333L} and SYTL4^{S363F} revealed repeated reactivity against these epitopes in the peripheral blood within a time frame of six months. The longitudinal observation of sustained neoepitope-specific reactivity is in line with other reports (Verdegaal et al., 2016).

TIL were screened for responses against eight mutated peptide ligands, which were detected in the first metastatic lesion resected in 2014. Reactivity was observed only against the epitope SYTL4^{S363F}, but not against the other ligands. Whether the second metastasis, from which the analyzed TIL were expanded, still contained the other mutations and whether they were presented on the cell surface, is under current investigation. Loss of mutations or presentation of mutated antigens during tumor progression has been observed before (Sucker et al., 2014; Verdegaal et al., 2016) and might explain lack of response, possibly caused by evolutionary pressure on the tumor and subsequent immune escape. Besides, TIL reactivity was assessed after in-vitro expansion due to limitations in tumor material, but not directly after metastasectomy. Thereby other mutation-specific T cells within the TIL compartment, that were not detected within performed stimulation procedures, might have been present but overgrown by T cells with other specificities. Likely, the relative proportion of SYLT4^{S363F}-specific cells after expansion possibly changed during in-vitro cultivation and therefore cannot be seen as a direct measure of the percentage of SYLT4^{S363F}-directed CTL within the original in-vivo TIL

repertoire. Nontheless, the high percentage of mutation-specific cells without any previous stimulation (Figure 23 and Figure 24) suggests the presence of clinically relevant amounts already in vivo at the tumor site. This notion is further supported by the high PD-L1 expression that we observed in some tumor areas within the resected metastatic region (Bassani-Sternberg et al., 2016).

The functional avidity of T cells and TCR displays an important determinant for the efficacy of target cell recognition (Ioannidou et al., 2017; Jenkins et al., 2009; Vigano et al., 2012). Within the second part of this thesis, several TCR with reactivity against mutated HLA ligands have been isolated. A detailed comparison of their functional capacity is still ongoing and will provide a further insight into neoantigen-driven immune responses.

Previous reports of source antigens, from which identified neoepitopes derived, hint towards a role in tumor progression and cell cycle control (Dulak et al., 2013; Ryu, Kim, Deluca, & Alani, 2007) but evidence of functional impact of the actually detected mutations has not been described so far. As only eleven ligands in total were identified within this approach, all mutated peptides were analyzed for their immunogenic potential irrespective of the original protein function or potential impairment of the detected alteration. In future experiments with maybe even a higher detection rate of altered ligands, integration of information on functionality and importance of affected proteins might be implemented into the selection process or later correlated to proven immunogenicity. In contrast, unbiased immunogenicity assessment of all detectable mutated ligands might provide a more comprehensive insight into neoantigen-driven tumor recognition and encompass the danger to miss clinically relevant rejection antigens.

4.2.2 Polyclonal neoepitope-specific immune responses as an example for complex anti-tumor reactivity

Within the proposed study, immune responses of patient Mel15 have been screened against those eight mutated peptide ligands that have been identified by MS. TAA-derived ligands detected within tumor samples of this patient have not been analyzed, but might play a role in immune-dependent tumor recognition as well. No cell line from patient Mel15's tumor could be grown, therefore the relative proportion of tumor-specific T cells within the TIL and the PBMC repertoire could not be determined. However, with regard to potential phenotypic changes of tumor cell lines during in vitro expansion, such analysis provide only limited information on the actual in-vivo tumor reactivity. It has been shown recently for melanoma patients and patients with cervical carcinoma that the composition of tumor-specific T cells comprises a broad spectrum of reactivities against different mutated epitopes, but also against unaltered ligands derived from overexpressed antigens (Stevanovic et al., 2017). In contrast, the proposed approach focuses on the determination of the

immunogenic potential of only those mutated peptide ligands which have been actually detected by mass spectrometry. Reactivity assessment against mutated peptide ligands which might have been missed by MS immunopeptidomic analyses is subject of ongoing investigations.

Recent data indicate monitoring of frequencies and dynamics may lead to a better understanding of stable and dynamic T-cell responses towards tumor antigens (Verdegaal et al., 2016). In order to specifically detect and trace isolated TCR with proven specificity in different samples of patient Mel15, a quantitative real-time PCR was established for each relevant TCR beta chain. A previous report of TCR quantification focusing on the quantification and comparison of distinct Vb-families (Ochsenreither et al., 2008) was used to track tyrosinase-specific T cells in a melanoma patient (Ochsenreither et al., 2010). In addition, Ochsenreither and colleagues monitored within this study one dominant T-cell clone by clone-specific real-time PCR emphasizing the high potential of PCR-based tracking of tumor-specific T cells. With regard to the established PCR for TCR of patient Mel15, DNA and cell dilutions showed a limit of detection in the range of 0.01% of specific T cells among all detected constant beta chain templates (Figure 31). In contrast, the sensitivity of other real-time PCR analyses such as the detection of minimal residual disease in chronic myeloid leukemia (CML) targeting the BCR-ABL translocation is reported as low as 5-10 copies per sample, however with the recommendation to analyze at least 1-2 * 10^7 cells (T. Hughes et al., 2006). Further possibilities of optimization, as for example the application of nested PCR (T. P. Hughes, Morgan, Martiat, & Goldman, 1991), might be elucidated to discriminate even lower percentages of tumor-specific T cells in the peripheral blood.

An alternative strategy for TCR quantification provides the method of TCR deep sequencing, as all TCR irrespective of their specificity are tracked and therefore frequencies of all detected TCR can be compared including ranking of tumor-antigen specific clones within the whole repertoire (Pasetto et al., 2016). Due to the unbiased assessment of all alpha and beta chains using TCR deep sequencing, the specificity of detected TCR can be assessed afterwards by cloning and transducing respective TCR chains. Nonetheless, this may result in large cloning and screening assays, as not all T-cell clones detected within TIL are neoantigen-specific. Alternatively, T cells might be sorted directly sequenced afterwards, however with only limited information on the original composition of specific clonal frequencies (Khodadoust et al., 2017).

4.2.3 Reactivity against two of eleven mutated ligands eliciting immune responses within healthy donors

Within the described collaborative project, the implementation of exome sequencing into mass spectrometry analysis of primary human tissue resulted for the first time in the detection of naturally presented mutated epitopes, what has been shown before only by using cell lines (Kalaora et al., 2016) or murine tissues (Gubin et al., 2014; Yadav et al., 2014). In the conduced stimulation approaches, two out of eleven tested mutation-bearing ligands (18.2%) elicited T-cell responses after in-vitro stimulation of HLA-matched healthy donors (HD). Another publication investigating HD-derived mutation-specific responses observed comparable percentages of immunogenic mutated HLA ligands with up to 19.3% using in-silico epitope prediction (Stronen et al., 2016). However, within this study only HLA-A0201 restricted peptides were investigated and the advantage relies in easier donor recruitment due to high prevalence of the desired allele. This focused approach facilitates the analysis of a broader spectrum of TCR repertoires from different donors, but other potentially relevant and actually presented peptide ligands are not considered at all. For some ligands, such as GABPA^{E161K}, the phenotype frequency of HLA-A*25 is reported as low as 4.6 % (German population)[12]. Therefore, only few donors could be tested leading to a biased assessment of the immunogenic potential. Including the fact of limited donor availability with respective HLA type, immune responses against ligands with restriction to rare HLA types might be better assessed by building up a larger donor bank.

4.2.4 Detailed analysis of AKAP6-specific T cells reveal cross reactivity against its wildtype counterpart

The characterization of AKAP6^{M1482}-specific T cells revealed on the one hand specific multimer staining without detectable binding of the wildtype peptide AKAP6^{WT}. On the other hand, peptide titration and detailed analysis of minigene reactivity showed a substantial cross reactivity against the wildtype counterpart. In the case of AKAP6, high antigen expression is described in brain tissue as well as in skeletal and cardiac muscle (Lee et al., 2015; McCartney, Little, & Scott, 1995). Cross reactivity of mutation-specific T cells against their wild-type counterpart may result in clinically relevant recognition of healthy tissues with high expression of non-mutated antigens. Thus, the impact of wild-type cross reactivity remains to be determined, for example by analysis of target cells with physiological expression of the non-mutated antigen.

The herein observed discrepancy between multimer staining and functional reactivity has been reported previously (Echchakir et al., 2002; McGranahan et al., 2016; Rubio-Godoy et al., 2001).

---

[12] http://www.allelefrequencies.net

Possible affection of multimer binding capacity by MHC micro-polymorphisms might prevent proper detection of relevant T cells (van Buuren et al., 2014). The relation of multimer-staining to functionality of respective T cells remains to be elucidated for each trimoleular complex consisting of TCR, peptide and MHC or HLA, respectively. TCR cloning and characterization still ongoing and may provide a deeper insight into the potential cross-reactivity of mutation-specific healthy donor-derived T cells. Future results will hopefully support the identification of decisive determinants for a well-informed decision whether isolated T cells might be suitable.

4.2.5 Targeting patient-specific mutations as a highly individualized approach?

UV-induced mutations are known as a frequent, but highly diverse mechanism of cancer induction in melanoma (Alexandrov et al., 2013). Therefore, a vast majority of tumor-specific mutations are individual for each single patient preventing the development of one single reagent targeting one specific tumor mutation, as it is possible for several differentiation antigens, such as CD19 (ref). So it was in the case of the proposed study, as none of the identified mutations could be found in a public database. Moreover, not all mutations are suitable rejection antigens due to their subclonal nature (McGranahan et al., 2015). However, taking a closer look at the acquisition of different mutations during the development of each individual tumor, clonal mutations may be identified within single patients or patient subgroups and used as targets for neoantigen-specific T cells (McGranahan et al., 2016). Targeting public mutations is in general limited to those mutational processes with frequent recurrence in different tumors, but might be a feasible in some cases (Tran et al., 2017). Recently, cytotoxic T-cell responses against a mutated HLA ligand containing the driver mutation KRAS^{G12D} were detected in a patient suffering from metastatic colon cancer (Tran et al., 2015) and therapeutic efficacy was observed after re-infusion of TIL targeting respective HLA-C*08:02 neoepitope (Tran et al., 2016). As this mutation occurs frequently in pancreatic adenocarcinoma and pancreatic cancer, the identified neoepitope might present an attractive target for broader immunotherapeutic approaches for those patients carrying respective HLA allele. However, as described above, this presents so far a rather rare example in the generally highly individual landscape of immunogenic tumor mutations.

4.3 Clinical applications and future perspectives

4.3.1 Adoptive T-cell therapy in solid cancers

Besides melanoma as a well-studied immunogenic tumor target, various malignancies are currently treated with the complex attempt of adoptive T-cell transfer. Whereas the application of ex-vivo expanded tumor-infiltrating lymphocytes and CAR-engineered T-cell products already facilitated treatment of several hundreds to thousands of patients (Andersen et al., 2016; Tran et al., 2017),

TCR-based therapy application is still at its infants. The main reason might rely in the absence of one distinct target antigen and the laborious procedures of TCR isolation and characterization. Nonetheless, the opportunity to specifically target peptide structures, also derived from intracellular proteins, in combination with persistence of adoptively transferred T cells still exhibits an attractive strategy.

Encouraging responses towards checkpoint blockade have been observed in several types of solid tumors including renal cell carcinoma (Motzer, Escudier, et al., 2015; Motzer, Rini, et al., 2015), NSCLC (Brahmer et al., 2012; Rizvi, Mazieres, et al., 2015), metastatic bladder cancer (Powles et al., 2014), and head and neck cancers (Seiwert et al., 2016). Efficient tumor lysis after checkpoint blockade emphasizes the high potential of immunotherapies with regard to various malignancies. Exhaustion of tumor-specific T cells may account as one major reason for therapy failure, rendering transfer of specific TCR into "fresh" potent T cells as an attractive strategy. In addition, the most suitable T-cell fraction, such as central memory T cells, capable of stable proliferation and long-term persistence in the host (Graef et al., 2014), can be selected and expanded for gene transfer and subsequent adoptive T cell therapy (Berger et al., 2008; X. Wang et al., 2016). The role of mutation-specific T cells in the clinical setting has been emphasized by reports on the presence of such T cells in adoptively transferred T-cell products mediating durable tumor regression (Lu et al., 2014; Prickett et al., 2016) but also by objective responses elicited by vaccination approaches with focus on neoantigens (Loffler et al., 2016).

4.3.2 Tumor evasion and intratumoral heterogeneity

Tumor cells are known to be flexible and this characteristic results amongst others in antigenic heterogeneity, which has been acknowledged already since a long time (Degiovanni, Lahaye, Herin, Hainaut, & Boon, 1988). As an important prerequisite towards the dissection of tumor- and T-cell dynamics, comprehensive insights in genetic plasticity of tumor cells have been gained. This has become feasible throughout the implementation of high-throughput methods leading to the improved understanding of tumor heterogeneity on the genomic and transcriptomic level. This was recently investigated in melanoma (Harbst et al., 2016) and variety of other malignancies (McGranahan & Swanton, 2017). In a comprehensive view taking also the part of T-cell recognition and immune-mediated shaping of tumors into consideration (Zaretsky et al., 2016), these insights shed a new light on the understanding of co-evolution of tumor- and T-cell interaction and may explain observed dynamics during tumor progression.

4.3.3 Combinatorial approaches for superior cancer eradication

Currently numerous alternative strategies employ combinatorial approaches to induce efficient immune responses or to overcome inherent or acquired immune resistance (Sharma, Hu-Lieskovan, Wargo, & Ribas, 2017). Regarding checkpoint inhibition, some factors relevant for therapy response could be identified, such as a high tumor burden (Huang et al., 2017). Tumor escape and immune inhibition might be overcome using several approaches. For example, modulation of the tumor microenvironment may lead to enhanced immunotherapeutic effects. Reverting the inhibitory influence of ionic changes on cancer specific T cells within the inflammatory or necrotic micro milieu displays a suitable target for improvement of T-cell mediated immunity (Eil et al., 2016). As the microbiome has been reported as a factor influencing response to immunotherapy (Sivan et al., 2015; Vetizou et al., 2015), combination of immunotherapeutic approaches with modulation of the gut microbiota might improve clinical outcome. Clinical investigations on the combination of checkpoint inhibitors with various immunomodulatory but also other approaches in the metastatic and adjuvant setting have been recently reviewed (Gotwals et al., 2017; Sharma et al., 2017) underpinning the high need of novel treatment regimens with superior efficacy compared to mono-therapies.

5 References

Abelin, J. G., Keskin, D. B., Sarkizova, S., Hartigan, C. R., Zhang, W., Sidney, J., . . . Wu, C. J. (2017). Mass Spectrometry Profiling of HLA-Associated Peptidomes in Mono-allelic Cells Enables More Accurate Epitope Prediction. *Immunity, 46*(2), 315-326. doi: 10.1016/j.immuni.2017.02.007

Alexandrov, L. B., Nik-Zainal, S., Wedge, D. C., Aparicio, S. A., Behjati, S., Biankin, A. V., . . . Stratton, M. R. (2013). Signatures of mutational processes in human cancer. *Nature, 500*(7463), 415-421. doi: 10.1038/nature12477

Altman, J. D., Moss, P. A., Goulder, P. J., Barouch, D. H., McHeyzer-Williams, M. G., Bell, J. I., . . . Davis, M. M. (1996). Phenotypic analysis of antigen-specific T lymphocytes. *Science, 274*(5284), 94-96.

Amir, A. L., van der Steen, D. M., van Loenen, M. M., Hagedoorn, R. S., de Boer, R., Kester, M. D., . . . Heemskerk, M. H. (2011). PRAME-specific Allo-HLA-restricted T cells with potent antitumor reactivity useful for therapeutic T-cell receptor gene transfer. *Clin Cancer Res, 17*(17), 5615-5625. doi: 10.1158/1078-0432.CCR-11-1066

Andersen, R., Donia, M., Ellebaek, E., Borch, T. H., Kongsted, P., Iversen, T. Z., . . . Svane, I. M. (2016). Long-Lasting Complete Responses in Patients with Metastatic Melanoma after Adoptive Cell Therapy with Tumor-Infiltrating Lymphocytes and an Attenuated IL2 Regimen. *Clin Cancer Res, 22*(15), 3734-3745. doi: 10.1158/1078-0432.CCR-15-1879

Bang, Y. J., Van Cutsem, E., Feyereislova, A., Chung, H. C., Shen, L., Sawaki, A., . . . To, G. A. T. I. (2010). Trastuzumab in combination with chemotherapy versus chemotherapy alone for treatment of HER2-positive advanced gastric or gastro-oesophageal junction cancer (ToGA): a phase 3, open-label, randomised controlled trial. *Lancet, 376*(9742), 687-697. doi: 10.1016/S0140-6736(10)61121-X

Barrett, D. M., Singh, N., Porter, D. L., Grupp, S. A., & June, C. H. (2014). Chimeric antigen receptor therapy for cancer. *Annu Rev Med, 65*, 333-347. doi: 10.1146/annurev-med-060512-150254

Bassani-Sternberg, M., Braunlein, E., Klar, R., Engleitner, T., Sinitcyn, P., Audehm, S., . . . Krackhardt, A. M. (2016). Direct identification of clinically relevant neoepitopes presented on native human melanoma tissue by mass spectrometry. *Nat Commun, 7*, 13404. doi: 10.1038/ncomms13404

Bassani-Sternberg, M., & Gfeller, D. (2016). Unsupervised HLA Peptidome Deconvolution Improves Ligand Prediction Accuracy and Predicts Cooperative Effects in Peptide-HLA Interactions. *J Immunol, 197*(6), 2492-2499. doi: 10.4049/jimmunol.1600808

Bassani-Sternberg, M., Pletscher-Frankild, S., Jensen, L. J., & Mann, M. (2015). Mass spectrometry of human leukocyte antigen class I peptidomes reveals strong effects of protein abundance and turnover on antigen presentation. *Mol Cell Proteomics, 14*(3), 658-673. doi: 10.1074/mcp.M114.042812

Bellantuono, I., Gao, L., Parry, S., Marley, S., Dazzi, F., Apperley, J., . . . Stauss, H. J. (2002). Two distinct HLA-A0201-presented epitopes of the Wilms tumor antigen 1 can function as targets for leukemia-reactive CTL. *Blood, 100*(10), 3835-3837. doi: 10.1182/blood.V100.10.3835

Belldegrun, A., Kasid, A., Uppenkamp, M., Topalian, S. L., & Rosenberg, S. A. (1989). Human tumor infiltrating lymphocytes. Analysis of lymphokine mRNA expression and relevance to cancer immunotherapy. *J Immunol, 142*(12), 4520-4526.

Bentzen, A. K., Marquard, A. M., Lyngaa, R., Saini, S. K., Ramskov, S., Donia, M., . . . Hadrup, S. R. (2016). Large-scale detection of antigen-specific T cells using peptide-MHC-I multimers labeled with DNA barcodes. *Nat Biotechnol, 34*(10), 1037-1045. doi: 10.1038/nbt.3662

Berger, C., Jensen, M. C., Lansdorp, P. M., Gough, M., Elliott, C., & Riddell, S. R. (2008). Adoptive transfer of effector CD8+ T cells derived from central memory cells establishes persistent T cell memory in primates. *J Clin Invest, 118*(1), 294-305. doi: 10.1172/JCI32103

References

Berlin, C., Kowalewski, D. J., Schuster, H., Mirza, N., Walz, S., Handel, M., . . . Stickel, J. S. (2015). Mapping the HLA ligandome landscape of acute myeloid leukemia: a targeted approach toward peptide-based immunotherapy. *Leukemia, 29*(3), 647-659. doi: 10.1038/leu.2014.233

Besser, M. J., Shapira-Frommer, R., Itzhaki, O., Treves, A. J., Zippel, D. B., Levy, D., . . . Schachter, J. (2013). Adoptive transfer of tumor-infiltrating lymphocytes in patients with metastatic melanoma: intent-to-treat analysis and efficacy after failure to prior immunotherapies. *Clin Cancer Res, 19*(17), 4792-4800. doi: 10.1158/1078-0432.CCR-13-0380

Brahmer, J. R., Tykodi, S. S., Chow, L. Q., Hwu, W. J., Topalian, S. L., Hwu, P., . . . Wigginton, J. M. (2012). Safety and activity of anti-PD-L1 antibody in patients with advanced cancer. *N Engl J Med, 366*(26), 2455-2465. doi: 10.1056/NEJMoa1200694

Caron, E., Kowalewski, D. J., Chiek Koh, C., Sturm, T., Schuster, H., & Aebersold, R. (2015). Analysis of Major Histocompatibility Complex (MHC) Immunopeptidomes Using Mass Spectrometry. *Mol Cell Proteomics, 14*(12), 3105-3117. doi: 10.1074/mcp.M115.052431

Carpenito, C., Milone, M. C., Hassan, R., Simonet, J. C., Lakhal, M., Suhoski, M. M., . . . June, C. H. (2009). Control of large, established tumor xenografts with genetically retargeted human T cells containing CD28 and CD137 domains. *Proc Natl Acad Sci U S A, 106*(9), 3360-3365. doi: 10.1073/pnas.0813101106

Chandran, S. S., Paria, B. C., Srivastava, A. K., Rothermel, L. D., Stephens, D. J., Dudley, M. E., . . . Kammula, U. S. (2015). Persistence of CTL clones targeting melanocyte differentiation antigens was insufficient to mediate significant melanoma regression in humans. *Clin Cancer Res, 21*(3), 534-543. doi: 10.1158/1078-0432.CCR-14-2208

Chen, Y. T., Scanlan, M. J., Sahin, U., Tureci, O., Gure, A. O., Tsang, S., . . . Old, L. J. (1997). A testicular antigen aberrantly expressed in human cancers detected by autologous antibody screening. *Proc Natl Acad Sci U S A, 94*(5), 1914-1918.

Cohen, C. J., Gartner, J. J., Horovitz-Fried, M., Shamalov, K., Trebska-McGowan, K., Bliskovsky, V. V., . . . Robbins, P. F. (2015). Isolation of neoantigen-specific T cells from tumor and peripheral lymphocytes. *J Clin Invest, 125*(10), 3981-3991. doi: 10.1172/JCI82416

Cohen, C. J., Zhao, Y., Zheng, Z., Rosenberg, S. A., & Morgan, R. A. (2006). Enhanced antitumor activity of murine-human hybrid T-cell receptor (TCR) in human lymphocytes is associated with improved pairing and TCR/CD3 stability. *Cancer Res, 66*(17), 8878-8886. doi: 10.1158/0008-5472.CAN-06-1450

Coiffier, B., Lepage, E., Briere, J., Herbrecht, R., Tilly, H., Bouabdallah, R., . . . Gisselbrecht, C. (2002). CHOP chemotherapy plus rituximab compared with CHOP alone in elderly patients with diffuse large-B-cell lymphoma. *N Engl J Med, 346*(4), 235-242. doi: 10.1056/NEJMoa011795

Cole, D. J., Weil, D. P., Shilyansky, J., Custer, M., Kawakami, Y., Rosenberg, S. A., & Nishimura, M. I. (1995). Characterization of the functional specificity of a cloned T-cell receptor heterodimer recognizing the MART-1 melanoma antigen. *Cancer Res, 55*(4), 748-752.

Couzin-Frankel, J. (2013). Breakthrough of the year 2013. Cancer immunotherapy. *Science, 342*(6165), 1432-1433. doi: 10.1126/science.342.6165.1432

Curti, B. D., Kovacsovics-Bankowski, M., Morris, N., Walker, E., Chisholm, L., Floyd, K., . . . Weinberg, A. D. (2013). OX40 is a potent immune-stimulating target in late-stage cancer patients. *Cancer Res, 73*(24), 7189-7198. doi: 10.1158/0008-5472.CAN-12-4174

D'Orsogna, L. J., Roelen, D. L., Doxiadis, II, & Claas, F. H. (2012). TCR cross-reactivity and allorecognition: new insights into the immunogenetics of allorecognition. *Immunogenetics, 64*(2), 77-85. doi: 10.1007/s00251-011-0590-0

Davis, M. M., Altman, J. D., & Newell, E. W. (2011). Interrogating the repertoire: broadening the scope of peptide-MHC multimer analysis. *Nat Rev Immunol, 11*(8), 551-558. doi: 10.1038/nri3020

Degiovanni, G., Lahaye, T., Herin, M., Hainaut, P., & Boon, T. (1988). Antigenic heterogeneity of a human melanoma tumor detected by autologous CTL clones. *Eur J Immunol, 18*(5), 671-676. doi: 10.1002/eji.1830180503

References

Dembic, Z., Haas, W., Weiss, S., McCubrey, J., Kiefer, H., von Boehmer, H., & Steinmetz, M. (1986). Transfer of specificity by murine alpha and beta T-cell receptor genes. *Nature, 320*(6059), 232-238. doi: 10.1038/320232a0

Donnelly, O. G., Errington-Mais, F., Steele, L., Hadac, E., Jennings, V., Scott, K., . . . Melcher, A. A. (2013). Measles virus causes immunogenic cell death in human melanoma. *Gene Ther, 20*(1), 7-15. doi: 10.1038/gt.2011.205

Dudley, M. E., Gross, C. A., Somerville, R. P., Hong, Y., Schaub, N. P., Rosati, S. F., . . . Rosenberg, S. A. (2013). Randomized selection design trial evaluating CD8+-enriched versus unselected tumor-infiltrating lymphocytes for adoptive cell therapy for patients with melanoma. *J Clin Oncol, 31*(17), 2152-2159. doi: 10.1200/JCO.2012.46.6441

Dudley, M. E., Wunderlich, J., Nishimura, M. I., Yu, D., Yang, J. C., Topalian, S. L., . . . Rosenberg, S. A. (2001). Adoptive transfer of cloned melanoma-reactive T lymphocytes for the treatment of patients with metastatic melanoma. *J Immunother, 24*(4), 363-373.

Dulak, A. M., Stojanov, P., Peng, S., Lawrence, M. S., Fox, C., Stewart, C., . . . Bass, A. J. (2013). Exome and whole-genome sequencing of esophageal adenocarcinoma identifies recurrent driver events and mutational complexity. *Nat Genet, 45*(5), 478-486. doi: 10.1038/ng.2591

Echchakir, H., Dorothee, G., Vergnon, I., Menez, J., Chouaib, S., & Mami-Chouaib, F. (2002). Cytotoxic T lymphocytes directed against a tumor-specific mutated antigen display similar HLA tetramer binding but distinct functional avidity and tissue distribution. *Proc Natl Acad Sci U S A, 99*(14), 9358-9363. doi: 10.1073/pnas.142308199

Eggermont, A. M., Chiarion-Sileni, V., Grob, J. J., Dummer, R., Wolchok, J. D., Schmidt, H., . . . Testori, A. (2016). Prolonged Survival in Stage III Melanoma with Ipilimumab Adjuvant Therapy. *N Engl J Med, 375*(19), 1845-1855. doi: 10.1056/NEJMoa1611299

Eil, R., Vodnala, S. K., Clever, D., Klebanoff, C. A., Sukumar, M., Pan, J. H., . . . Restifo, N. P. (2016). Ionic immune suppression within the tumour microenvironment limits T cell effector function. *Nature, 537*(7621), 539-543. doi: 10.1038/nature19364

Engell-Noerregaard, L., Hansen, T. H., Andersen, M. H., Thor Straten, P., & Svane, I. M. (2009). Review of clinical studies on dendritic cell-based vaccination of patients with malignant melanoma: assessment of correlation between clinical response and vaccine parameters. *Cancer Immunol Immunother, 58*(1), 1-14. doi: 10.1007/s00262-008-0568-4

Engels, B., Cam, H., Schuler, T., Indraccolo, S., Gladow, M., Baum, C., . . . Uckert, W. (2003). Retroviral vectors for high-level transgene expression in T lymphocytes. *Hum Gene Ther, 14*(12), 1155-1168. doi: 10.1089/104303403322167993

Foran, J. M., Rohatiner, A. Z., Cunningham, D., Popescu, R. A., Solal-Celigny, P., Ghielmini, M., . . . Lister, T. A. (2000). European phase II study of rituximab (chimeric anti-CD20 monoclonal antibody) for patients with newly diagnosed mantle-cell lymphoma and previously treated mantle-cell lymphoma, immunocytoma, and small B-cell lymphocytic lymphoma. *J Clin Oncol, 18*(2), 317-324. doi: 10.1200/JCO.2000.18.2.317

Gotwals, P., Cameron, S., Cipolletta, D., Cremasco, V., Crystal, A., Hewes, B., . . . Dranoff, G. (2017). Prospects for combining targeted and conventional cancer therapy with immunotherapy. *Nat Rev Cancer, 17*(5), 286-301. doi: 10.1038/nrc.2017.17

Graef, P., Buchholz, V. R., Stemberger, C., Flossdorf, M., Henkel, L., Schiemann, M., . . . Busch, D. H. (2014). Serial transfer of single-cell-derived immunocompetence reveals stemness of CD8(+) central memory T cells. *Immunity, 41*(1), 116-126. doi: 10.1016/j.immuni.2014.05.018

Gros, A., Parkhurst, M. R., Tran, E., Pasetto, A., Robbins, P. F., Ilyas, S., . . . Rosenberg, S. A. (2016). Prospective identification of neoantigen-specific lymphocytes in the peripheral blood of melanoma patients. *Nat Med, 22*(4), 433-438. doi: 10.1038/nm.4051

Grupp, S. A., Kalos, M., Barrett, D., Aplenc, R., Porter, D. L., Rheingold, S. R., . . . June, C. H. (2013). Chimeric antigen receptor-modified T cells for acute lymphoid leukemia. *N Engl J Med, 368*(16), 1509-1518. doi: 10.1056/NEJMoa1215134

References

Gubin, M. M., Zhang, X., Schuster, H., Caron, E., Ward, J. P., Noguchi, T., . . . Schreiber, R. D. (2014). Checkpoint blockade cancer immunotherapy targets tumour-specific mutant antigens. *Nature, 515*(7528), 577-581. doi: 10.1038/nature13988

Gudgeon, N. H., Taylor, G. S., Long, H. M., Haigh, T. A., & Rickinson, A. B. (2005). Regression of Epstein-Barr virus-induced B-cell transformation in vitro involves virus-specific CD8+ T cells as the principal effectors and a novel CD4+ T-cell reactivity. *J Virol, 79*(9), 5477-5488. doi: 10.1128/JVI.79.9.5477-5488.2005

Hamid, O., Robert, C., Daud, A., Hodi, F. S., Hwu, W. J., Kefford, R., . . . Ribas, A. (2013). Safety and tumor responses with lambrolizumab (anti-PD-1) in melanoma. *N Engl J Med, 369*(2), 134-144. doi: 10.1056/NEJMoa1305133

Harbst, K., Lauss, M., Cirenajwis, H., Isaksson, K., Rosengren, F., Torngren, T., . . . Jonsson, G. (2016). Multiregion Whole-Exome Sequencing Uncovers the Genetic Evolution and Mutational Heterogeneity of Early-Stage Metastatic Melanoma. *Cancer Res, 76*(16), 4765-4774. doi: 10.1158/0008-5472.CAN-15-3476

Himoudi, N., Nabarro, S., Yan, M., Gilmour, K., Thrasher, A. J., & Anderson, J. (2007). Development of anti-PAX3 immune responses; a target for cancer immunotherapy. *Cancer Immunol Immunother, 56*(9), 1381-1395. doi: 10.1007/s00262-007-0294-3

Hirschhorn-Cymerman, D., Rizzuto, G. A., Merghoub, T., Cohen, A. D., Avogadri, F., Lesokhin, A. M., . . . Houghton, A. N. (2009). OX40 engagement and chemotherapy combination provides potent antitumor immunity with concomitant regulatory T cell apoptosis. *J Exp Med, 206*(5), 1103-1116. doi: 10.1084/jem.20082205

Hodi, F. S., O'Day, S. J., McDermott, D. F., Weber, R. W., Sosman, J. A., Haanen, J. B., . . . Urba, W. J. (2010). Improved survival with ipilimumab in patients with metastatic melanoma. *N Engl J Med, 363*(8), 711-723. doi: 10.1056/NEJMoa1003466

Hombrink, P., Hassan, C., Kester, M. G., de Ru, A. H., van Bergen, C. A., Nijveen, H., . . . van Veelen, P. A. (2013). Discovery of T cell epitopes implementing HLA-peptidomics into a reverse immunology approach. *J Immunol, 190*(8), 3869-3877. doi: 10.4049/jimmunol.1202351

Huang, A. C., Postow, M. A., Orlowski, R. J., Mick, R., Bengsch, B., Manne, S., . . . Wherry, E. J. (2017). T-cell invigoration to tumour burden ratio associated with anti-PD-1 response. *Nature, 545*(7652), 60-65. doi: 10.1038/nature22079

Hudecek, M., Lupo-Stanghellini, M. T., Kosasih, P. L., Sommermeyer, D., Jensen, M. C., Rader, C., & Riddell, S. R. (2013). Receptor affinity and extracellular domain modifications affect tumor recognition by ROR1-specific chimeric antigen receptor T cells. *Clin Cancer Res, 19*(12), 3153-3164. doi: 10.1158/1078-0432.CCR-13-0330

Hughes, T., Deininger, M., Hochhaus, A., Branford, S., Radich, J., Kaeda, J., . . . Goldman, J. M. (2006). Monitoring CML patients responding to treatment with tyrosine kinase inhibitors: review and recommendations for harmonizing current methodology for detecting BCR-ABL transcripts and kinase domain mutations and for expressing results. *Blood, 108*(1), 28-37. doi: 10.1182/blood-2006-01-0092

Hughes, T. P., Morgan, G. J., Martiat, P., & Goldman, J. M. (1991). Detection of residual leukemia after bone marrow transplant for chronic myeloid leukemia: role of polymerase chain reaction in predicting relapse. *Blood, 77*(4), 874-878.

Hugo, W., Zaretsky, J. M., Sun, L., Song, C., Moreno, B. H., Hu-Lieskovan, S., . . . Lo, R. S. (2016). Genomic and Transcriptomic Features of Response to Anti-PD-1 Therapy in Metastatic Melanoma. *Cell, 165*(1), 35-44. doi: 10.1016/j.cell.2016.02.065

Hunt, D. F., Henderson, R. A., Shabanowitz, J., Sakaguchi, K., Michel, H., Sevilir, N., . . . Engelhard, V. H. (1992). Characterization of peptides bound to the class I MHC molecule HLA-A2.1 by mass spectrometry. *Science, 255*(5049), 1261-1263.

Ioannidou, K., Baumgaertner, P., Gannon, P. O., Speiser, M. F., Allard, M., Hebeisen, M., . . . Speiser, D. E. (2017). Heterogeneity assessment of functional T cell avidity. *Sci Rep, 7*, 44320. doi: 10.1038/srep44320

References

Jenkins, M. R., La Gruta, N. L., Doherty, P. C., Trapani, J. A., Turner, S. J., & Waterhouse, N. J. (2009). Visualizing CTL activity for different CD8+ effector T cells supports the idea that lower TCR/epitope avidity may be advantageous for target cell killing. *Cell Death Differ, 16*(4), 537-542. doi: 10.1038/cdd.2008.176

Johnson, L. A., Morgan, R. A., Dudley, M. E., Cassard, L., Yang, J. C., Hughes, M. S., . . . Rosenberg, S. A. (2009). Gene therapy with human and mouse T-cell receptors mediates cancer regression and targets normal tissues expressing cognate antigen. *Blood, 114*(3), 535-546. doi: 10.1182/blood-2009-03-211714

Jonker, D. J., O'Callaghan, C. J., Karapetis, C. S., Zalcberg, J. R., Tu, D., Au, H. J., . . . Moore, M. J. (2007). Cetuximab for the treatment of colorectal cancer. *N Engl J Med, 357*(20), 2040-2048. doi: 10.1056/NEJMoa071834

Kalaora, S., Barnea, E., Merhavi-Shoham, E., Qutob, N., Teer, J. K., Shimony, N., . . . Samuels, Y. (2016). Use of HLA peptidomics and whole exome sequencing to identify human immunogenic neo-antigens. *Oncotarget, 7*(5), 5110-5117. doi: 10.18632/oncotarget.6960

Khodadoust, M. S., Olsson, N., Wagar, L. E., Haabeth, O. A., Chen, B., Swaminathan, K., . . . Alizadeh, A. A. (2017). Antigen presentation profiling reveals recognition of lymphoma immunoglobulin neoantigens. *Nature, 543*(7647), 723-727. doi: 10.1038/nature21433

Kirschner, A., Thiede, M., Blaeschke, F., Richter, G. H., Gerke, J. S., Baldauf, M. C., . . . Thiel, U. (2016). Lysosome-associated membrane glycoprotein 1 predicts fratricide amongst T cell receptor transgenic CD8+ T cells directed against tumor-associated antigens. *Oncotarget, 7*(35), 56584-56597. doi: 10.18632/oncotarget.10647

Klar, R., Schober, S., Rami, M., Mall, S., Merl, J., Hauck, S. M., . . . Krackhardt, A. M. (2014). Therapeutic targeting of naturally presented myeloperoxidase-derived HLA peptide ligands on myeloid leukemia cells by TCR-transgenic T cells. *Leukemia, 28*(12), 2355-2366. doi: 10.1038/leu.2014.131

Kohrt, H. E., Colevas, A. D., Houot, R., Weiskopf, K., Goldstein, M. J., Lund, P., . . . Levy, R. (2014). Targeting CD137 enhances the efficacy of cetuximab. *J Clin Invest, 124*(6), 2668-2682. doi: 10.1172/JCI73014

Koks, C. A., Garg, A. D., Ehrhardt, M., Riva, M., Vandenberk, L., Boon, L., . . . Van Gool, S. W. (2015). Newcastle disease virotherapy induces long-term survival and tumor-specific immune memory in orthotopic glioma through the induction of immunogenic cell death. *Int J Cancer, 136*(5), E313-325. doi: 10.1002/ijc.29202

Kreiter, S., Vormehr, M., van de Roemer, N., Diken, M., Lower, M., Diekmann, J., . . . Sahin, U. (2015). Mutant MHC class II epitopes drive therapeutic immune responses to cancer. *Nature, 520*(7549), 692-696. doi: 10.1038/nature14426

Kumari, S., Walchli, S., Fallang, L. E., Yang, W., Lund-Johansen, F., Schumacher, T. N., & Olweus, J. (2014). Alloreactive cytotoxic T cells provide means to decipher the immunopeptidome and reveal a plethora of tumor-associated self-epitopes. *Proc Natl Acad Sci U S A, 111*(1), 403-408. doi: 10.1073/pnas.1306549111

Larkin, J., Chiarion-Sileni, V., Gonzalez, R., Grob, J. J., Cowey, C. L., Lao, C. D., . . . Wolchok, J. D. (2015). Combined Nivolumab and Ipilimumab or Monotherapy in Untreated Melanoma. *N Engl J Med, 373*(1), 23-34. doi: 10.1056/NEJMoa1504030

Lawson, D. H., Lee, S., Zhao, F., Tarhini, A. A., Margolin, K. A., Ernstoff, M. S., . . . Kirkwood, J. M. (2015). Randomized, Placebo-Controlled, Phase III Trial of Yeast-Derived Granulocyte-Macrophage Colony-Stimulating Factor (GM-CSF) Versus Peptide Vaccination Versus GM-CSF Plus Peptide Vaccination Versus Placebo in Patients With No Evidence of Disease After Complete Surgical Resection of Locally Advanced and/or Stage IV Melanoma: A Trial of the Eastern Cooperative Oncology Group-American College of Radiology Imaging Network Cancer Research Group (E4697). *J Clin Oncol, 33*(34), 4066-4076. doi: 10.1200/JCO.2015.62.0500

References

Lee, S. W., Won, J. Y., Yang, J., Lee, J., Kim, S. Y., Lee, E. J., & Kim, H. S. (2015). AKAP6 inhibition impairs myoblast differentiation and muscle regeneration: Positive loop between AKAP6 and myogenin. *Sci Rep, 5*, 16523. doi: 10.1038/srep16523

Leisegang, M., Engels, B., Meyerhuber, P., Kieback, E., Sommermeyer, D., Xue, S. A., . . . Uckert, W. (2008). Enhanced functionality of T cell receptor-redirected T cells is defined by the transgene cassette. *J Mol Med (Berl), 86*(5), 573-583. doi: 10.1007/s00109-008-0317-3

Leisegang, M., Wilde, S., Spranger, S., Milosevic, S., Frankenberger, B., Uckert, W., & Schendel, D. J. (2010). MHC-restricted fratricide of human lymphocytes expressing survivin-specific transgenic T cell receptors. *J Clin Invest, 120*(11), 3869-3877. doi: 10.1172/JCI43437

Lennerz, V., Fatho, M., Gentilini, C., Frye, R. A., Lifke, A., Ferel, D., . . . Wolfel, T. (2005). The response of autologous T cells to a human melanoma is dominated by mutated neoantigens. *Proc Natl Acad Sci U S A, 102*(44), 16013-16018. doi: 10.1073/pnas.0500090102

Linette, G. P., Stadtmauer, E. A., Maus, M. V., Rapoport, A. P., Levine, B. L., Emery, L., . . . June, C. H. (2013). Cardiovascular toxicity and titin cross-reactivity of affinity-enhanced T cells in myeloma and melanoma. *Blood, 122*(6), 863-871. doi: 10.1182/blood-2013-03-490565

Linnemann, C., Heemskerk, B., Kvistborg, P., Kluin, R. J., Bolotin, D. A., Chen, X., . . . Schumacher, T. N. (2013). High-throughput identification of antigen-specific TCRs by TCR gene capture. *Nat Med, 19*(11), 1534-1541. doi: 10.1038/nm.3359

Linnemann, C., van Buuren, M. M., Bies, L., Verdegaal, E. M., Schotte, R., Calis, J. J., . . . Schumacher, T. N. (2015). High-throughput epitope discovery reveals frequent recognition of neo-antigens by CD4+ T cells in human melanoma. *Nat Med, 21*(1), 81-85. doi: 10.1038/nm.3773

Livak, K. J., & Schmittgen, T. D. (2001). Analysis of relative gene expression data using real-time quantitative PCR and the 2(-Delta Delta C(T)) Method. *Methods, 25*(4), 402-408. doi: 10.1006/meth.2001.1262

Loffler, M. W., Chandran, P. A., Laske, K., Schroeder, C., Bonzheim, I., Walzer, M., . . . Rammensee, H. G. (2016). Personalized peptide vaccine-induced immune response associated with long-term survival of a metastatic cholangiocarcinoma patient. *J Hepatol, 65*(4), 849-855. doi: 10.1016/j.jhep.2016.06.027

Lu, Y. C., Yao, X., Crystal, J. S., Li, Y. F., El-Gamil, M., Gross, C., . . . Robbins, P. F. (2014). Efficient identification of mutated cancer antigens recognized by T cells associated with durable tumor regressions. *Clin Cancer Res, 20*(13), 3401-3410. doi: 10.1158/1078-0432.CCR-14-0433

Mall, S., Yusufi, N., Wagner, R., Klar, R., Bianchi, H., Steiger, K., . . . Krackhardt, A. M. (2016). Immuno-PET Imaging of Engineered Human T Cells in Tumors. *Cancer Res, 76*(14), 4113-4123. doi: 10.1158/0008-5472.CAN-15-2784

Maloney, D. G., Grillo-Lopez, A. J., White, C. A., Bodkin, D., Schilder, R. J., Neidhart, J. A., . . . Levy, R. (1997). IDEC-C2B8 (Rituximab) anti-CD20 monoclonal antibody therapy in patients with relapsed low-grade non-Hodgkin's lymphoma. *Blood, 90*(6), 2188-2195.

Martinuzzi, E., Afonso, G., Gagnerault, M. C., Naselli, G., Mittag, D., Combadiere, B., . . . Mallone, R. (2011). acDCs enhance human antigen-specific T-cell responses. *Blood, 118*(8), 2128-2137. doi: 10.1182/blood-2010-12-326231

Matsushita, H., Vesely, M. D., Koboldt, D. C., Rickert, C. G., Uppaluri, R., Magrini, V. J., . . . Schreiber, R. D. (2012). Cancer exome analysis reveals a T-cell-dependent mechanism of cancer immunoediting. *Nature, 482*(7385), 400-404. doi: 10.1038/nature10755

Maude, S. L., Frey, N., Shaw, P. A., Aplenc, R., Barrett, D. M., Bunin, N. J., . . . Grupp, S. A. (2014). Chimeric antigen receptor T cells for sustained remissions in leukemia. *N Engl J Med, 371*(16), 1507-1517. doi: 10.1056/NEJMoa1407222

Maury, S., Chevret, S., Thomas, X., Heim, D., Leguay, T., Huguet, F., . . . for, G. (2016). Rituximab in B-Lineage Adult Acute Lymphoblastic Leukemia. *N Engl J Med, 375*(11), 1044-1053. doi: 10.1056/NEJMoa1605085

McCartney, S., Little, B. M., & Scott, J. D. (1995). Analysis of a novel A-kinase anchoring protein 100, (AKAP 100). *Biochem Soc Trans, 23*(2), 268S.

McGranahan, N., Favero, F., de Bruin, E. C., Birkbak, N. J., Szallasi, Z., & Swanton, C. (2015). Clonal status of actionable driver events and the timing of mutational processes in cancer evolution. *Sci Transl Med, 7*(283), 283ra254. doi: 10.1126/scitranslmed.aaa1408

McGranahan, N., Furness, A. J., Rosenthal, R., Ramskov, S., Lyngaa, R., Saini, S. K., . . . Swanton, C. (2016). Clonal neoantigens elicit T cell immunoreactivity and sensitivity to immune checkpoint blockade. *Science, 351*(6280), 1463-1469. doi: 10.1126/science.aaf1490

McGranahan, N., & Swanton, C. (2017). Clonal Heterogeneity and Tumor Evolution: Past, Present, and the Future. *Cell, 168*(4), 613-628. doi: 10.1016/j.cell.2017.01.018

Melero, I., Shuford, W. W., Newby, S. A., Aruffo, A., Ledbetter, J. A., Hellstrom, K. E., . . . Chen, L. (1997). Monoclonal antibodies against the 4-1BB T-cell activation molecule eradicate established tumors. *Nat Med, 3*(6), 682-685.

Morgan, R. A., Chinnasamy, N., Abate-Daga, D., Gros, A., Robbins, P. F., Zheng, Z., . . . Rosenberg, S. A. (2013). Cancer regression and neurological toxicity following anti-MAGE-A3 TCR gene therapy. *J Immunother, 36*(2), 133-151. doi: 10.1097/CJI.0b013e3182829903

Morgan, R. A., Dudley, M. E., Wunderlich, J. R., Hughes, M. S., Yang, J. C., Sherry, R. M., . . . Rosenberg, S. A. (2006). Cancer regression in patients after transfer of genetically engineered lymphocytes. *Science, 314*(5796), 126-129. doi: 10.1126/science.1129003

Moris, A., Teichgraber, V., Gauthier, L., Buhring, H. J., & Rammensee, H. G. (2001). Cutting edge: characterization of allorestricted and peptide-selective alloreactive T cells using HLA-tetramer selection. *J Immunol, 166*(8), 4818-4821.

Morton, D. L., Eilber, F. R., Joseph, W. L., Wood, W. C., Trahan, E., & Ketcham, A. S. (1970). Immunological factors in human sarcomas and melanomas: a rational basis for immunotherapy. *Ann Surg, 172*(4), 740-749.

Motzer, R. J., Escudier, B., McDermott, D. F., George, S., Hammers, H. J., Srinivas, S., . . . CheckMate, I. (2015). Nivolumab versus Everolimus in Advanced Renal-Cell Carcinoma. *N Engl J Med, 373*(19), 1803-1813. doi: 10.1056/NEJMoa1510665

Motzer, R. J., Rini, B. I., McDermott, D. F., Redman, B. G., Kuzel, T. M., Harrison, M. R., . . . Hammers, H. J. (2015). Nivolumab for Metastatic Renal Cell Carcinoma: Results of a Randomized Phase II Trial. *J Clin Oncol, 33*(13), 1430-1437. doi: 10.1200/JCO.2014.59.0703

Nestle, F. O., Alijagic, S., Gilliet, M., Sun, Y., Grabbe, S., Dummer, R., . . . Schadendorf, D. (1998). Vaccination of melanoma patients with peptide- or tumor lysate-pulsed dendritic cells. *Nat Med, 4*(3), 328-332.

Obst, R., Munz, C., Stevanovic, S., & Rammensee, H. G. (1998). Allo- and self-restricted cytotoxic T lymphocytes against a peptide library: evidence for a functionally diverse allorestricted T cell repertoire. *Eur J Immunol, 28*(8), 2432-2443. doi: 10.1002/(SICI)1521-4141(199808)28:08<2432::AID-IMMU2432>3.0.CO;2-0

Ochsenreither, S., Fusi, A., Busse, A., Letsch, A., Haase, D., Thiel, E., . . . Keilholz, U. (2010). Long term presence of a single predominant tyrosinase-specific T-cell clone associated with disease control in a patient with metastatic melanoma. *Int J Cancer, 126*(10), 2497-2502. doi: 10.1002/ijc.24939

Ochsenreither, S., Fusi, A., Busse, A., Nagorsen, D., Schrama, D., Becker, J., . . . Keilholz, U. (2008). Relative quantification of TCR Vbeta-chain families by real time PCR for identification of clonal T-cell populations. *J Transl Med, 6*, 34. doi: 10.1186/1479-5876-6-34

Overwijk, W. W. (2005). Breaking tolerance in cancer immunotherapy: time to ACT. *Curr Opin Immunol, 17*(2), 187-194. doi: 10.1016/j.coi.2005.01.011

Palmer, D. H., Midgley, R. S., Mirza, N., Torr, E. E., Ahmed, F., Steele, J. C., . . . Adams, D. H. (2009). A phase II study of adoptive immunotherapy using dendritic cells pulsed with tumor lysate in patients with hepatocellular carcinoma. *Hepatology, 49*(1), 124-132. doi: 10.1002/hep.22626

Parkhurst, M. R., Yang, J. C., Langan, R. C., Dudley, M. E., Nathan, D. A., Feldman, S. A., . . . Rosenberg, S. A. (2011). T cells targeting carcinoembryonic antigen can mediate regression of metastatic colorectal cancer but induce severe transient colitis. *Mol Ther, 19*(3), 620-626. doi: 10.1038/mt.2010.272

References

Pasetto, A., Gros, A., Robbins, P. F., Deniger, D. C., Prickett, T. D., Matus-Nicodemos, R., . . . Rosenberg, S. A. (2016). Tumor- and Neoantigen-Reactive T-cell Receptors Can Be Identified Based on Their Frequency in Fresh Tumor. *Cancer Immunol Res, 4*(9), 734-743. doi: 10.1158/2326-6066.CIR-16-0001

Perren, T. J., Swart, A. M., Pfisterer, J., Ledermann, J. A., Pujade-Lauraine, E., Kristensen, G., . . . Investigators, I. (2011). A phase 3 trial of bevacizumab in ovarian cancer. *N Engl J Med, 365*(26), 2484-2496. doi: 10.1056/NEJMoa1103799

Piccart-Gebhart, M. J., Procter, M., Leyland-Jones, B., Goldhirsch, A., Untch, M., Smith, I., . . . Herceptin Adjuvant Trial Study, T. (2005). Trastuzumab after adjuvant chemotherapy in HER2-positive breast cancer. *N Engl J Med, 353*(16), 1659-1672. doi: 10.1056/NEJMoa052306

Pirker, R., Pereira, J. R., Szczesna, A., von Pawel, J., Krzakowski, M., Ramlau, R., . . . Team, F. S. (2009). Cetuximab plus chemotherapy in patients with advanced non-small-cell lung cancer (FLEX): an open-label randomised phase III trial. *Lancet, 373*(9674), 1525-1531. doi: 10.1016/S0140-6736(09)60569-9

Porter, D. L., Levine, B. L., Kalos, M., Bagg, A., & June, C. H. (2011). Chimeric antigen receptor-modified T cells in chronic lymphoid leukemia. *N Engl J Med, 365*(8), 725-733. doi: 10.1056/NEJMoa1103849

Postow, M. A., Chesney, J., Pavlick, A. C., Robert, C., Grossmann, K., McDermott, D., . . . Hodi, F. S. (2015). Nivolumab and ipilimumab versus ipilimumab in untreated melanoma. *N Engl J Med, 372*(21), 2006-2017. doi: 10.1056/NEJMoa1414428

Powles, T., Eder, J. P., Fine, G. D., Braiteh, F. S., Loriot, Y., Cruz, C., . . . Vogelzang, N. J. (2014). MPDL3280A (anti-PD-L1) treatment leads to clinical activity in metastatic bladder cancer. *Nature, 515*(7528), 558-562. doi: 10.1038/nature13904

Prickett, T. D., Crystal, J. S., Cohen, C. J., Pasetto, A., Parkhurst, M. R., Gartner, J. J., . . . Robbins, P. F. (2016). Durable Complete Response from Metastatic Melanoma after Transfer of Autologous T Cells Recognizing 10 Mutated Tumor Antigens. *Cancer Immunol Res, 4*(8), 669-678. doi: 10.1158/2326-6066.CIR-15-0215

Radvanyi, L. G., Bernatchez, C., Zhang, M., Fox, P. S., Miller, P., Chacon, J., . . . Hwu, P. (2012). Specific lymphocyte subsets predict response to adoptive cell therapy using expanded autologous tumor-infiltrating lymphocytes in metastatic melanoma patients. *Clin Cancer Res, 18*(24), 6758-6770. doi: 10.1158/1078-0432.CCR-12-1177

Ressing, M. E., Sette, A., Brandt, R. M., Ruppert, J., Wentworth, P. A., Hartman, M., . . . Kast, W. M. (1995). Human CTL epitopes encoded by human papillomavirus type 16 E6 and E7 identified through in vivo and in vitro immunogenicity studies of HLA-A*0201-binding peptides. *J Immunol, 154*(11), 5934-5943.

Rizvi, N. A., Hellmann, M. D., Snyder, A., Kvistborg, P., Makarov, V., Havel, J. J., . . . Chan, T. A. (2015). Cancer immunology. Mutational landscape determines sensitivity to PD-1 blockade in non-small cell lung cancer. *Science, 348*(6230), 124-128. doi: 10.1126/science.aaa1348

Rizvi, N. A., Mazieres, J., Planchard, D., Stinchcombe, T. E., Dy, G. K., Antonia, S. J., . . . Ramalingam, S. S. (2015). Activity and safety of nivolumab, an anti-PD-1 immune checkpoint inhibitor, for patients with advanced, refractory squamous non-small-cell lung cancer (CheckMate 063): a phase 2, single-arm trial. *Lancet Oncol, 16*(3), 257-265. doi: 10.1016/S1470-2045(15)70054-9

Robbins, P. F., Kassim, S. H., Tran, T. L., Crystal, J. S., Morgan, R. A., Feldman, S. A., . . . Rosenberg, S. A. (2015). A pilot trial using lymphocytes genetically engineered with an NY-ESO-1-reactive T-cell receptor: long-term follow-up and correlates with response. *Clin Cancer Res, 21*(5), 1019-1027. doi: 10.1158/1078-0432.CCR-14-2708

Robbins, P. F., Lu, Y. C., El-Gamil, M., Li, Y. F., Gross, C., Gartner, J., . . . Rosenberg, S. A. (2013). Mining exomic sequencing data to identify mutated antigens recognized by adoptively transferred tumor-reactive T cells. *Nat Med, 19*(6), 747-752. doi: 10.1038/nm.3161

Robbins, P. F., Morgan, R. A., Feldman, S. A., Yang, J. C., Sherry, R. M., Dudley, M. E., . . . Rosenberg, S. A. (2011). Tumor regression in patients with metastatic synovial cell sarcoma and melanoma

using genetically engineered lymphocytes reactive with NY-ESO-1. *J Clin Oncol, 29*(7), 917-924. doi: 10.1200/JCO.2010.32.2537

Rosenberg, J. C., Assimacoupoulos, C., Lober, P., Rosenberg, S. A., & Zimmermann, B. (1961). The malignant melanoma of hamsters. I. Pathologic characteristics of a transplanted melanotic and amelanotic tumor. *Cancer Res, 21*, 627-631.

Rosenberg, S. A., Packard, B. S., Aebersold, P. M., Solomon, D., Topalian, S. L., Toy, S. T., . . . et al. (1988). Use of tumor-infiltrating lymphocytes and interleukin-2 in the immunotherapy of patients with metastatic melanoma. A preliminary report. *N Engl J Med, 319*(25), 1676-1680. doi: 10.1056/NEJM198812223192527

Rosenberg, S. A., Spiess, P., & Lafreniere, R. (1986). A new approach to the adoptive immunotherapy of cancer with tumor-infiltrating lymphocytes. *Science, 233*(4770), 1318-1321.

Rosenberg, S. A., Yang, J. C., Schwartzentruber, D. J., Hwu, P., Marincola, F. M., Topalian, S. L., . . . White, D. E. (1998). Immunologic and therapeutic evaluation of a synthetic peptide vaccine for the treatment of patients with metastatic melanoma. *Nat Med, 4*(3), 321-327.

Rosenberg, S. A., Yang, J. C., Sherry, R. M., Kammula, U. S., Hughes, M. S., Phan, G. Q., . . . Dudley, M. E. (2011). Durable complete responses in heavily pretreated patients with metastatic melanoma using T-cell transfer immunotherapy. *Clin Cancer Res, 17*(13), 4550-4557. doi: 10.1158/1078-0432.CCR-11-0116

Rubio-Godoy, V., Dutoit, V., Rimoldi, D., Lienard, D., Lejeune, F., Speiser, D., . . . Valmori, D. (2001). Discrepancy between ELISPOT IFN-gamma secretion and binding of A2/peptide multimers to TCR reveals interclonal dissociation of CTL effector function from TCR-peptide/MHC complexes half-life. *Proc Natl Acad Sci U S A, 98*(18), 10302-10307. doi: 10.1073/pnas.181348898

Ryu, B., Kim, D. S., Deluca, A. M., & Alani, R. M. (2007). Comprehensive expression profiling of tumor cell lines identifies molecular signatures of melanoma progression. *PLoS One, 2*(7), e594. doi: 10.1371/journal.pone.0000594

Sadovnikova, E., Jopling, L. A., Soo, K. S., & Stauss, H. J. (1998). Generation of human tumor-reactive cytotoxic T cells against peptides presented by non-self HLA class I molecules. *Eur J Immunol, 28*(1), 193-200. doi: 10.1002/(SICI)1521-4141(199801)28:01<193::AID-IMMU193>3.0.CO;2-K

Scheibenbogen, C., Schmittel, A., Keilholz, U., Allgauer, T., Hofmann, U., Max, R., . . . Schadendorf, D. (2000). Phase 2 trial of vaccination with tyrosinase peptides and granulocyte-macrophage colony-stimulating factor in patients with metastatic melanoma. *J Immunother, 23*(2), 275-281.

Scholten, K. B., Kramer, D., Kueter, E. W., Graf, M., Schoedl, T., Meijer, C. J., . . . Hooijberg, E. (2006). Codon modification of T cell receptors allows enhanced functional expression in transgenic human T cells. *Clin Immunol, 119*(2), 135-145. doi: 10.1016/j.clim.2005.12.009

Schumacher, T. N., & Schreiber, R. D. (2015). Neoantigens in cancer immunotherapy. *Science, 348*(6230), 69-74. doi: 10.1126/science.aaa4971

Schuster, I. G., Busch, D. H., Eppinger, E., Kremmer, E., Milosevic, S., Hennard, C., . . . Krackhardt, A. M. (2007). Allorestricted T cells with specificity for the FMNL1-derived peptide PP2 have potent antitumor activity against hematologic and other malignancies. *Blood, 110*(8), 2931-2939. doi: 10.1182/blood-2006-11-058750

Seiwert, T. Y., Burtness, B., Mehra, R., Weiss, J., Berger, R., Eder, J. P., . . . Chow, L. Q. (2016). Safety and clinical activity of pembrolizumab for treatment of recurrent or metastatic squamous cell carcinoma of the head and neck (KEYNOTE-012): an open-label, multicentre, phase 1b trial. *Lancet Oncol, 17*(7), 956-965. doi: 10.1016/S1470-2045(16)30066-3

Sharma, P., Hu-Lieskovan, S., Wargo, J. A., & Ribas, A. (2017). Primary, Adaptive, and Acquired Resistance to Cancer Immunotherapy. *Cell, 168*(4), 707-723. doi: 10.1016/j.cell.2017.01.017

Shu, S. Y., & Rosenberg, S. A. (1985). Adoptive immunotherapy of newly induced murine sarcomas. *Cancer Res, 45*(4), 1657-1662.

References

Simpson, A. A., Mohammed, F., Salim, M., Tranter, A., Rickinson, A. B., Stauss, H. J., . . . Willcox, B. E. (2011). Structural and energetic evidence for highly peptide-specific tumor antigen targeting via allo-MHC restriction. *Proc Natl Acad Sci U S A, 108*(52), 21176-21181. doi: 10.1073/pnas.1108422109

Sivan, A., Corrales, L., Hubert, N., Williams, J. B., Aquino-Michaels, K., Earley, Z. M., . . . Gajewski, T. F. (2015). Commensal Bifidobacterium promotes antitumor immunity and facilitates anti-PD-L1 efficacy. *Science, 350*(6264), 1084-1089. doi: 10.1126/science.aac4255

Slamon, D. J., Leyland-Jones, B., Shak, S., Fuchs, H., Paton, V., Bajamonde, A., . . . Norton, L. (2001). Use of chemotherapy plus a monoclonal antibody against HER2 for metastatic breast cancer that overexpresses HER2. *N Engl J Med, 344*(11), 783-792. doi: 10.1056/NEJM200103153441101

Snyder, A., Makarov, V., Merghoub, T., Yuan, J., Zaretsky, J. M., Desrichard, A., . . . Chan, T. A. (2014). Genetic basis for clinical response to CTLA-4 blockade in melanoma. *N Engl J Med, 371*(23), 2189-2199. doi: 10.1056/NEJMoa1406498

Stancovski, I., Schindler, D. G., Waks, T., Yarden, Y., Sela, M., & Eshhar, Z. (1993). Targeting of T lymphocytes to Neu/HER2-expressing cells using chimeric single chain Fv receptors. *J Immunol, 151*(11), 6577-6582.

Stevanovic, S., Pasetto, A., Helman, S. R., Gartner, J. J., Prickett, T. D., Howie, B., . . . Hinrichs, C. S. (2017). Landscape of immunogenic tumor antigens in successful immunotherapy of virally induced epithelial cancer. *Science, 356*(6334), 200-205. doi: 10.1126/science.aak9510

Stitz, J., Buchholz, C. J., Engelstadter, M., Uckert, W., Bloemer, U., Schmitt, I., & Cichutek, K. (2000). Lentiviral vectors pseudotyped with envelope glycoproteins derived from gibbon ape leukemia virus and murine leukemia virus 10A1. *Virology, 273*(1), 16-20. doi: 10.1006/viro.2000.0394

Strausser, J. L., Mazumder, A., Grimm, E. A., Lotze, M. T., & Rosenberg, S. A. (1981). Lysis of human solid tumors by autologous cells sensitized in vitro to alloantigens. *J Immunol, 127*(1), 266-271.

Stronen, E., Toebes, M., Kelderman, S., van Buuren, M. M., Yang, W., van Rooij, N., . . . Schumacher, T. N. (2016). Targeting of cancer neoantigens with donor-derived T cell receptor repertoires. *Science, 352*(6291), 1337-1341. doi: 10.1126/science.aaf2288

Sucker, A., Zhao, F., Real, B., Heeke, C., Bielefeld, N., Mabetaen, S., . . . Paschen, A. (2014). Genetic evolution of T-cell resistance in the course of melanoma progression. *Clin Cancer Res, 20*(24), 6593-6604. doi: 10.1158/1078-0432.CCR-14-0567

Sugiyama, D., Nishikawa, H., Maeda, Y., Nishioka, M., Tanemura, A., Katayama, I., . . . Sakaguchi, S. (2013). Anti-CCR4 mAb selectively depletes effector-type FoxP3+CD4+ regulatory T cells, evoking antitumor immune responses in humans. *Proc Natl Acad Sci U S A, 110*(44), 17945-17950. doi: 10.1073/pnas.1316796110

Svennevig, J. L., Lovik, M., & Svaar, H. (1979). Isolation and characterization of lymphocytes and macrophages from solid, malignant human tumours. *Int J Cancer, 23*(5), 626-631.

Tewari, K. S., Sill, M. W., Long, H. J., 3rd, Penson, R. T., Huang, H., Ramondetta, L. M., . . . Monk, B. J. (2014). Improved survival with bevacizumab in advanced cervical cancer. *N Engl J Med, 370*(8), 734-743. doi: 10.1056/NEJMoa1309748

Topalian, S. L., Hodi, F. S., Brahmer, J. R., Gettinger, S. N., Smith, D. C., McDermott, D. F., . . . Sznol, M. (2012). Safety, activity, and immune correlates of anti-PD-1 antibody in cancer. *N Engl J Med, 366*(26), 2443-2454. doi: 10.1056/NEJMoa1200690

Topalian, S. L., Solomon, D., & Rosenberg, S. A. (1989). Tumor-specific cytolysis by lymphocytes infiltrating human melanomas. *J Immunol, 142*(10), 3714-3725.

Tran, E., Ahmadzadeh, M., Lu, Y. C., Gros, A., Turcotte, S., Robbins, P. F., . . . Rosenberg, S. A. (2015). Immunogenicity of somatic mutations in human gastrointestinal cancers. *Science, 350*(6266), 1387-1390. doi: 10.1126/science.aad1253

References

Tran, E., Robbins, P. F., Lu, Y. C., Prickett, T. D., Gartner, J. J., Jia, L., . . . Rosenberg, S. A. (2016). T-Cell Transfer Therapy Targeting Mutant KRAS in Cancer. *N Engl J Med, 375*(23), 2255-2262. doi: 10.1056/NEJMoa1609279

Tran, E., Robbins, P. F., & Rosenberg, S. A. (2017). 'Final common pathway' of human cancer immunotherapy: targeting random somatic mutations. *Nat Immunol, 18*(3), 255-262. doi: 10.1038/ni.3682

Turk, M. J., Guevara-Patino, J. A., Rizzuto, G. A., Engelhorn, M. E., Sakaguchi, S., & Houghton, A. N. (2004). Concomitant tumor immunity to a poorly immunogenic melanoma is prevented by regulatory T cells. *J Exp Med, 200*(6), 771-782. doi: 10.1084/jem.20041130

Vacchelli, E., Pol, J., Bloy, N., Eggermont, A., Cremer, I., Fridman, W. H., . . . Galluzzi, L. (2015). Trial watch: Tumor-targeting monoclonal antibodies for oncological indications. *Oncoimmunology, 4*(1), e985940. doi: 10.4161/2162402X.2014.985940

Van Allen, E. M., Miao, D., Schilling, B., Shukla, S. A., Blank, C., Zimmer, L., . . . Garraway, L. A. (2015). Genomic correlates of response to CTLA-4 blockade in metastatic melanoma. *Science, 350*(6257), 207-211. doi: 10.1126/science.aad0095

van Buuren, M. M., Dijkgraaf, F. E., Linnemann, C., Toebes, M., Chang, C. X., Mok, J. Y., . . . Schumacher, T. N. (2014). HLA micropolymorphisms strongly affect peptide-MHC multimer-based monitoring of antigen-specific CD8+ T cell responses. *J Immunol, 192*(2), 641-648. doi: 10.4049/jimmunol.1301770

van den Berg, J. H., Gomez-Eerland, R., van de Wiel, B., Hulshoff, L., van den Broek, D., Bins, A., . . . Haanen, J. B. (2015). Case Report of a Fatal Serious Adverse Event Upon Administration of T Cells Transduced With a MART-1-specific T-cell Receptor. *Mol Ther, 23*(9), 1541-1550. doi: 10.1038/mt.2015.60

van der Bruggen, P., Traversari, C., Chomez, P., Lurquin, C., De Plaen, E., Van den Eynde, B., . . . Boon, T. (1991). A gene encoding an antigen recognized by cytolytic T lymphocytes on a human melanoma. *Science, 254*(5038), 1643-1647.

Verdegaal, E. M., de Miranda, N. F., Visser, M., Harryvan, T., van Buuren, M. M., Andersen, R. S., . . . van der Burg, S. H. (2016). Neoantigen landscape dynamics during human melanoma-T cell interactions. *Nature, 536*(7614), 91-95. doi: 10.1038/nature18945

Vetizou, M., Pitt, J. M., Daillere, R., Lepage, P., Waldschmitt, N., Flament, C., . . . Zitvogel, L. (2015). Anticancer immunotherapy by CTLA-4 blockade relies on the gut microbiota. *Science, 350*(6264), 1079-1084. doi: 10.1126/science.aad1329

Viatte, S., Alves, P. M., & Romero, P. (2006). Reverse immunology approach for the identification of CD8 T-cell-defined antigens: advantages and hurdles. *Immunol Cell Biol, 84*(3), 318-330. doi: 10.1111/j.1440-1711.2006.01447.x

Vigano, S., Utzschneider, D. T., Perreau, M., Pantaleo, G., Zehn, D., & Harari, A. (2012). Functional avidity: a measure to predict the efficacy of effector T cells? *Clin Dev Immunol, 2012*, 153863. doi: 10.1155/2012/153863

Visseren, M. J., van Elsas, A., van der Voort, E. I., Ressing, M. E., Kast, W. M., Schrier, P. I., & Melief, C. J. (1995). CTL specific for the tyrosinase autoantigen can be induced from healthy donor blood to lyse melanoma cells. *J Immunol, 154*(8), 3991-3998.

von Minckwitz, G., Eidtmann, H., Rezai, M., Fasching, P. A., Tesch, H., Eggemann, H., . . . Arbeitsgemeinschaft Gynakologische Onkologie-Breast Study, G. (2012). Neoadjuvant chemotherapy and bevacizumab for HER2-negative breast cancer. *N Engl J Med, 366*(4), 299-309. doi: 10.1056/NEJMoa1111065

Walz, S., Stickel, J. S., Kowalewski, D. J., Schuster, H., Weisel, K., Backert, L., . . . Stevanovic, S. (2015). The antigenic landscape of multiple myeloma: mass spectrometry (re)defines targets for T-cell-based immunotherapy. *Blood, 126*(10), 1203-1213. doi: 10.1182/blood-2015-04-640532

Wang, R. F. (2009). Molecular cloning and characterization of MHC class I- and II-restricted tumor antigens recognized by T cells. *Curr Protoc Immunol, Chapter 20*, Unit 20 10. doi: 10.1002/0471142735.im2010s84

References

Wang, X., Wong, C. W., Urak, R., Taus, E., Aguilar, B., Chang, W. C., . . . Jensen, M. C. (2016). Comparison of naive and central memory derived CD8+ effector cell engraftment fitness and function following adoptive transfer. *Oncoimmunology, 5*(1), e1072671. doi: 10.1080/2162402X.2015.1072671

Wehler, T. C., Nonn, M., Brandt, B., Britten, C. M., Grone, M., Todorova, M., . . . Herr, W. (2007). Targeting the activation-induced antigen CD137 can selectively deplete alloreactive T cells from antileukemic and antitumor donor T-cell lines. *Blood, 109*(1), 365-373. doi: 10.1182/blood-2006-04-014100

Weigand, L. U., Liang, X., Schmied, S., Mall, S., Klar, R., Stotzer, O. J., . . . Krackhardt, A. M. (2012). Isolation of human MHC class II-restricted T cell receptors from the autologous T-cell repertoire with potent anti-leukaemic reactivity. *Immunology, 137*(3), 226-238. doi: 10.1111/imm.12000

Whelan, J. A., Russell, N. B., & Whelan, M. A. (2003). A method for the absolute quantification of cDNA using real-time PCR. *J Immunol Methods, 278*(1-2), 261-269.

Wilde, S., Geiger, C., Milosevic, S., Mosetter, B., Eichenlaub, S., & Schendel, D. J. (2012). Generation of allo-restricted peptide-specific T cells using RNA-pulsed dendritic cells: A three phase experimental procedure. *Oncoimmunology, 1*(2), 129-140. doi: 10.4161/onci.1.2.18216

Wilde, S., Sommermeyer, D., Frankenberger, B., Schiemann, M., Milosevic, S., Spranger, S., . . . Schendel, D. J. (2009). Dendritic cells pulsed with RNA encoding allogeneic MHC and antigen induce T cells with superior antitumor activity and higher TCR functional avidity. *Blood, 114*(10), 2131-2139. doi: 10.1182/blood-2009-03-209387

Wolfel, T., Van Pel, A., De Plaen, E., Lurquin, C., Maryanski, J. L., & Boon, T. (1987). Immunogenic (tum-) variants obtained by mutagenesis of mouse mastocytoma P815. VIII. Detection of stable transfectants expressing a tum- antigen with a cytolytic T cell stimulation assay. *Immunogenetics, 26*(3), 178-187.

Wolfl, M., Kuball, J., Ho, W. Y., Nguyen, H., Manley, T. J., Bleakley, M., & Greenberg, P. D. (2007). Activation-induced expression of CD137 permits detection, isolation, and expansion of the full repertoire of CD8+ T cells responding to antigen without requiring knowledge of epitope specificities. *Blood, 110*(1), 201-210. doi: 10.1182/blood-2006-11-056168

Yadav, M., Jhunjhunwala, S., Phung, Q. T., Lupardus, P., Tanguay, J., Bumbaca, S., . . . Delamarre, L. (2014). Predicting immunogenic tumour mutations by combining mass spectrometry and exome sequencing. *Nature, 515*(7528), 572-576. doi: 10.1038/nature14001

Yu, G., Li, Y., Cui, Z., Morris, N. P., Weinberg, A. D., Fox, B. A., . . . Hu, H. M. (2016). Combinational Immunotherapy with Allo-DRibble Vaccines and Anti-OX40 Co-Stimulation Leads to Generation of Cross-Reactive Effector T Cells and Tumor Regression. *Sci Rep, 6*, 37558. doi: 10.1038/srep37558

Zajac, P., Schultz-Thater, E., Tornillo, L., Sadowski, C., Trella, E., Mengus, C., . . . Spagnoli, G. C. (2017). MAGE-A Antigens and Cancer Immunotherapy. *Front Med (Lausanne), 4*, 18. doi: 10.3389/fmed.2017.00018

Zaretsky, J. M., Garcia-Diaz, A., Shin, D. S., Escuin-Ordinas, H., Hugo, W., Hu-Lieskovan, S., . . . Ribas, A. (2016). Mutations Associated with Acquired Resistance to PD-1 Blockade in Melanoma. *N Engl J Med, 375*(9), 819-829. doi: 10.1056/NEJMoa1604958

Zhou, D., Srivastava, R., Grummel, V., Cepok, S., Hartung, H. P., & Hemmer, B. (2006). High throughput analysis of TCR-beta rearrangement and gene expression in single T cells. *Lab Invest, 86*(3), 314-321. doi: 10.1038/labinvest.3700381

6 Appendix

6.1 Characteristics of all patients subjected to MS analyses

Patient	Gender	Age at biopsy	Location of biopsy
Mel3	female	56	Soft tissue
Mel4	male	80	Bone, soft tissue
Mel5	male	50	Lymph node
Mel8	female	66	Lymph node
Mel12	male	65	Lymph node
Mel15	male	63	Small intestine
Mel16	female	61	Lymph node
Mel20	male	78	Lymph node
Mel21	male	60	Lymph node
Mel24	male	37	Lymph node
Mel25	male	44	Lymph node
Mel26	female	69	Lymph node
Mel27	female	71	Lymph node
Mel28	female	66	Lymph node
Mel29	female	67	Lymph node
Mel30	female	68	Lymph node
Mel33	male	54	Lymph node
Mel34	male	37	Lung
Mel35	male	43	Lymph node
Mel36	male	40	Lymph node
Mel38	male	59	Adrenal gland
Mel39	male	72	Lymph node
Mel40	male	91	Soft tissue
Mel41	male	68	Lymph node
Mel42	female	69	Soft tissue

6.2 Information of patients selected for neoepitope identification

Patient	Stage[A]	Stage at biopsy	LDH[B]	S100[C]	Defined mutations	HLA type[D]
Mel5	IV	M1C	426	1253	-	A*01, A*25, B*08, B*18
Mel8	IV	M1C	340	668	cKIT p.L576P (Exon 11)	A*01:01:01, A*03:01:01, B*07:02:01, B*08:01:01, C*07:01:01, C*07:02:01
Mel12	IV	M1C	266	56	-	A* 01:01:01, B* 08:01:01, C* 07:01:01
Mel15	IV	M1C	174	82	-	A*03:01:01, A*68:01:01, B*27:05:02, B*35:03:01, C*02:02:02, C*04:01:01
Mel16	IV	M1C	215	94	BRAF V600E	A*01:01:01, A*24:02:01, B*07:02:01, B*08:01:01, C*07:01:01, C*07:02:01

[A] Tumor staging according to Union international contre le cancer (UICC)

[B] At time of metastasectomy (U/L), physiological range < 244 U/L

[C] At time of metastasectomy (pg/ml), physiological range < 100pg/ml

[D] Mel5: determined by HLA miner; all other patients: typed by next-generation sequencing

6.3 Clinical courses of patients Mel5, Mel8, Mel12, Mel15 and Mel16

Mel5

	03/2012	12/2012	04/2013	07/2013	12/2013
Diagnostics	Initial diagnosis of metastasized melanoma	Progression: new lesions in adrenal glands, lung, soft tissue and abdomen	Progression of intraabdominal lesion	Minor progression	Disease progression, death
Therapy	Resection of CNS and lung metastases; Brain irradiation	4 cycles Ipilimumab	Surgery of obstructive intestinal metastasis; Initiation Nivolumab therapy → Immunopeptidomics	Continuation Nivolumab	

Mel8

	03/2003	09/2011	07/2012	11/2012	02/2013	05/2013	11/2013	02/2014
Diagnostics	Initial diagnosis of acral lentiginous melanoma	Local relapse	CNS metastases	Progression of peritoneal and mediastinal LN metastases	Disease progression	Progression of multiple LN metastases	Progression of lung and brain metastasis	Disease progression, death
Therapy	Complete resection; Adjuvant IFN alpha therapy	Lisfranc amputation of left foot	Metastatectomy + whole brain irradiation	Ipilimumab (4 cycles)	DTIC (2 cycles)	Inguinal + axillary Metastatectomy; Imatinib → Immuno-peptidomics	Stereotactic irradiation of CNS metastasis	

Mel12

	02/2010	02/2012	07/2012	11/2012	08/2013	05/2014	07/2016
Diagnostics	Initial diagnosis: primary amelanotic melanoma	Metastatic disease: skin, LN and lung metastases	Systemic progression (lung, axillary + mediastinal LN)	Major response, progression of one bone metastasis	Progression of multiple LN metastases	Progression of LN metastases	Progression of mediastinal LN metastases
Therapy	Excision of primary lesion + LN dissection; Adjuvant IFN alpha therapy	Resection of skin metastasis + irradiation; DTIC (3 cycles)	Ipilimumab (4 cycles)	Irradiation	Diagnostic excision of axillary LN; Carboplatin + Paclitaxel (6 cycles) → Immuno-peptidomics	Ipilimumab (4 cycles)	Initiation Nivolumab

Mel15

	08/2008	09/2013	11/2013	02/2014	01/2016	07/2016
Diagnostics	Initial diagnosis of malignant melanoma (right arm)	Systemic manifestation: thoracal and intestinal metastases	Mixed response	Response of thoracal metastasis, progression of abdominal manifestation	Progression of thoracal lesion	Complete remission
Therapy	Tumor resection pT2a N0 M0, Clark IV	Carboplatin/ Paclitaxel (2 cycles)	Ipilimumab (4 cycles)	Resection of abdominal metastases → Immuno-peptidomics	Resection	

Mel16

	03/2005	04/2014	11/2014	01/2016	04/2016
Diagnostics	Initial diagnosis: skin metastasis of local melanoma	Metastatic disease: axillary LN	Bone metastasis in the left femur	CNS metastasis with FDG uptake	Stable disease
Therapy	Resection	Resection + irradiation → Immunopeptidomics	Ipilimumab (4 cycles) + irradiation	Resection + irradiation	Nivolumab (ongoing)

CNS = central nervous system; LN = lymph node; DTIC = Dacarbazine.

6.4 Sequence of TCR 8D4om

ATGGGCTGTAGACTGCTGTGCTGCGTCGTGTTTTGCCTGCTGCAGGCCGGACCACTGGATACCGCCGTGAGCC
AGACTCCTAAATACCTGGTGACCCAGATGGGGAACGATAAGTCCATCAAATGCGAGCAGAATCTGGGACACG
ATACAATGTACTGGTATAAGCAGGACTCTAAGAAATTCCTGAAGATCATGTTCAGTTACAACAATAAGGAACT
GATCATTAACGAGACTGTGCCTAATAGGTTCTCACCAAAGAGCCCCGATAAAGCCCACCTGAACCTGCATATCA
ATAGTCTGGAACTGGGAGACAGCGCCGTGTACTTTTGCGCAAGCTCCCAGGAGCGGAGCGGAGTCACAGGAG
AACTGTTCTTTGGAGAGGGCAGCCGCCTGACAGTGCTGGAAGACCTGCGAAACGTGACTCCCCCTAAAGTCTC
ACTGTTCGAACCAAGCAAGGCTGAGATTGCAAACAAGCAGAAGGCCACCCTGGTGTGCCTGGCTAGAGGCTT
CTTTCCCGATCACGTGGAACTGTCTTGGTGGGTCAACGGAAAAGAGGTGCATTCCGGCGTCTCTACAGACCCT
CAGGCCTACAAGGAGAGTAATTACTCATATTGCCTGTCTAGTCGGCTGCGGGTGTGCGCTACTTTTTGGCACAA
CCCCCGAAATCATTTCCGGTGCCAGGTCCAGTTTCACGGCCTGTCAGAGGAGGATAAGTGGCCTGAAGGGAG
CCCTAAACCCGTGACACAGAACATCTCCGCCGAGGCTTGGGGAAGGGCAGACTGTGGGATTACTTCCGCCTCT
TATCATCAGGGCGTGCTGTCCGCAACTATCCTGTACGAGATTCTGCTGGGAAAGGCAACCCTGTATGCCGTGCT
GGTCTCTGGCCTGGTGCTGATGGCTATGGTCAAGAAAAGAACAGTGGAAGCGGCGCCACGAACTTCTCTCTG
TTAAAGCAAGCAGGAGACGTGGAAGAAAACCCCGGTCCCATGGAAAGCTTTCTGGGCGGGGTCCTGCTGATC
CTGTGGCTGCAGGTGGACTGGGTCAAGAGCCAGAAAATCGAACAGAACTCCGAGGCACTGAATATTCAGGAG
GGGAAGACTGCCACCCTGACATGCAACTACACCAATTATAGCCCAGCCTACCTGCAGTGGTATAGACAGGATC
CTGGCAGGGGGCCAGTGTTCCTGCTGCTGATCCGAGAGAACGAAAAGAGAAGAGGAAAGAGCGCCTGAAA
GTGACCTTCGATACCACACTGAAGCAGAGCCTGTTTCATATTACCGCCTCCCAGCCAGCCGACTCTGCTACATA
CCTGTGCGCTCGGCCCTTCTTTAGCGGCTCCGCAAGACAGCTGACATTCGGAAGCGGCACACAGCTGACTGTG
CTGCCTGACATCCAGAACCCCGAACCTGCCGTCTATCAGCTGAAGGACCCACGCAGCCAGGATAGCACCCTGT
GCCTGTTCACCGACTTTGATTCTCAGATCAATGTGCCCAAAACCATGGAGAGTGGCACCTTTATTACAGACAAG
ACTGTCCTGGATATGAAGGCCATGGACTCTAAAAGTAACGGGGCAATCGCCTGGTCTAATCAGACCAGTTTCA
CATGTCAGGATATCTTCAAGGAGACTAACGCTTGCTACCCCTCAAGCGACGTGCCTTGTGATGCAACTCTGACC
GAAAGTCCTTCGAGACCGACATGAACCTGAATTTTCAGAATCTGTCTGTGATGGGCCTGCGGATCCTGCTGCT
GAAAGTCGCTGGGTTTAATCTGCTGATGACACTGCGGCTGTGGAGTAGTTGA

6.5 List of figures

6.6   List of Tables

6.7 Abbreviations

µl	Microliter
µM	Micromolar
4-1BB = TNFRSF9	TNF receptor superfamily member 9
ADCC	Antibody-dependent cell-mediated cytotoxicity
AEC	3-Amino-9-ethylcarbazole
AKAP6	A-kinase anchoring protein 6
APC	Allophycocyanin
BSA	Bovine serum albumine
CAR	Chimeric antigen receptor
CAR	Chimeric antigen receptors
CD	Cluster of Differentiation
CDC	Complement-dependent cytotoxicity
CDR3	Complementary-determining region 3
c_{END}	Endconcentration
CML	Chronic myeloid leukemia
c_{STOCK}	Stock concentration
CTLA-4	Cytotoxic T-lymphocyte associated protein 4
c_{WORK}	Concentration of working dilution
DC	Dendritic cell
DEPC	Diethyl pyrocarbonate
DMEM	Dulbecco's Modified Eagle Medium
DMF	Dimethylformamide
DMSO	Dimethyl sulfoxide
DNAa	Deoxyribonucleic acid
dNTP	Deoxynucleotide triphosphates
DsRed	Discosoma sp. red fluorescent protein
EBV	Epstein-Barr virus
EC50	Half maximal effective concentration
EDTA	Ethylenediaminetetraacetic acid
EF	Endotoxin-free
EGFR	Epidermal growth factor receptor
ELISA	Enzyme-linked immunosorbent assay
ELIspot	Enzyme-linked immunospot
FACS	Fluorescence activated cell sorting
FCS	Fetal calf serum
FITC	Fluorescein isothiocyanate
GaLV	Gibbon ape Leukemia Virus
GFP	Green fluorescent protein
GM-CSF	Granulocyte-macrophage colony-stimulating factor
GvHD	Graft-versus-Host disease
h	Hour
HD	Healthy donor
HEPES	4-(2-hydroxyethyl)-1-piperazineethanesulfonic acid
HER2	Human epidermal growth factor receptor 2
HLA	Human leukocyte antigen
HRP	Horseradish peroxidase
HS	Human serum

IFN	Interferon
IL	Interleukin
LB	Lysogeny broth
LCL	Lymphoblastoid cell line
MHC	Major histocompatiblity complex
min	Minute
Mio	Million
ml	Milliliter
mM	Millimolar
MS	Mass spectrometry
NCAPG2	Non-SMC condensin II complex subunit G2
NEAA	Non-essential amio acids
nM	Nanomolar
NSCLC	Non-small-cell lung cancer
OX40 = TNFRSF4	TNF receptor superfamily member 4
P2A	Peptide 2A
PAX3	Paired box 3
PBC	Peripheral blood cell
PBMC	Peripheral blood mononuclear cells
PBS	Phosphate-Buffered Saline
PCR	Polymerase chain reaction
PCR	Polymerase chain reaction
PD-1	Programmed cell death 1
PE	Phycoerythrin
PFA	Paraformaldehyde
PI	Propidium Iodide
Poly-I:C	Polyinosinic-polycytidylic acid
PRAME	Preferentially expressed antigen in melanoma
rh	Recombinant human
RNA	Ribonucleic acid
RPMI 1640	Roswell Park Memorial Institute 1640
RT	Room temperature
s	Second
SYTL4	Synaptotagmin like 4
TAA	Tumor-associated antigen
TAE	Tris-acetate-EDTA
TCR	T-cell receptor
TIL	Tumor-infiltrating lymphocytes
TNF	Tumor-necrosis factor
TRAC	T cell receptor alpha constant
TRBC	T cell receptor beta constant
Treg	Regulatory T cell
TSA	Tumor-specific antigen
TYR	Tyrosinase
U	Unit
UV	Ultraviolet
VEGF	Vascular endothelial growth factor
V_{END}	Endvolume
VLE	Very low endotoxin
WES	Whole exome sequencing

7 Acknowlegdements